

Utah State University

DigitalCommons@USU

All Graduate Theses and Dissertations

Graduate Studies

12-2016

Characterization of the Substrate Interactions and Regulation of Protein Arginine Methyltransferase

Yalemi Morales
Utah State University

Follow this and additional works at: <https://digitalcommons.usu.edu/etd>



Part of the [Biochemistry Commons](#)

Recommended Citation

Morales, Yalemi, "Characterization of the Substrate Interactions and Regulation of Protein Arginine Methyltransferase" (2016). *All Graduate Theses and Dissertations*. 5074.
<https://digitalcommons.usu.edu/etd/5074>

This Dissertation is brought to you for free and open access by the Graduate Studies at DigitalCommons@USU. It has been accepted for inclusion in All Graduate Theses and Dissertations by an authorized administrator of DigitalCommons@USU. For more information, please contact digitalcommons@usu.edu.



CHARACTERIZATION OF THE SUBSTRATE INTERACTIONS AND
REGULATION OF PROTEIN ARGININE
METHYLTRANSFERASE 1

by

Yalemi Morales

A dissertation submitted in partial fulfillment
of the requirements for the degree

of

DOCTOR OF PHILOSOPHY

in

Biochemistry

Approved:

Joan M. Hevel, Ph.D.
Major Professor

Lance C. Seefeldt, Ph.D.
Committee Member

Sean J. Johnson, Ph.D.
Committee Member

Scott A. Ensign, Ph.D.
Committee Member

Gregory J. Podgorski, Ph.D.
Committee Member

Mark R. McLellan, Ph.D.
Vice President for Research and
Dean of the School of Graduate Studies

UTAH STATE UNIVERSITY
Logan, Utah

2016

Copyright © Yalemi Morales 2016

All Rights Reserved

ABSTRACT

Characterization of the Substrate Interactions and Regulation of Protein Arginine
Methyltransferase 1 (PRMT1)

by

Yalemi Morales, Doctor of Philosophy

Utah State University, 2016

Major Professor: Dr. Joan M. Hevel
Department: Chemistry and Biochemistry

Protein arginine methylation is a posttranslational modification catalyzed by the family of proteins known as the protein arginine methyltransferases (PRMTs). Thousands of methylated arginines have been found in mammalian cells. Many targets of arginine regulation are involved in important cellular processes like transcription, RNA transport and processing, translation, cellular signaling, and DNA repair. Since PRMT dysregulation has been linked to a variety of disease states, understanding how the activity of the PRMTs is regulated is of paramount importance. PRMT1 is the predominant PRMT, responsible for about 85% of all arginine methylation in cells, but very little is known about how PRMT1 is regulated. Although a few methods to regulate PRMT1 activity have been reported, the details of interaction and regulatory mechanisms remain largely unknown.

To better understand how PRMT1 is able to bind its substrates and how PRMT1 activity is regulated, we followed a mechanistic and structural biology approach to better

understand how PRMT1 interacts with its substrates and protein regulators. In this study the regulation of Hmt1 methyltransferase activity by the Air1 and Air2 proteins was analyzed and only one was determined to affect Hmt1 activity. The posttranslational phosphorylation of Hmt1 had also been reported to affect Hmt1 activity *in vivo* and our preliminary studies suggest that additional factors may help influence the regulatory effect of phosphorylation. Lastly, we report a new method of PRMT regulation through the reversible oxidation of key PRMT1 cysteine residues. We are also able to show that this regulation occurs in cells and affects several PRMT isoforms.

(195 pages)

PUBLIC ABSTRACT

Protein Arginine Methyltransferase 1 Interactions and Regulation

Yalemi Morales

Protein arginine methyltransferases, or PRMTs, are enzymes that can add one or two methyl groups to certain arginine residues in target proteins. The modification of the target protein, or substrate, changes the substrate just enough to affect its function. This typically occurs by allowing the target protein to interact with new proteins or molecules, or by preventing interactions that occur with the unmodified target protein. In mammalian cells, there are thousands of arginines that can be methylated and many of those are found in proteins involved in critical cellular processes like RNA transport and processing, transcription, and translation. Therefore, it is important to understand how the PRMTs select which arginine substrates to methylate, and how this activity is regulated.

The work presented in this dissertation includes several lines of investigation that together aimed to describe how PRMT1, the predominant PRMT in mammalian cells, interacts with substrates and can be regulated. The visualization of PRMT1 interactions with target proteins was sought out through protein crystallography, but could not be achieved within the scope of this study. The regulation of the yeast PRMT1 (Hmt1) protein by the Air1 and Air2 proteins was analyzed and only one was determined to affect the rate of methyl groups transferred. The modification of the yeast PRMT1 through phosphorylation was also investigated and preliminary results suggest that additional factors are likely involved in the regulatory effect of phosphorylation. Lastly, a new method of PRMT1 regulation through reversible oxidation was reported and was confirmed to be conserved method of regulation for several members of the PRMT family of enzymes.

ACKNOWLEDGMENTS

I would like to take this opportunity to thank my major advisor Dr. Joanie Hevel for her patience, guidance, encouragement, and support throughout my studies at Utah State University. I am very grateful for her mentorship which has helped me grow as a student, teacher, scientist, and mother. I would also like to thank my supervisory committee members, Dr. Sean Johnson, Dr. Lance Seefeldt, Dr. Scott Ensign, and Dr. Gregory Podgorski, for their advice, suggestions, and encouragement.

I also have to thank my lab mates and peers for their lessons and their friendship. Dr. Whitney Wooderchak-Donahue, Dr. Laurel Gui, Dr. Brenda Suh-Lailam, Dr. Ryan Jackson, Dr. Jeremy Bakelar, Dr. Bradley Hintze, Owen Price, Damon Nitzel, Betsy Caceres, Heather Tarbet, Lacy Taylor, Brooke Siler, Drake Smith, and many others have helped me tremendously and made my PhD years some of my best.

Most importantly, I would like to thank my family for supporting me through this time in my life. I especially want to thank Todd Gary for always being there to listen and encourage me through the many failures and long days of work. My daughter Allisen Gary also helped me realize how strong I can be and helped me realize the things that are truly important to me. Without the support of my family, friends, mentors, and peers, I would not have made it through this journey. Thank you all very much!

Yalemi Morales

CONTENTS

	Page
ABSTRACT	iii
PUBLIC ABSTRACT	v
ACKNOWLEDGMENTS	vi
LIST OF TABLES	ix
LIST OF FIGURES	x
 CHAPTER	
1. INTRODUCTION	1
References	6
2. LITERATURE REVIEW	9
References	36
3. INVESTIGATING PRMT1: SUBSTRATE INTERACTIONS.....	52
Introduction.....	53
Experimental Procedures	57
Results.....	62
Discussion	71
References.....	76
4. HMT1 REGULATION BY THE AIR1/2 PROTEINS	79
Introduction.....	80
Experimental Procedures	85
Results.....	93
Discussion	103
References.....	105
5. INVESTIGATING THE EFFECTS OF PHOSPHORYLATION ON HMT1 ACTIVITY	110
Introduction.....	111
Experimental Procedures	112
Results.....	115
Discussion	120
References.....	121

6.	REDOX CONTROL OF PROTEIN ARGININE METHYLTRANSFERASE 1 (PRMT1) ACTIVITY	124
	Introduction.....	125
	Experimental Procedures	128
	Results.....	135
	Discussion	147
	References.....	153
7.	SUMMARY AND FUTURE DIRECTIONS	160
	References.....	167
	APPENDIX.....	174
	CURRICULUM VITAE	181

LIST OF TABLES

Table	Page
2-1. PRMT protein regulators	24
3-1. Npl3 construct interaction with Hmt1	70
4-1. Data collection statistics for Air2-Hmt1 crystal	103

LIST OF FIGURES

Figure	Page
2-1. Structure of AdoMet and S _N 2 mechanism of AdoMet-dependent methyltransferases	10
2-2. Reactions catalyzed by the PRMTs	12
2-3. Schematic comparison of the nine mammalian PRMT isoforms	13
2-4. Structural overview of a PRMT monomer.....	15
2-5. Zoomed in view of the PRMT1 active site (PDB: 1OR8).....	18
2-6. PRMT substrate binding modes.....	20
2-7. PRMT dimer interacting regions	30
3-1. Reactions catalyzed by the mammalian protein arginine methyltransferases.....	54
3-2. Structure of rat PRMT1 bound to R3 peptide (PDB: 1OR8).....	56
3-3. Summary of initial S14-PRMT1 crystallization conditions.....	64
3-4. Diffraction pattern and electron density of PRMT1 crystal containing the eIF4A1-CH ₃ peptide	65
3-5. Npl3 sequence and arginine methylation sites.....	68
3-6. Npl3 constructs designed	69
3-7. Summary of Hmt1 and Cterm Npl3 crystallization conditions	72
4-1. Reactions catalyzed by yeast protein arginine methyltransferases	81
4-2. The TRAMP complex is an essential nuclear exosome cofactor	83
4-3. Air1 and Air2 sequence alignment	85
4-4. Air1 and Air2 truncated constructs used to test binding to Hmt1 as well as ability to inhibit Hmt1 activity	95
4-5. Effect of Air1 and Air1 on the methylation of Npl3 by Hmt1	97
4-6. Air1 zinc binding is required for inhibitory effect on Hmt1.....	98
4-7. Air1 zinc knuckles 4 and 5 are required for Hmt1 inhibition.....	99
4-8. Sequence alignment of Air2 and Air1 zinc knuckles 4 through 5	99
4-9. Air1 N-ZnK5 and Δ N22+2 Hmt1 complex crystals and diffraction patterns	102

4-10. Initial Air1-Hmt1 electron density map created after molecular replacement using Δ N22+2 Hmt1 hexamer as search model	102
5-1. Methylation of Npl3 by Hmt1 phosphorylation variants	117
5-2. Activity of Hmt1 phosphorylation variants at two AdoMet concentrations	117
5-3. Activity of Hmt1 phosphorylation variants with varying [Npl3], or with R3 peptide.....	119
5-4. Effect of N-terminal tags on Npl3 methylation by Hmt1 phosphorylation variants	120
6-1. ADMA formation and degradation.....	126
6-2. PRMT1 activity is (A) inhibited by H ₂ O ₂ in a concentration dependent manner and (B) activity lost can be recovered by reduction	136
6-3. The effect of reducing agents on PRMT1 enzymatic activity	138
6-4. The enhancing effect of DTT on PRMT1 methyltransferase activity is independent of the His ₆ -tag.....	140
6-5. Oligomeric state of PRMT1 proteins assessed by size exclusion chromatography	142
6-6. Methyltransferase activity of PRMT1 cysteine variants in the absence or presence of DTT	144
6-7. Sulfenic acid detection and free thiol content in PRMT1.....	148
6-8. Cysteine residues in rPRMT1	149
6-9. Redox control is conserved among PRMT family members	151
7-1. PRMT1 methyltransferase activity is impaired by oxidation <i>in vivo</i>	162
7-2. Sulfenic acid levels in PRMT1 increase with increasing cellular oxidative stress.....	163
7-3. PRMT6 structures in (A) oxidized and (B) reduced forms.....	165
7-4. Position of PRMT6 active site E167 in (A) oxidized and (B) reduced forms	165
7-5. PRMT1 product formation on the R3 peptide depends on the redox state.....	167

CHAPTER 1

INTRODUCTION

Posttranslational modification of proteins allows organisms to expand upon the limits of the proteome by influencing protein localization, protein-protein or protein-nucleic acid interactions, and protein stability. Protein arginine methylation is a type of posttranslational modification that has been implicated in a many fundamental biological pathways such as RNA transport and processing, DNA repair, transcriptional regulation, and signal transduction (reviewed in (1-4)). The family of enzymes responsible for the catalysis of protein arginine methylation is the protein arginine methyltransferases (PRMTs). Due to the significant role PRMTs play in many cellular pathways, dysregulation of PRMT expression and/or activity has been linked to several human diseases including cardiovascular disease (5-7), stroke (8,9), asthma (10), viral pathogenesis (11-13), multiple sclerosis (14), and carcinogenesis (15-17).

Unlike other posttranslational modifications such as phosphorylation and even lysine methylation which can be reversed by phosphatases or lysine demethylases, no enzyme has yet been found to reverse the posttranslational methylation of arginine residues. The seemingly irreversible nature of this modification underscores the importance of proper regulation over the activity of the protein arginine methyltransferases. Yet, although much progress has been made in understanding the pathways in which the PRMTs are involved, surprisingly little is known about how the PRMTs select and interact with substrates, or how their activity is regulated.

The goal of this dissertation is to understand how PRMT1, the predominant protein arginine methyltransferase, functions by characterizing the molecular details of substrate interactions, and to determine how the methyltransferase activity of PRMT1 is regulated.

In Chapter 3, I used structural biology techniques in an attempt to observe the interactions of PRMT1 with a substrate. A previously solved structure of PRMT1 was co-crystallized with a substrate containing three methylatable arginines (18). This structure contained clear density only for the active site arginine, while only broken tracks of backbone density were observed for the other residues in the substrate peptide. The poor resolution observed for the peptide in this structure was hypothesized to be due to crystal heterogeneity resulting from the three possible methylatable arginines each binding the active site on different PRMT1 molecules. In order to limit the binding modes, only peptide substrates containing a single arginine were used in my crystallization attempts. Furthermore, since the initial structure was able to depict the residues coordinating the binding of the substrate arginine, a peptide substrate containing a monomethylated arginine was chosen for our attempts in order to decipher how the MMA substrate is coordinated in the PRMT1 active site for the second catalytic step. Unfortunately, we have been unable to solve a structure with clear electron density for any bound substrate. To overcome this problem, a new strategy of co-crystallizing PRMT1 with a protein substrate was put in place. The yeast PRMT1, Hmt1, and a truncated Npl3 protein substrate were chosen for this approach. The structure of Hmt1 had been previously solved by X-ray crystallography (19) and Npl3 is the best characterized Hmt1 substrate. The Npl3 protein was truncated to remove a flexible N-terminal region that is not required for Hmt1 interaction in order to improve the favorability of crystallization. Crystals have been obtained containing both

Hmt1 and the substrate Npl3 construct; however, these crystals have failed to provide X-ray diffraction patterns of sufficient quality to solve a structure. Further optimization of crystallization conditions is recommended in order to improve diffraction resolution and produce a structure capable of revealing the molecular details of how PRMT1 interacts with substrate proteins.

Beginning in Chapter 4, my work shifts towards characterizing the regulation of PRMT1. In this chapter, I worked in collaboration with the Johnson lab to investigate the previously reported regulation of Hmt1 by the Air1 and Air2 proteins (20). The Air1/2 proteins are part of the TRAMP (Trf4/Mtr4/Air1 or Trf5/Mtr4/Air2) nuclear RNA surveillance complex studied in the Johnson lab. However, the Air (arginine methyltransferase-interacting RING finger) proteins were both initially identified and named after their ability to interact with Hmt1 substrates in a yeast two hybrid study. In this initial report, Air1 was shown to inhibit Hmt1 methylation both *in vivo* and *in vitro*. A large degree of sequence similarity between Air1 and Air2, in combination with a knockout screen indicating the two might be functionally redundant led to the conclusion that both may be Hmt1 regulators. Investigations using C-terminally truncated constructs of both Air1 and Air2 quickly showed that while Air1 is indeed an Hmt1 inhibitor, Air2 was unable to inhibit Hmt1 methylation of any of the substrates tested. To further probe the Hmt1 inhibition by Air1, several constructs of Air1 were created to map both the regions of interaction with Hmt1, as well as the minimal region required for inhibition. We were able to determine that a ~60 amino acid region of Air1 containing the fourth and fifth zinc knuckle motifs of the protein are enough to inhibit methyltransferase activity. Further work should be done to finalize the minimal Air1 construct required for Hmt1 inhibition and

characterize the method of inhibition. Additionally, since discovering that Air2 does not seem to inhibit Hmt1, but is still able to form a stable complex, we have attempted to solve the crystal structure of the complex and provide the first insights on how the PRMTs interact with other proteins. Crystals containing both proteins have been optimized and have produced diffraction data suitable to ~ 3.2 Å. This structure has not yet been solved, but molecular replacement using a previously solved Hmt1 structure has produced initial electron density maps in which the structure of the complex will be built. Similar efforts to crystallize and solve the structure of an Air1/Hmt1 complex are recommended.

In Chapter 5, I attempt to validate results indicating that Hmt1 activity and oligomeric state could be regulated by posttranslational phosphorylation on the N-terminus of Hmt1 (21). This report indicated that *in vivo* phosphorylation of Hmt1 at Ser9 results in an increase in the methylation of Npl3. However, because *in vitro* studies were not performed, it is unclear if phosphorylation affected the intrinsic activity of Hmt1 or if this PTM resulted in recruitment of another factor that modulated the methyltransferase activity. Since this report elegantly demonstrated that the phosphorylation effects could be mimicked using a glutamate substitution at position 9, I set out to characterize the mechanism by which phosphorylation affects Hmt1 activity. Hmt1 S9E (phosphorylation mimic) and S9A (unable to be phosphorylated) constructs were expressed, purified, and their activities measured in order to corroborate the *in vivo* published results. However, despite the use of several different solubility tags and a variety of substrates, it was impossible to validate the previous results with our *in vitro* methylation assay. This discrepancy hints at the possibility that the published results were a result of recruitment of an unknown factor, rather than solely due to the phosphorylation event.

In Chapter 6, I followed the discovery of Dr. Shanying Gui and Damon Nitzel, previous students in the Hevel lab, who had observed that PRMT1 activity changes as a function of the redox state and that this effect is cysteine-dependent. I was able to further characterize that PRMT1 activity decreases in a hydrogen peroxide (H₂O₂) concentration-dependent manner and is reversible within physiologically relevant levels of H₂O₂. Additionally, I was able to identify the cysteine residues necessary for this redox effect to occur and determine that the two critical cysteines are oxidized to sulfenic acid. Furthermore, I then looked at cysteine conservation among the PRMT isoforms and found that PRMT3, PRMT6, and PRMT7 are also under redox control. This work not only reveals the details of a novel PRMT1 regulatory mechanism, but also indicates that redox regulation is a conserved feature of several members of the PRMT family.

Chapter 7 includes preliminary results from several ongoing projects and discusses possible future directions. Follow up work on the redox regulation of PRMT1 is discussed. *Ex-vivo* assays show that oxidation of PRMT1 in cells results in increased sulfenic acid formation and diminished PRMT1 activity, indicating that the redox regulation described *in vitro* is likely also occurring *in vivo*. In addition, a detailed comparison between PRMT1 and PRMT6 suggests that while redox regulation is conserved, the mechanism through which oxidation impairs enzymatic activity may be different among the two isoforms. Constructs created to validate this hypothesis will be discussed, as well as avenues for future investigation. Lastly, preliminary data seems to indicate that the redox state of PRMT1 may influence product specificity. A summary of the initial data and suggestions for future work will be discussed.

In summary, this dissertation provides new insights into regulatory mechanisms poised to control PRMT methyltransferase activity in cells. The investigation/validation of previously reported regulators along with the discovery of a new PRMT regulatory mechanism provide a strong foundation for future avenues of investigation.

REFERENCES

1. Bedford, M. T. (2007) Arginine methylation at a glance. *J. Cell Sci.* **120**, 4243-4246
2. Bedford, M. T., and Clarke, S. G. (2009) Protein arginine methylation in mammals: who, what, and why. *Mol. Cell* **33**, 1-13
3. Bedford, M. T., and Richard, S. (2005) Arginine methylation an emerging regulator of protein function. *Mol. Cell* **18**, 263-272
4. Di Lorenzo, A., and Bedford, M. T. (2011) Histone arginine methylation. *FEBS Lett.* **585**, 2024-2031
5. Boger, R. H. (2003) The emerging role of asymmetric dimethylarginine as a novel cardiovascular risk factor. *Cardiovasc. Res.* **59**, 824-833
6. De Gennaro Colonna, V., Bianchi, M., Pascale, V., Ferrario, P., Morelli, F., Pascale, W., Tomasoni, L., and Turiel, M. (2009) Asymmetric dimethylarginine (ADMA): an endogenous inhibitor of nitric oxide synthase and a novel cardiovascular risk molecule. *Med. Sci. Monit.* **15**, RA91-101
7. Kielstein, J. T., Impraim, B., Simmel, S., Bode-Boger, S. M., Tsikas, D., Frolich, J. C., Hoepfer, M. M., Haller, H., and Fliser, D. (2004) Cardiovascular effects of systemic nitric oxide synthase inhibition with asymmetrical dimethylarginine in humans. *Circulation* **109**, 172-177
8. Chen, S., Li, N., Deb-Chatterji, M., Dong, Q., Kielstein, J. T., Weissenborn, K., and Worthmann, H. (2012) Asymmetric dimethylarginine as marker and mediator in ischemic stroke. *Int. J. Mol. Sci.* **13**, 15983-16004
9. Yoo, J. H., and Lee, S. C. (2001) Elevated levels of plasma homocyst(e)ine and asymmetric dimethylarginine in elderly patients with stroke. *Atherosclerosis* **158**, 425-430

10. Wells, S. M., Buford, M. C., Migliaccio, C. T., and Holian, A. (2009) Elevated asymmetric dimethylarginine alters lung function and induces collagen deposition in mice. *Am. J. Respir. Cell Mol. Biol.* **40**, 179-188
11. Benhenda, S., Ducroux, A., Riviere, L., Sobhian, B., Ward, M. D., Dion, S., Hantz, O., Protzer, U., Michel, M. L., Benkirane, M., Semmes, O. J., Buendia, M. A., and Neuveut, C. (2013) Methyltransferase PRMT1 is a binding partner of HBx and a negative regulator of hepatitis B virus transcription. *J. Virol.* **87**, 4360-4371
12. Shire, K., Kapoor, P., Jiang, K., Hing, M. N., Sivachandran, N., Nguyen, T., and Frappier, L. (2006) Regulation of the EBNA1 Epstein-Barr virus protein by serine phosphorylation and arginine methylation. *J. Virol.* **80**, 5261-5272
13. Singhroy, D. N., Mesplede, T., Sabbah, A., Quashie, P. K., Falgoutyret, J. P., and Wainberg, M. A. (2013) Automethylation of protein arginine methyltransferase 6 (PRMT6) regulates its stability and its anti-HIV-1 activity. *Retrovirology* **10**, 73
14. Kim, J. K., Mastronardi, F. G., Wood, D. D., Lubman, D. M., Zand, R., and Moscarello, M. A. (2003) Multiple sclerosis: an important role for post-translational modifications of myelin basic protein in pathogenesis. *Mol. Cell. Proteomics* **2**, 453-462
15. Cheung, N., Chan, L. C., Thompson, A., Cleary, M. L., and So, C. W. (2007) Protein arginine-methyltransferase-dependent oncogenesis. *Nature Cell Biol.* **9**, 1208-1215
16. Baldwin, R. M., Moretton, A., and Cote, J. (2014) Role of PRMTs in cancer: Could minor isoforms be leaving a mark? *World J. Biol. Chem.* **5**, 115-129
17. Yang, Y., and Bedford, M. T. (2013) Protein arginine methyltransferases and cancer. *Nat. Rev. Cancer* **13**, 37-50
18. Zhang, X., and Cheng, X. (2003) Structure of the predominant protein arginine methyltransferase PRMT1 and analysis of its binding to substrate peptides. *Structure* **11**, 509-520
19. Weiss, V. H., McBride, A. E., Soriano, M. A., Filman, D. J., Silver, P. A., and Hogle, J. M. (2000) The structure and oligomerization of the yeast arginine methyltransferase, Hmt1. *Nat. Struct. Biol.* **7**, 1165-1171
20. Inoue, K., Mizuno, T., Wada, K., and Hagiwara, M. (2000) Novel RING finger proteins, Air1p and Air2p, interact with Hmt1p and inhibit the arginine methylation of Npl3p. *The Journal of Biological Chemistry* **275**, 32793-32799

21. Messier, V., Zenklusen, D., and Michnick, S. W. (2013) A nutrient-responsive pathway that determines M phase timing through control of B-cyclin mRNA stability. *Cell* **153**, 1080-1093

CHAPTER 2

LITERATURE REVIEW

Methylation

Cellular methylation requires the presence of a methyl group donor such as S-adenosyl-L-methionine (AdoMet/SAM) (Figure 2-1-A) or tetrahydrofolate (THF) and a methyl acceptor. AdoMet is the second most commonly used enzyme cofactor after adenosine triphosphate (ATP) (1). Methionine and ATP are used by methionine adenosyltransferase to synthesize AdoMet, which can be used by AdoMet-dependent methyltransferases (MTases) as a methyl group donor, leaving the product S-adenosyl-L-homocysteine (AdoHcy/SAH). AdoMet is the preferred methyl group donor in biological systems likely due to the favorable energetics of the methyl transfer reaction which releases -17 kcal/mol, more than twice the energy released during ATP hydrolysis (1). AdoMet-dependent methyltransferases are remarkably diverse enzymes, utilizing any of five different structural folds to bind AdoMet and catalyze the transfer of a methyl group to substrates ranging from small molecules, to nucleic acids, to proteins (2). At the atomic level, the targets for MTases can be carbon, oxygen, nitrogen, sulfur, or even halides (1,3). The diversity in methyl group acceptors means that MTases have evolved a wide variety of mechanisms to activate the catalytic nucleophile. However, despite the many differences among the AdoMet-dependent MTases, all are thought to proceed in an S_N2 -like mechanism and transfer the methyl group from AdoMet to the substrate with an inversion of symmetry (Figure 2-1-B) (3).

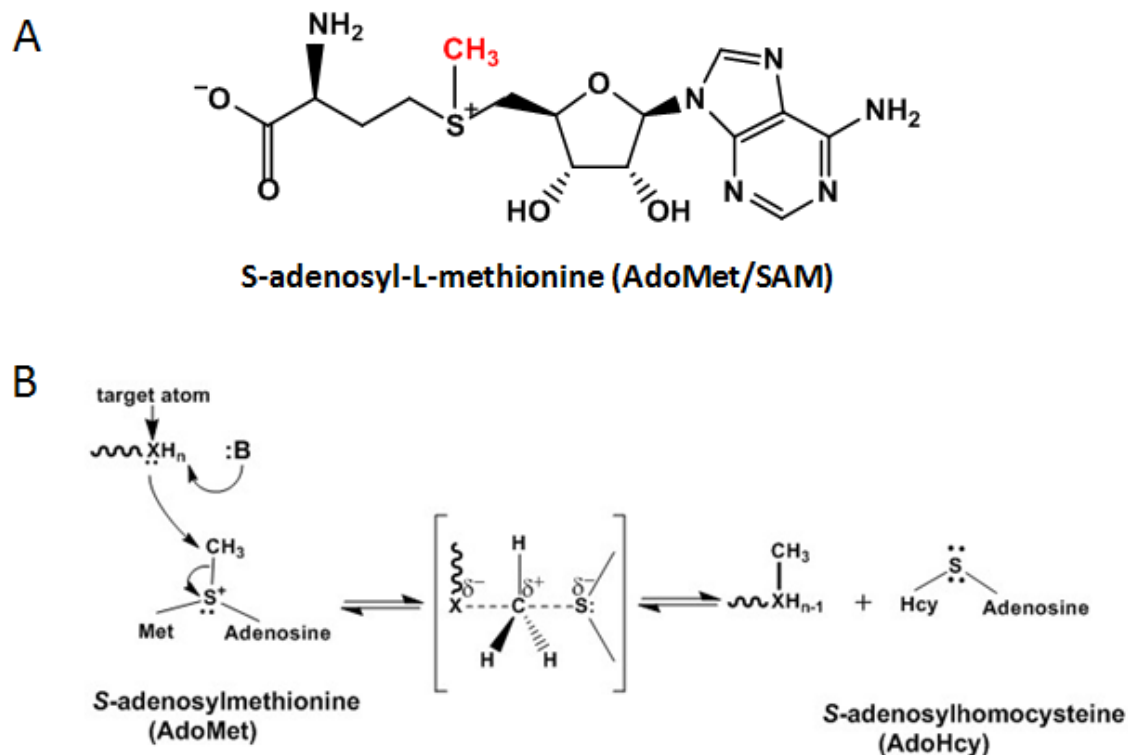


FIGURE 2-1. Structure of AdoMet and S_N2 mechanism of AdoMet-dependent methyltransferases. (A) Structure of S-adenosyl-L-methionine (AdoMet) which includes the adenosine moiety and the methionine moiety. (B) In this general S_N2 reaction mechanism, a general base (:B) deprotonates the target atom ($X=N, O, S,$ or C) prior, during, or after methyl transfer. A transition state forms from the nucleophilic attack of the target atom onto the methyl group carbon of AdoMet, resulting in the methyl group transfer from AdoMet to the target atom.

Protein Arginine Methylation

Protein arginine methylation is a type of posttranslational modification (PTM) which enables organisms to expand the limits of their genomes and enlarge the functionality of proteins. The AdoMet-dependent methylation of arginine residues does not alter the positive charge of the amino acid, but it does increase the hydrophobicity and steric bulk, thereby affecting how modified proteins interact with other proteins or nucleic acids. Arginine methylated proteins are involved in a wide array of cellular processes,

including transcription (4), translation (5), RNA transport and metabolism (6,7), and DNA damage repair (8).

This widespread PTM is catalyzed by nine known mammalian protein arginine methyltransferases (PRMTs), as well as homologs present in yeast, protozoa, plants, nematodes, and fish, but not in bacteria (2). The PRMTs are classified based on their product formation as either type I, type II, type III, or type IV enzymes (Figure 2-2). Types I, II, and III PRMTs methylate the terminal (ω) guanidino nitrogen atoms of arginine residues in protein substrates, resulting in a modified monomethylarginine (MMA) residue. While PRMT7, the only known type III PRMT can only make MMA, type I and II enzymes are capable of catalyzing the addition of a second methyl group. Type I PRMTs (PRMT1, 2, 3, 4, 6, 8) can add a second methyl group to the same nitrogen atom, making asymmetric dimethylarginine (ADMA). Type II PRMTs (PRMT5, 9) can also add a second methyl group to the unmodified terminal nitrogen atom, making symmetric dimethylarginine (SDMA). Type IV PRMTs, which have thus far been identified only in yeast, catalyze the monomethylation of the internal (δ) guanidino nitrogen atom (Figure 2-2). Correct product formation is critical given that different products can have different biological consequences (9,10). Yet, very little is currently known regarding how product specificity is regulated for the PRMTs.

Protein Arginine Methyltransferase Family

Each of the nine members of the mammalian PRMT family contain four conserved amino acid sequence motifs (I, post-I, II, and III) characteristic of the class I seven β -strand

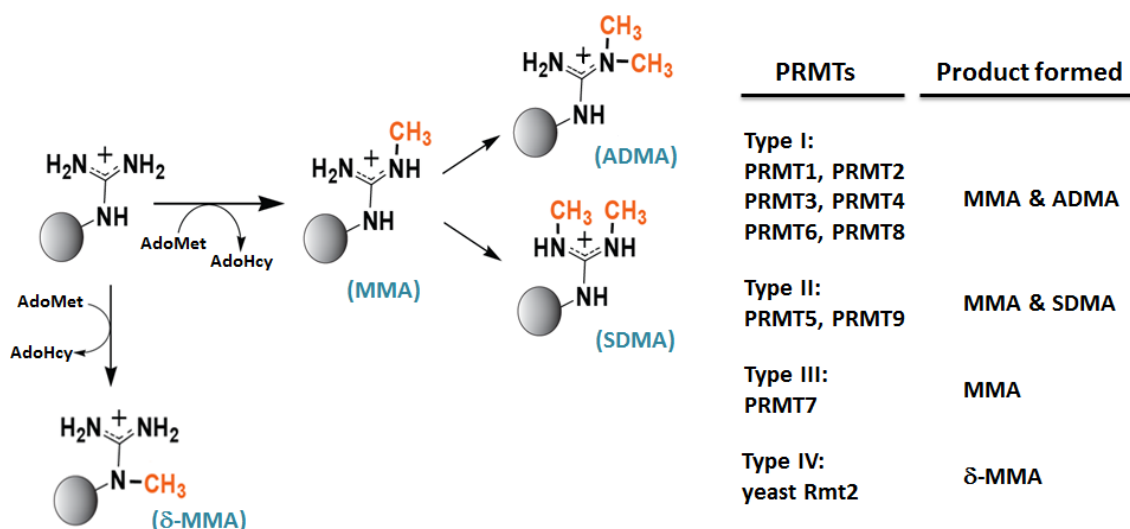


FIGURE 2-2. Reactions catalyzed by the PRMTs. The four types of PRMTs are classified based on the products formed. All catalyze the transfer of a methyl group from AdoMet to a substrate arginine residue making δ -MMA, MMA, ADMA, or SDMA.

AdoMet-dependent methyltransferases (2,11), as well as a highly conserved THW loop (Figure 2-3). Although the PRMTs vary widely in length, a 310 amino acid conserved core (gray in Figure 2-3) is present in all isoforms. Most isoforms also have extended N-terminal additions (blue and green in Figure 2-3) that are unique to each isoforms and may be responsible for altering substrate recognition (12), dictating protein-protein interactions (13), specifying cellular localization (14), or even regulating methyltransferase activity (15), thus facilitating the unique function of each PRMT isoform.

PRMT1 is the predominant type I PRMT in mammalian cells, catalyzing 85% of cellular protein arginine methylation (16). PRMT1 has been found to localize in both the cytoplasm and the nucleus and is ubiquitously expressed in all tissues (17,18). Seven PRMT1 splice variants have been found in humans that display distinct activity, substrate specificity, and subcellular localization (12). PRMT2 is also a ubiquitously expressed type

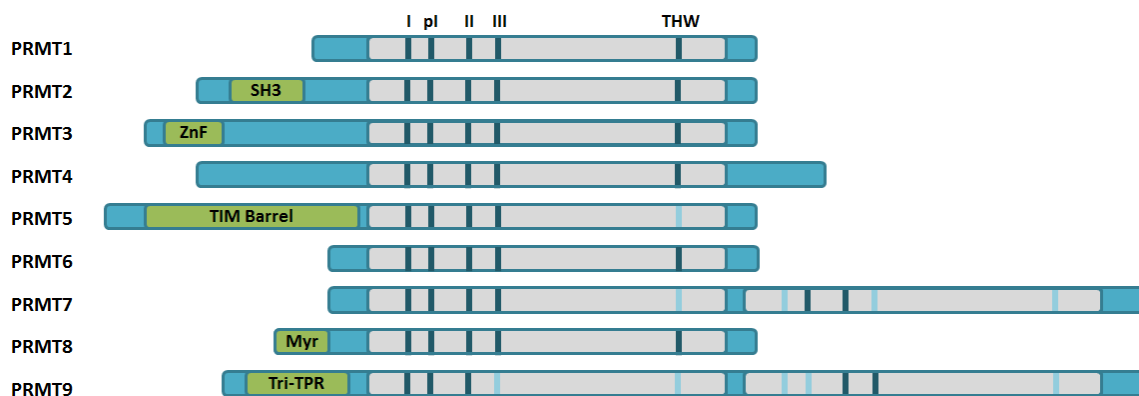


FIGURE 2-3. Schematic comparison of the nine mammalian PRMT isoforms. The catalytic core is colored in gray with each conserved motif (I, post-I, II, III, and THW loop) highlighted in dark blue, or light blue if not strictly conserved. Various N-terminal modules are also shown in green. PRMT2 has an SH3 domain, PRMT3 has a zinc finger domain (ZnF), PRMT5 has a TIM barrel motif, PRMT8 has a myristoylation site (Myr), and PRMT9 has a tetratricopeptide repeat (Tri-TPR).

I PRMT (19). PRMT2 contains an N-terminal SH3 domain which is essential for interactions with proline-rich proteins (20). PRMT2 functions as a coactivator for the estrogen receptor (21,22) and has been shown to directly interact with and stimulate the activity of PRMT1 in cells (23). PRMT3 is an exclusively cytoplasmic type I PRMT isoform which contains an N-terminal zinc finger domain shown to play a role in PRMT3 substrate recognition (24,25). PRMT3 is found mostly in association with ribosomes, where it methylates the S2 protein of the small ribosomal subunit (13,26). The type I PRMT4 (also commonly called CARM1) is a transcriptional coactivator that can function synergistically with PRMT1 and histone acetyltransferases (27). PRMT4 has also been found to methylate mRNA stabilizing proteins and splicing factors, indicative of a role in coupling transcription and RNA processing (28). PRMT5 is the predominant type II PRMT and can be found as part of several different protein complexes (29). In the cytoplasm, PRMT5 is part of the “methylosome” complex where its activity is implicated in snRNP

biogenesis through the methylation of Sm proteins (30). In the nucleus, PRMT5 can complex with chromatin remodeling proteins which are able to enhance PRMT5 activity towards selected targets (31). PRMT6 is a primarily nuclear type I PRMT (32). PRMT6 has been implicated in viral immunity since methylation by PRMT6 negatively regulates the activity of the HIV transactivator protein Tat, thereby acting as a restriction factor for viral replication (33). PRMT7 is the only known type III PRMT, capable of catalyzing only MMA formation (34). PRMT7 contains a duplicated core catalytic domain, both of which are required for activity (35). PRMT8 is a type I PRMT found primarily in the human brain (14). It is uniquely found to be localized at the plasma membrane through N-terminal myristoylation (14). PRMT8 has been found to associate with PRMT1 and to self-regulate through automethylation on its N-terminal region (36). PRMT9 has been recently determined to have type II PRMT activity (37). PRMT9 also contains a duplicated catalytic core, along with an N-terminal tetratricopeptide repeat, although the functional importance of these domains for PRMT9 activity is unknown (38).

PRMT Structure and Substrate Binding

The crystal structures of many of the PRMT isoforms have been solved (39-50), revealing a striking structural conservation of the PRMT catalytic core. The monomeric structure of all PRMTs can be divided into three conserved parts (Figure 2-4): an AdoMet binding domain (green), a β barrel domain (gray), and a dimerization arm (blue). The AdoMet binding domain adopts a typical Rossmann fold conserved in other class I AdoMet-dependent methyltransferases (51), while the β barrel domain is unique to the PRMT family and is thought to participate in substrate binding (39,41). The dimerization

arm is inserted into the β barrel domain and although the length and sequence composition varies among the PRMT isoforms, a highly similar helical fold is observed in all PRMT crystal structures. The conservation of the dimeric interface coincides with the formation of head-to-tail homodimers observed in all PRMT structures (43) (human, mouse, and *C. elegans* PRMT7 are the exception since they contain a duplicated core which mimics the dimeric structure (48)). Dimerization appears required for methyltransferase activity, as experiments in PRMT1, PRMT3, and *A. thaliana* PRMT10 (AtPRMT10) have shown that removal or mutation of the dimerization arm results in abolished methyltransferase activity (39-41,43).

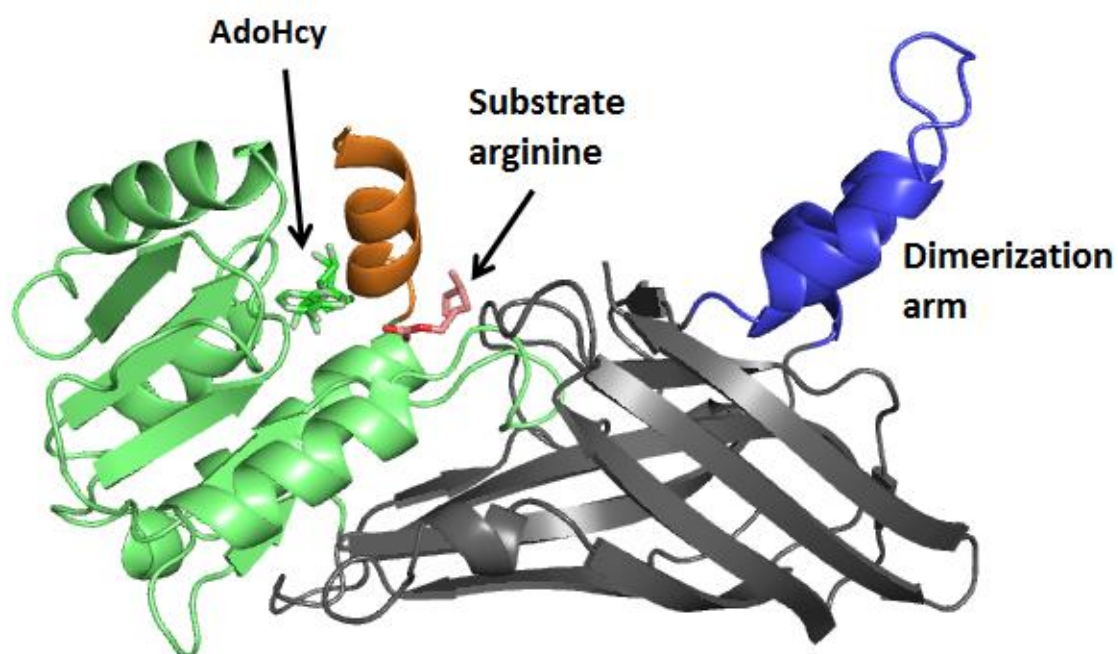


FIGURE 2-4. Structural overview of a PRMT monomer. The structure of rat PRMT1 (PDB: 1OR8) is used to illustrate the general fold of all PRMT isoforms. The AdoMet binding domain adopts a typical Rossmann fold (green) to bind the AdoMet cofactor (green) and is capped by N-terminal helices (helix αY is shown in orange, while αX is not present in this structure). The substrate arginine residue is colored in pink, while the β barrel domain is in gray and the dimerization arm is in blue.

AdoMet binding by PRMTs is coordinated primarily through the conserved motifs found in the typical Rossmann fold of class I AdoMet-dependent methyltransferases. Motif I (VLD/EVGxGxG) forms the base of the AdoMet binding site. The carboxylate of the acidic residues within the post-I motif (L/V/IxG/AxD/E) form hydrogen bonds with the hydroxyl groups of the ribose moiety of AdoMet. While motif II (F/I/VDI/L/K) stabilizes motif I through the formation of a parallel B sheet, and motif III (LR/Kxxg) forms a parallel B sheet with motif II. The THW loop is close to the active site cavity and helps stabilize the N-terminal helix, which is important for arginine substrate recognition. In addition to these conserved motifs, the AdoMet binding pocket is completed by a conserved structural element composed of two helical segments, helices αX and αY , that fold onto the bound cofactor and provides a physical division between the cofactor binding site and the arginine binding site (see helix αY , orange in Figure 2-4). Most of the available PRMT crystal structures are missing most or all of the αX helix, suggesting that dynamics may be involved in cofactor binding and release. In support of this theory, the mouse PRMT6 crystal structure was recently published in both oxidized and reduced states (49), capturing the αX helix in an unfolded, inactive state when oxidized, and a properly folded active state when reduced, and thus providing direct evidence of the protein dynamics involved in cofactor binding.

The active site of all PRMTs contains a pair of conserved glutamate residues (E144 and E153 in rat PRMT1). These residues commonly referred to as the “double-E loop”, hydrogen bond with the positively charged guanidino nitrogen of the target arginine residue and thereby create the correct orientation for catalysis (magenta in Figure 2-5) (41).

The active site of type I PRMTs also contain a pair of conserved methionine residues (M48 and M155 in rat PRMT1) which are positioned very close to the guanidino group of the target arginine residue and have been found to affect the type and degree of methylation (blue in Figure 2-5). Mutation of both methionines in rat PRMT1 was found to affect the MMA/ADMA ratios (52). Mutation of M48 of rat PRMT1 to the correspondingly conserved phenylalanine residue in the type II PRMT5 led to the transformation of rPRMT1 into a mixed type I/type II enzyme (53). The equivalent mutation in PRMT5 (F379 in *C. elegans* PRMT5 to methionine) also transformed this type II enzyme into a mixed type II/type I PRMT (44). This result is intriguing since the equivalent position on the other type II PRMT, PRMT9, is a methionine; indicating that other unidentified factors collaborate to confer the product specificity of the PRMTs. Current work in the Hevel lab is also investigating the role of residues in the type III PRMT7 in conferring this isoform its strict type III activity.

While much has been revealed on the details of AdoMet binding and the PRMT catalytic mechanism (reviewed in (54)), the structures of PRMTs with peptide substrates bound have only revealed pieces of information on how PRMTs recognize and bind their substrates. Recently, the *Trypanosoma brucei* PRMT7 (TbPRMT7) and human PRMT5 (hPRMT5) structures were both solved in the presence of a histone H4 peptide, providing the first clear images of how these PRMTs interact with the H4 substrate. In the PRMT5 structure, the substrate arginine is presented/projected into the active site at the tip of a sharp β -turn in the peptide substrate (55)(Figure 2-6-A), and in the PRMT7 structure, the peptide substrate forms a wide turn on the surface of the active site (50)(Figure 2-6-B).

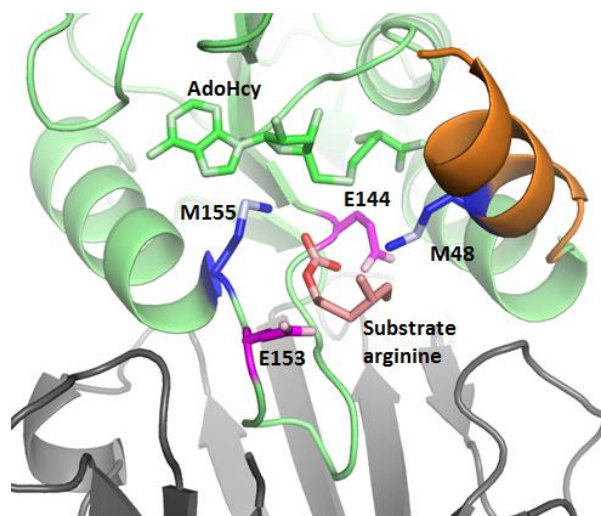


FIGURE 2-5. Zoomed in view of PRMT1 active site (PDB: 1OR8). Double-E-loop glutamates (E144 and E153) are in magenta; two methionines involved in product specificity (M48 and M155) are in blue. Substrate arginine (pink) and AdoHcy (green) are also shown. Note that E153 in this structure points away from the active site arginine (inactive conformation) due to the low pH of the crystallization conditions.

However, both the type II hPRMT5 and the type III TbPRMT7 recognize the substrate primarily through peptide backbone interactions. Because of the wide array of substrates and substrate sequences methylated by these enzymes, structures with additional substrates will be needed in order to determine if the observed binding modes (turns in the backbone bracketing the arginine) are inherent for these PRMTs, or rather are substrate-specific, a possibility suggested by PRMT1 studies.

The structure of rat PRMT1 (rPRMT1) was solved with a substrate peptide containing three arginines (R3; GGRGGFGGRGGFGGRGGFG) (39). Heterogeneity likely caused by the three different methylatable arginines each binding the active site of different molecules resulted in clear electron density only for an arginine residue in the active site, while the rest of the substrate peptide side chains could not be observed. However, patches of electron density revealed three possible peptide binding grooves

(39)(Figure 2-6-C), suggesting that different PRMT1 substrates might interact with PRMT1 using different binding modes. In support of this theory, biochemical manipulation of a residue on one of these grooves altered the pattern of PRMT1 methylation on hypomethylated cell extracts, inhibiting methylation of some proteins while leaving methylation of others unchanged (56). Interestingly, the PRMT4 structure also revealed multiple potential binding grooves on the surface of this isoform (42).

Similar to what was observed in the hPRMT5 and TbPRMT7 structures, binding of the R3 peptide to rPRMT1 seems to occur mainly through backbone interactions. This observation is also supported by substrate profiling studies which have shown little to no consensus sequence for substrate recognition by PRMT1 (57,58), (although there is a prevalence of 'RGG', 'RXR', and 'RG' sequences observed *in vivo*). The presence of glycine around the targeted arginine builds conformational flexibility into the region of methylation that may be a requirement of specific binding modes. Alternatively, the prevalence of glycine could reflect the physical contortions that substrates must commit to in order to access an active site situated in the rim of the dimeric structure.

Although the PRMTs seem somewhat promiscuous, small changes in the sequences of *protein* substrates can have profound effects on methyltransferase activity. For example, a single amino acid change in the helicase eIF4A1 (a PRMT1 protein substrate) from 'RGG' to 'RSG' (to mimic the sequence found in eIF4A3, which is not normally a PRMT1 substrate) abolished methylation by PRMT1 (57). Surprisingly, when the same RGG → RSG change was made in a peptide substrate methylation was retained, suggesting that other interactions distant from the target arginine are important in influencing the substrate

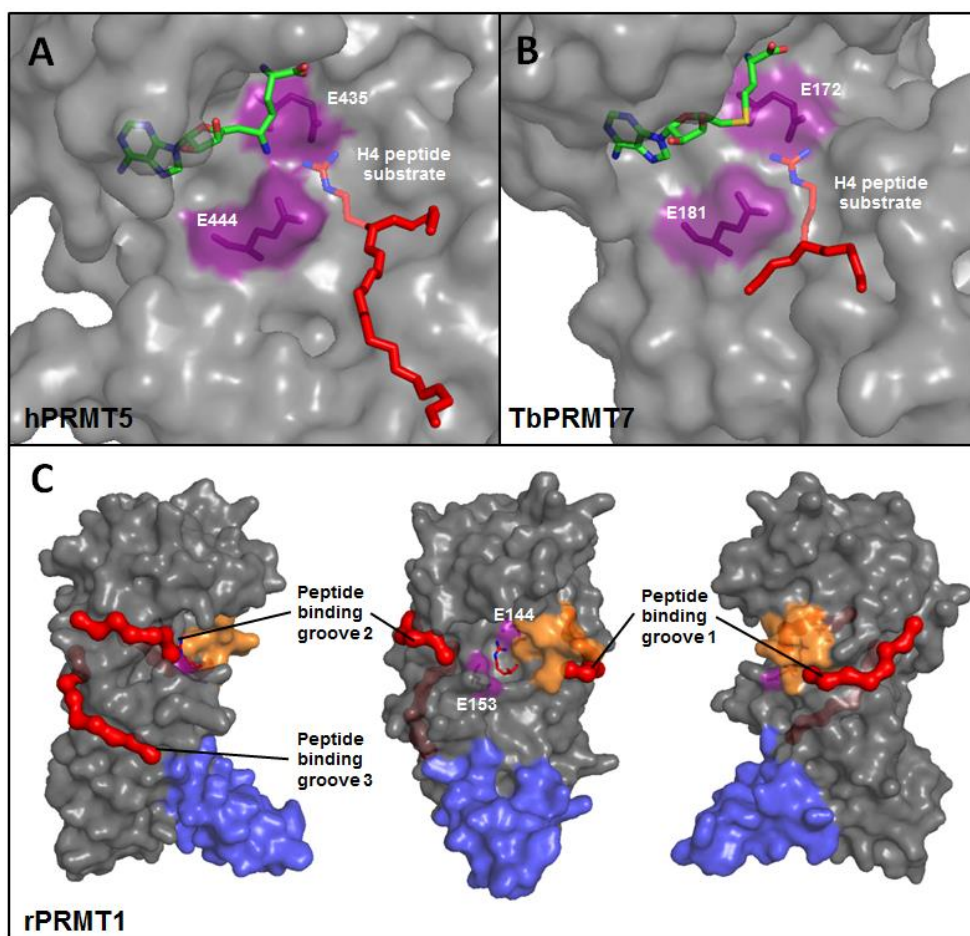


FIGURE 2-6. PRMT substrate binding modes. Surface representations of (A) hPRMT5 (4GQB, residues 331-636) and (B) TbPRMT7 (4M38, residues 82-374) binding to a histone H4 peptide fragment (red) and AdoMet analog or AdoHcy (green). In both, active site glutamates are shown in purple to provide orientation, while the backbone of the H4 peptide fragment (SGRGKRRK in (A) and SRGK in (B)) is in red with only the arginine side chain shown for clarity. In (A), the H4 peptide forms a sharp β -turn to present the arginine into the hPRMT5 active site. In (B), the H4 peptide forms a wide turn on the surface of the TbPRMT7 active site. (C) Surface representation of a rPRMT1 monomer (PDB ID: 1OR8). Gray core with blue dimerization arm and orange helix α Y. Active site glutamates are shown in purple. The active site arginine is shown in red, along with the three peptide binding grooves.

specificity (57). This idea is supported by a study showing that mutation of positively charged or polar residues distal from the arginine within peptide substrates of PRMT1 to non-charged residues led to decreased catalytic efficiency of the PRMT1 enzyme (59).

Although the field has made advances in understanding facets of substrate recognition and binding (particularly for PRMT1), the current studies also show that recognition and binding are complex and emphasize the need for a structure of a PRMT with a *protein* substrate bound, a goal that was attempted as described in chapter 3. However, even upon determination of such a structure, we may find that different classes of protein substrates bind the PRMT isoforms using a *set* of binding modes instead of a single binding site.

PRMT Mechanism

The kinetic mechanisms of the type I PRMT1 and PRMT6, as well as the type II PRMT5 have all shown a rapid equilibrium sequential random mechanism in which either one of the two substrates can bind in a random fashion (60,61). Methyl transfer seems to be the rate limiting step (62), and subsequent product release also occurs in a random fashion. However, an investigation of the PRMT2 mechanism found ordered substrate binding and product release with AdoMet binding first and AdoHcy release occurring last (63).

The determination that different methyl marks on substrates can lead to opposing biological consequences, highlights the importance of understanding the factors that may influence the distributive or processive methylation of type I and type II PRMTs. Although

all type I and type II PRMTs have the potential to be processive and synthesize a dimethylated product without releasing the monomethylated product, only PRMT1, PRMT6, and PRMT5 have been carefully examined. Interestingly, our lab has found PRMT1 activity is semi-processive, with the degree of processivity varying depending on the substrate tested (64). The type II PRMT5 enzyme works through a distributive mechanism, where the dimethylated product only appears after the monomethylated product exceeds the unmodified substrate (65). Since proper control over the processivity of these enzymes is essential for biological wellness, it is striking how little is known about what factors may PRMT enzyme processivity. A careful investigation of how regulators affect PRMT activity may lead to identification of factors that affect processivity as well.

PRMT Regulators

Protein regulators— A variety of PRMT-binding proteins have been reported to regulate methyltransferase activity by inhibiting, activating, or even changing the PRMT substrate specificity (see Table 2-1). Several proteins have been reported to inhibit the activity of PRMTs (Table 2-1). In one example, hCAF1 inhibited PRMT1 methylation of Sam68 and histone H4, but not hnRNPA1 (66). The hCAF1 protein is part of the mammalian CCR4-NOT complex which is involved in the regulation of transcription and RNA metabolism in yeast and mammalian cells. Interestingly, multiple components of the yeast CCR4-NOT complex have also been shown to associate with the PRMT1 homolog, Hmt1 (67). Since many PRMT1 substrates are RNA-binding proteins involved in various aspects of RNA processing and transport, PRMT1 regulation by hCAF1 and association

with the CCR4-NOT complex suggests these proteins are involved in crosstalk between transcription and RNA processing. The exact mechanism of regulation and substrates involved remain unknown and will prove to be a strong avenue for future investigations.

The PRMT5-MEP50 complex is a prime example of protein-induced activation since binding by the MEP50 protein is necessary for PRMT5 activity in mammalian cells (30,68). Current evidence points to a mechanism in which MEP50 binding is required for the PRMT5-MEP50 complex to simultaneously engage the protein substrate and orient the target arginine to the catalytic site (55,68). Other binding proteins can function as modulators of the PRMT5-MEP50 complex enhancing activity towards specific substrates (see Table 2-1). One well-characterized example is the SWI/SNF chromatin remodeling complex which can bind PRMT5-MEP50 and enhance methyltransferase activity toward histone substrates. Thus, the components present at a specific time in complex with PRMT5 and MEP50 function to fine-tune PRMT5 methylation activity and preferred targets depending on the precise cellular needs. While many regulatory complexes have been well described for PRMT5, the high number of PRMT-interacting proteins (69-71) may suggest that similar multi-protein regulatory mechanisms have yet to be identified for the other PRMTs.

Posttranslational modifications— Automethylation activity has been reported for several PRMTs; the functional significance of these modifications remains under investigation, but thus far seem specific to particular PRMT isoforms. PRMT6 automethylation on its N-terminal region (R29, R35, R37 of human PRMT6) contributes

Table 2-1. PRMT protein regulators

PRMT Isoform	Protein regulator	Effect of interaction
PRMT1	hCAF1	Inhibition towards certain substrates (66)
	Btg1	Stimulates activity towards selected substrates (72)
	Tis1/Btg2	Stimulates activity towards selected substrates (72)
	orphan nuclear receptor TR3 (NR4A1)	Inhibition of PRMT1 activity (73)
	PP2Ac	Inhibition of PRMT1 activity (74)
	PRMT2	Enhances PRMT1 activity (23)
	Air1	Inhibition of Hmt1 (yeast PRMT1) activity (75)
PRMT3	DAL-1/4.1B	Inhibition of PRMT3 activity (76)
PRMT4	NUMAC	Targets CARM1 to nucleosomal H3 <i>in vivo</i> (77)
PRMT5	MEP50	Required for PRMT5 activity in mammalian cells (30)
	COPR5	Changes balance of activity from H3R8 toward H4R3 <i>in vivo</i> (78)
	hSWI/SNF complex (BRG and BRM)	Enhances PRMT5 activity towards histones (31)
	RIOK1	Regulates PRMT5 substrate specificity (79)
	pICLN	Regulates PRMT5 substrate specificity (79)
	CDK4	Enhances PRMT5 activity and triggers neoplastic growth <i>in vitro</i> (80)
	Exon junction complex (RNA binding protein Y14)	Increased activity of MEP50:PRMT5 towards Sm proteins of the small nuclear ribonucleoprotein core (81)
	DAL-1/4.1B	Mediates PRMT5 methylation in a substrate-specific manner (82)
PRMT6	HMGA1	Increased MIF methylation by PRMT6 <i>in vitro</i> (83)
PRMT7	CTCFL	Enhanced PRMT7* activity (84)*

* The reported CTCFL regulation of PRMT7 needs to be re-evaluated. PRMT7 is now known to be a type III PRMT, and is therefore unable to catalyze SDMA formation. In the report by Jelinic *et al.* CTCFL was shown to increase SDMA formation *in vivo* on Histone H4R3 (84), which neither indicates, nor discounts PRMT7 activity enhancement since it did not directly measure PRMT7 activity.

to PRMT6 protein stability and regulates its anti-HIV-1 activity (85). PRMT4 automethylation occurs on its C-terminal end at R551 of the mouse sequence, which exhibits strict conservation in vertebrates. Preventing automethylation impaired both PRMT4-activated transcription and pre-mRNA splicing (86). PRMT8 automethylation occurs *in cis* at N-terminal arginines R58 and R73 of the human sequence and is independent of PRMT8 G2 myristoylation. Preventing PRMT8 automethylation increased the turnover rate and decreased K_M of AdoMet, but not of peptide substrates (36), indicating that automethylation regulates PRMT8 activity by decreasing the affinity of the enzyme for AdoMet (87). PRMT1, PRMT3, and PRMT7 automethylation has also been reported, but neither the location of the methylated arginines nor functional significance have yet been uncovered (52,88-90). While there are reports showing that PRMT4 automethylation is regulated at the level of alternative splicing (91), the significance and regulation of automethylation on other PRMT isoforms remains to be determined.

Phosphorylation has also been reported to regulate several PRMTs. A constitutively active JAK2 mutant found in leukemia phosphorylates PRMT5 at three conserved tyrosines (Tyr297, Tyr304, and Tyr307 of the human PRMT5 sequence) on the N-terminal domain, diminishing PRMT5 activity, likely by disrupting the substrate binding pocket, resulting in decreased PRMT5 activity and contributing to the myeloproliferative phenotype (55,92,93). Two distinct mechanisms for phosphor-inhibition of PRMT4 function have been reported. An initial report indicated that phosphorylation in the PRMT4 dimerization arm (Ser229 mouse/rat, Ser228 human) severely impacted dimer formation and led to reduced AdoMet binding and methyltransferase activity (94). A second report has revealed that PRMT4 phosphorylation of Ser217 (Ser216 human PRMT4) abolished AdoMet

binding and methyltransferase activity *in vitro*, while promoting cytoplasmic localization and abrogating its coactivator function *in vivo*. The side chain hydroxyl group of Ser217 forms a hydrogen bond with the backbone carbonyl of Tyr154 which is believed to close the AdoMet cavity (95), phosphorylation likely disrupts this interaction and as a result the enzyme no longer binds AdoMet. This data led Feng *et al.* to propose a model in which Ser217 phosphorylation serves as a molecular switch to control PRMT4 activity during the cell cycle (95). Interestingly, Ser217 and Tyr154 are strictly conserved among type I PRMTs, suggesting the possibility for a conserved regulatory mechanism. Reports have also indicated that PRMT1 may be phosphorylated, although they differ on the site and effect of phosphorylation. Rust *et al.* found that PRMT1 phosphorylation on Tyr291 (in a region conserved for type I PRMTs called the THW loop) alters both substrate specificity and protein-protein interactions (96). Messier *et al.* reported yeast PRMT1 (Hmt1) phosphorylation on Ser9 activates Hmt1 activity *in vivo* (97). Hmt1 Ser9 is conserved in rat and human PRMT1 (Ser21) and it will be interesting to determine whether phosphorylation at this residue is conserved and can regulate function in higher eukaryotes.

Regulation by modification or masking of substrate arginines— Posttranslational modifications adjacent to arginine methylation sites have also been shown to regulate PRMT activity by masking or blocking methylation. Histone tails are heavily modified in order to regulate transcription and are a perfect example of the interplay different PTMs can have in regulating other modifications. In one example, PRMT5 methylation of histone H3R8 leads to a decrease in transcription; however this methylation can be blocked by H3K9 acetylation (98). In turn, the H3R8me2a or H3R8me2s marks can block methylation of H3K9 (99). In another example, H3R2 methylation by PRMT6 is inhibited, but not

completely blocked by the H3K4me3 mark (100) and H3K4 methylation is also blocked by prior H3R2 methylation (101). In a striking example, acetylation of H4K5 shifts H4R3 from being a primarily PRMT1 substrate to a preferred PRMT5 substrate, shifting the balance from ADMA to SDMA and thus leading to suppressed transcription (102). The interplay between histone tails modifications thus regulates PRMTs by varying the substrate accessibility or preference, and may also regulate product specificity. Examples of this substrate masking effect are now also beginning to emerge for non-histone substrates. It was recently shown that PRMT6 methylation of the androgen receptor occurs at AKT consensus site motifs and is mutually exclusive with serine phosphorylation by AKT (103,104). Phosphorylation of the C-terminal tail of RNA Polymerase II at Ser2 or Ser5 has also been reported to block Arg1810 methylation by PRMT4, resulting in misexpression of a variety of small nuclear RNAs and small nucleolar RNAs (105). Since many PRMT non-histone substrates are also heavily modified (hnRNPk, Npl3, Sam68, PABPN1, etc.), it is not difficult to imagine that similar masking of substrate arginines will continue to emerge and be found to play a regulatory role in many PRMT-regulated signaling pathways.

Another indirect path of regulating protein arginine methylation is through the activity of protein arginine deiminase (PAD4), which removes an amino group from the guanidino side chain of arginine, converting a previous arginine substrate into a non-substrate citrulline (106,107)(for a recent in-depth review of protein arginine deiminases see Fuhrmann *et al.* (54)). Although PAD4 was initially believed to also convert MMA (but not DMA) to citrulline (107), later work by Raijmakers *et al.* showed that monomethylarginine is a poor substrate for PAD4 (108). PAD4 was the first enzyme shown

to antagonize histone methylation and it has subsequently been shown to also deiminate at least one site on p300, preventing PRMT4 methylation (109). Other examples of antagonistic effects of citrullination at methylation sites in non-histone proteins are continually emerging (110,111). It will be interesting to see how many of the PRMT substrates can become citrullinated, what regulates PAD4 activity and substrate selection, and whether this is truly an irreversibly process or one that can be reversed by a yet undiscovered aminotransferase.

Impact of oligomeric state on PRMT activity— As previously discussed, the PRMT field has widely accepted that PRMTs must form at least a dimer in order to be catalytically active (39,40,43). This concept has been supported by dimer observations in all known PRMT crystal structures (39,41-43,45-48,50), as well as by biochemical characterizations indicating loss of activity when the dimerization arm is removed or mutated (39-41,43). Most dimer molecular interactions occur between the dimerization arm of one monomer and the outer surface (αY , αZ , αA , and αB) of the AdoMet binding domain of the other monomer (Figure 2-7). Although the dimerization arm sequences for different PRMTs vary widely in length and amino acid composition, in each case hydrophobic interactions make up the majority of the dimer interface, complemented by a small network of hydrogen bonds (note that the residues on the surface of the AdoMet binding domain are highly conserved among PRMTs).

Cheng *et al.* calculated the atomic position fluctuations (APFs) of AtPRMT10 C α atoms in monomeric and dimeric states. The αY - αZ region, which both forms direct contacts with AdoMet and contributes to the conserved substrate binding groove I, and the

dimerization arm region displayed significantly reduced APFs in the dimeric form. These reduced fluctuations are a result of direct involvement in forming the dimer interface and suggest that stabilization of this region by dimerization likely improves the binding of AdoMet and substrate proteins (43). This stabilizing effect of dimerization is consistent with the report that the PRMT4 dimerization arm phosphorylation mimic S229E exhibits decreased AdoMet binding and methyltransferase activity (94). To date, the only data suggesting any PRMT may exist as a monomer was presented by Tang *et al.* in the initial characterization of PRMT3, where PRMT3 isolated from mammalian cell extracts migrated as a monomer over gel filtration, although no activity was shown for this monomeric PRMT3 (24). Herrmann *et al.* corroborated the presence of PRMT3 monomers using glycerol gradient experiments and additionally observed that PRMT6 behaved as a monomer in fluorescence correlation spectroscopy experiments (18). However, it should be noted that there is no evidence to suggest methyltransferase activity can be obtained from a PRMT monomer. FRET experiments yielding K_D of dimerization for PRMT1 and PRMT6 homodimers indicate that the strength of dimer formation varies among the PRMTs and can be impacted by the presence of AdoMet (112). Together, the data thus far indicates that dimerization is conserved throughout the PRMTs and serves to stabilize cofactor binding and orient the active site for catalysis.

In addition to dimers, several PRMTs have been detected as high molecular weight oligomers in solution both *in vivo* and *in vitro* (18,39,40,62,113). Feng *et al.* introduced the idea that changing the oligomeric state of PRMT1 affects methyltransferase activity (62). In these studies, crosslinking data showed an increase in oligomerization with increasing

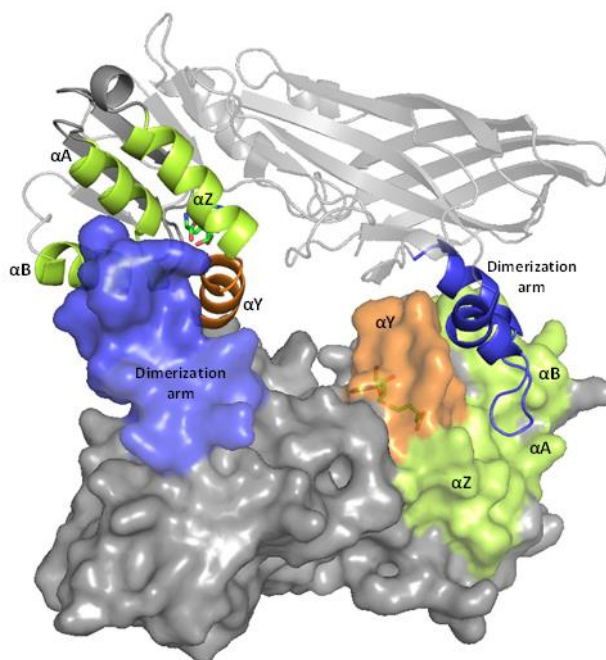


FIGURE 2-7. PRMT dimer interacting regions. rPRMT1 (IOR8) dimer interactions occur through the dimerization arm (blue, residues 188-216) of one monomer and the outer surface of the AdoMet binding domain (helices αY , αZ , αA , and αB shown in lime) of the second monomer.

protein concentration correlated to an increase in the turnover rate per PRMT1 monomer reaching a plateau around $0.5\mu\text{M}$ PRMT1 (62). Recently, the oligomeric state of PRMT1 was also shown to change as a function of the redox state (114). However, while this work showed that reduced PRMT1 is more active and forms a lower molecular weight oligomer than oxidized PRMT1, a clear explanation for this effect could not be discerned. Future work should address the factors driving the formation of PRMT1 high molecular weight aggregates and exactly how these affect methyltransferase activity.

Redox control of PRMT activity— A novel redox-based PRMT regulatory mechanism was also recently discovered and published as described in chapter 6. We were

able to show that rPRMT1, hPRMT3, hPRMT6, and TbPRMT7 all display a reversible increase in methyltransferase activity in the presence of reductant (PRMT8 is also believed to be under redox control, but was not tested) (114). Further biochemical characterization revealed that two PRMT1 cysteine residues (C101 and C208 of rat PRMT1) can become reversibly oxidized to sulfenic acid. Preventing oxidation at these two sites abolished the typical increase in methyltransferase activity in the presence of reductant, indicating that these two cysteine residues allow rPRMT1 activity to be regulated by the redox environment. Sequence alignment shows that one of these two cysteines (Cys208 in rPRMT1) is conserved in all but one (TbPRMT7) of the PRMTs shown to be redox regulated. Only PRMT8 shows conservation of both cysteine residues, while the type III TbPRMT7 contains only three cysteines, none of which are conserved in the other PRMTs. These variations in cysteine conservation imply that while redox regulation may be a conserved trait for several PRMT family members, the mechanism of redox control likely varies among them.

The biological implications of redox regulation remain to be determined. However, it is impossible not to speculate on the potential involvement of PRMT1 in the cellular oxidative stress response. In one example, Lafleur *et al.* suggests that PRMT1 may be important for the cellular hypoxic response (115). PRMT1 acts as a repressor of both HIF-1 and HIF-2 which are essential mediators for the adaptive transcriptional response to low oxygen conditions (115). It will be interesting to determine if during hypoxia and HIF activation, PRMT1 activity is decreased by increased oxidative stress resulting in a decrease on PRMT1-dependent HIF repression to maintain elevated HIF-1 α levels. Although Lafleur *et al.* did not observe this phenomenon under their hypoxic conditions,

it was suggested that this feedback regulation may only be observed under longer periods of hypoxic exposure (115). The impact of this newly discovered redox regulatory mechanism on several PRMT family members will surely be the focus of much investigation in years to come.

Biological Importance of PRMTs

The continued development of techniques for detecting PRMT substrates has allowed the identification of thousands of *in vivo* arginine methylation sites in proteins involved in a plethora of biological pathways (2,5,69,89,116-118). However, in order to truly understand the impact of the PRMTs, the effects of methylation on the substrate protein structure and on its molecular interactions must be related to the corresponding cellular function of the substrate protein. This level of understanding often requires the creative application of a combination of *in vivo* and *in vitro* techniques. A brief representation of the many ways PRMTs are involved in critical biological pathways, with particular focus on PRMT1, is presented below.

Transcription—The PRMTs have a well-established involvement in the regulation of gene transcription (119). PRMTs have been shown to form numerous interactions with transcription factors and transcriptional coactivators in addition to their ability to directly methylate histones and RNA polymerase II (28). PRMT1 and PRMT4/CARM1 can cooperatively enhance gene expression and are generally considered transcriptional activators (120), while PRMT5-dependent SDMA formation is generally associated with

transcriptional repression (65,121). Additionally, methyltransferase activity in yeast has also been found to regulate transcription elongation and termination (122)

Cell signaling— Posttranslational modifications drive cellular signaling by altering protein function through the promotion or prevention of specific protein-protein interactions. PRMT1 binds the type I interferon α/β (INF α/β) receptor and PRMT1 knockdown interfere with the biological function of this receptor (123). Knockdown of PRMT1 expression similarly was shown to attenuate the signaling cascade from the insulin receptor (IR) (124), indicating that PRMT1 methylation is a positive regulator of IR function and subsequent glucose uptake.

mRNA transport and splicing— Many of the known PRMT substrates are RNA-binding proteins (RBPs) that contain GAR (glycine-arginine rich) or PGM (proline-glycine-methionine) motifs, which are some of the preferred sites of PRMT1 and CARM1 methylation, respectively (28,125). In many RBP binding sites, arginine residues are key amino acids for RNA-protein interactions (126). Arginine methylation has been found to both negatively (methylation can block hydrogen bonding) and positively (increased arginine hydrophobicity when methylated may facilitate stacking with RNA bases) regulate protein-RNA interactions (127). In yeast, the PRMT1 homolog Hmt1 methylates mRNA export factor Npl3 (128), an activity which is required for the mRNA shuttling function of Npl3 (129). Hmt1 also methylates Snp1, a U1 small nuclear RNP (snRNP)–specific protein (130). The deletion of *HMT1* was found to deregulate the recruitment of U1 snRNP and its associated components to intron-containing genes (130), therefore implicating arginine methylation in the promoting target specificity in splicing.

DNA damage repair— The loss of PRMT1 has been linked to genome instability (131). PRMT1 is known to methylate and regulate the exonuclease activity of MRE11, a key enzyme in DNA double-strand break repair and overall genome stability (132). Importantly, arginine methylation seems to be required for MRE11 localization to the site of DNA damage (133). The p53-binding protein 1 (53BP1), which is important for the early events of detection, signaling, and repair of DNA double-strand breaks is also methylated by PRMT1 (134), and methyltransferase activity was also found to be required for 53BP1 localization to DNA damage sites (135).

Protein Arginine Methylation and Diseases

Cardiovascular disease— All type I PRMTs have the ability to make ADMA, but the predominant arginine methyltransferase, PRMT1, is responsible for most of the ADMA formation in cells (16). Altered levels of free ADMA, which is generated by the proteolysis of asymmetrically dimethylated proteins, have been found in a variety of disease states (136). Recently, plasma ADMA levels have been used as a biomarker for prognosis after a cardiac event (137,138). ADMA is a competitive inhibitor of nitric oxide synthase (NOS) (139), which is responsible for the production of nitric oxide, a potent vasodilator. Therefore, the inhibition of NOS by ADMA has major consequences on the cardiovascular system (139,140). Elevated expression of PRMT1, the primary generator of ADMA in cells, has been found in coronary heart disease (141), implicating the dysregulation of PRMT1 activity with cardiovascular disease (142) as well as other pathophysiological conditions such as kidney failure (143,144) and chronic pulmonary disease (145,146).

Cancer— The role of PRMTs in cancer has been extensively reviewed recently (147). Overexpression or aberrant splicing of PRMT1 has been reported in leukemia (148,149), as well as breast (150-153), prostate (154,155), colon (156,157), and lung cancer (158). In Mixed Lineage Leukemia (MLL), PRMT1 was shown to be an essential component of an MLL oncogenic transcriptional complex which unitizes both histone acetylation and arginine methylation (H4R3) activities to enhance the expression of critical MLL targets (148). The essential role of PRMT1 in this oncogenic complex has made it as a prominent therapeutic target (159).

Viral pathogenesis— Arginine methylation has been shown to regulate the viral replication of both the human immunodeficiency virus (HIV-1) and the hepatitis delta virus (HDV). The HIV-1 transactivator protein (Tat) is methylated by PRMT6, which negatively regulates its transactivation activity (160). Correspondingly, knocking down PRMT6 increased HIV-1 production and viral infectiousness (160), indicating that arginine methylation offers some protection against HIV infection (33). In contrast, PRMT1 methylation of the small hepatitis delta antigen (sHDAg) appears to enhance its nuclear transport and therefore facilitate viral replication (161), suggesting that blocking methylation may offer protection against some viruses (162).

CONCLUSIONS

Protein arginine methylation is critical for organismal well-being. The vast array of PRMT substrates implicates this posttranslational modification in important cellular pathways. Not surprisingly, the dysregulation of PRMT activity has been implicated in a number of high-profile human diseases like cardiovascular disease, cancer, and viral

pathogenesis. Yet, despite the important role of the PRMTs, how these proteins are regulated remains mostly unclear. We have aimed to understand how PRMT1, the predominant PRMT in cells, interacts with its substrates and is regulated. This dissertation provides increased understanding of both existing and novel PRMT1 regulatory mechanisms, which will contribute to the PRMT research field, and provide a foundation for an advanced understanding of PRMT roles *in vivo*.

REFERENCES

1. Cantoni, G. L. (1975) Biological methylation: selected aspects. *Annu. Rev. Biochem.* **44**, 435-451
2. Clarke, S. G., and Tamanoi, F. (2006) *Protein methyltransferases*, Academic Press, Amsterdam ; London
3. Salvatore, F., and Accademia nazionale dei Lincei. (1977) *The Biochemistry of adenosylmethionine : [proceedings of an international symposium on the biochemistry of adenosylmethionine, sponsored by the Accademia nazionale dei Lincei, held in Rome, Italy May 21-26, 1974]*, Columbia University Press, New York
4. Chen, D. (1999) Regulation of transcription by a protein methyltransferase. *Science* **284**, 2174-2177
5. Boisvert, F. M., Cote, J., Boulanger, M. C., and Richard, S. (2003) A proteomic analysis of arginine-methylated protein complexes. *Mol. Cell. Proteomics* **2**, 1319-1330
6. Kuhn, P., Chumanov, R., Wang, Y., Ge, Y., Burgess, R. R., and Xu, W. (2011) Automethylation of CARM1 allows coupling of transcription and mRNA splicing. *Nucleic Acids Res.* **39**, 2717-2726
7. Blackwell, E., and Ceman, S. (2012) Arginine methylation of RNA-binding proteins regulates cell function and differentiation. *Mol. Reprod. Dev.* **79**, 163-175
8. Lee, Y. H., and Stallcup, M. R. (2011) Roles of protein arginine methylation in DNA damage signaling pathways is CARM1 a life-or-death decision point? *Cell Cycle* **10**, 1343-1344

9. Wysocka, J., Allis, C. D., and Coonrod, S. (2006) Histone arginine methylation and its dynamic regulation. *Front. Biosci.* **11**, 344-355
10. Kirmizis, A., Santos-Rosa, H., Penkett, C. J., Singer, M. A., Green, R. D., and Kouzarides, T. (2009) Distinct transcriptional outputs associated with mono- and dimethylated histone H3 arginine 2. *Nat. Struct. Mol. Biol.* **16**, 449-451
11. Katz, J. E., Dlakic, M., and Clarke, S. (2003) Automated identification of putative methyltransferases from genomic open reading frames. *Mol. Cell. Proteomics* **2**, 525-540
12. Goulet, I., Gauvin, G., Boisvenue, S., and Cote, J. (2007) Alternative splicing yields protein arginine methyltransferase 1 isoforms with distinct activity, substrate specificity, and subcellular localization. *The Journal of Biological Chemistry* **282**, 33009-33021
13. Swiercz, R., Person, M. D., and Bedford, M. T. (2005) Ribosomal protein S2 is a substrate for mammalian PRMT3 (protein arginine methyltransferase 3). *Biochem. J.* **386**, 85-91
14. Lee, J., Sayegh, J., Daniel, J., Clarke, S., and Bedford, M. T. (2005) PRMT8, a new membrane-bound tissue-specific member of the protein arginine methyltransferase family. *J. Biol. Chem.* **280**, 32890-32896
15. Sayegh, J., Webb, K., Cheng, D., Bedford, M. T., and Clarke, S. G. (2007) Regulation of protein arginine methyltransferase 8 (PRMT8) activity by its N-terminal domain. *J. Biol. Chem.* **282**, 36444-36453
16. Tang, J., Frankel, A., Cook, R. J., Kim, S., Paik, W. K., Williams, K. R., Clarke, S., and Herschman, H. R. (2000) PRMT1 is the predominant type I protein arginine methyltransferase in mammalian cells. *J. Biol. Chem.* **275**, 7723-7730
17. Herrmann, F., and Fackelmayer, F. O. (2009) Nucleo-cytoplasmic shuttling of protein arginine methyltransferase 1 (PRMT1) requires enzymatic activity. *Genes Cells* **14**, 309-317
18. Herrmann, F., Pably, P., Eckerich, C., Bedford, M. T., and Fackelmayer, F. O. (2009) Human protein arginine methyltransferases in vivo--distinct properties of eight canonical members of the PRMT family. *J. Cell Sci.* **122**, 667-677
19. Scott, H. S., Antonarakis, S. E., Lalioti, M. D., Rossier, C., Silver, P. A., and Henry, M. F. (1998) Identification and characterization of two putative human arginine methyltransferases (HRMT1L1 and HRMT1L2). *Genomics* **48**, 330-340

20. Alexandropoulos, K., Cheng, G., and Baltimore, D. (1995) Proline-rich sequences that bind to Src homology 3 domains with individual specificities. *Proceedings of the National Academy of Sciences* **92**, 3110-3114
21. Qi, C. (2002) Identification of protein arginine methyltransferase 2 as a coactivator for estrogen receptor [alpha]. *J. Biol. Chem.* **277**, 28624-28630
22. Meyer, R., Wolf, S. S., and Obendorf, M. (2007) PRMT2, a member of the protein arginine methyltransferase family, is a coactivator of the androgen receptor. *J. Steroid Biochem. Mol. Biol.* **107**, 1-14
23. Pak, M. L., Lakowski, T. M., Thomas, D., Vhuiyan, M. I., Husecken, K., and Frankel, A. (2011) A protein arginine N-methyltransferase 1 (PRMT1) and 2 heteromeric interaction increases PRMT1 enzymatic activity. *Biochemistry* **50**, 8226-8240
24. Tang, J., Gary, J. D., Clarke, S., and Herschman, H. R. (1998) PRMT 3, a type I protein arginine N-methyltransferase that differs from PRMT1 in its oligomerization, subcellular localization, substrate specificity, and regulation. *J. Biol. Chem.* **273**, 16935-16945
25. Frankel, A., and Clarke, S. (2000) PRMT3 is a distinct member of the protein arginine N-methyltransferase family. Conferral of substrate specificity by a zinc-finger domain. *The Journal of Biological Chemistry* **275**, 32974-32982
26. Swiercz, R., Cheng, D., Kim, D., and Bedford, M. T. (2007) Ribosomal protein rpS2 is hypomethylated in PRMT3-deficient mice. *J. Biol. Chem.* **282**, 16917-16923
27. Lee, Y. H., Koh, S. S., Zhang, X., Cheng, X., and Stallcup, M. R. (2002) Synergy among nuclear receptor coactivators: selective requirement for protein methyltransferase and acetyltransferase activities. *Mol. Cell. Biol.* **22**, 3621-3632
28. Cheng, D., Cote, J., Shaaban, S., and Bedford, M. T. (2007) The arginine methyltransferase CARM1 regulates the coupling of transcription and mRNA processing. *Mol. Cell* **25**, 71-83
29. Branscombe, T. L. (2001) Prmt5 (janus kinase-binding protein 1) catalyzes the formation of symmetric dimethylarginine residues in proteins. *The Journal of Biological Chemistry* **276**, 32971-32976
30. Friesen, W. J., Wyce, A., Paushkin, S., Abel, L., Rappsilber, J., Mann, M., and Dreyfuss, G. (2002) A novel WD repeat protein component of the methylosome binds Sm proteins. *J. Biol. Chem.* **277**, 8243-8247

31. Pal, S., Vishwanath, S. N., Erdjument-Bromage, H., Tempst, P., and Sif, S. (2004) Human SWI/SNF-associated PRMT5 methylates histone H3 arginine 8 and negatively regulates expression of ST7 and NM23 tumor suppressor genes. *Mol. Cell. Biol.* **24**, 9630-9645
32. Frankel, A., Yadav, N., Lee, J., Branscombe, T. L., Clarke, S., and Bedford, M. T. (2002) The novel human protein arginine N-methyltransferase PRMT6 is a nuclear enzyme displaying unique substrate specificity. *The Journal of Biological Chemistry* **277**, 3537-3543
33. Singhroy, D. N., Mesplede, T., Sabbah, A., Quashie, P. K., Falgoutyret, J. P., and Wainberg, M. A. (2013) Automethylation of protein arginine methyltransferase 6 (PRMT6) regulates its stability and its anti-HIV-1 activity. *Retrovirology* **10**, 73
34. Zurita-Lopez, C. I., Sandberg, T., Kelly, R., and Clarke, S. G. (2012) Human protein arginine methyltransferase 7 (PRMT7) is a type III enzyme forming omega-NG-monomethylated arginine residues. *J. Biol. Chem.* **287**, 7859-7870
35. Miranda, T. B., Miranda, M., Frankel, A., and Clarke, S. (2004) PRMT7 is a member of the protein arginine methyltransferase family with a distinct substrate specificity. *J. Biol. Chem.* **279**, 22902-22907
36. Dillon, M. B., Rust, H. L., Thompson, P. R., and Mowen, K. A. (2013) Automethylation of protein arginine methyltransferase 8 (PRMT8) regulates activity by impeding S-adenosylmethionine sensitivity. *The Journal of Biological Chemistry* **288**, 27872-27880
37. Yang, Y., Hadjikyriacou, A., Xia, Z., Gayatri, S., Kim, D., Zurita-Lopez, C., Kelly, R., Guo, A., Li, W., Clarke, S. G., and Bedford, M. T. (2015) PRMT9 is a type II methyltransferase that methylates the splicing factor SAP145. *Nat Commun* **6**, 6428
38. Hadjikyriacou, A., Yang, Y., Espejo, A., Bedford, M. T., and Clarke, S. G. (2015) Unique Features of Human Protein Arginine Methyltransferase 9 (PRMT9) and Its Substrate RNA Splicing Factor SF3B2. *The Journal of Biological Chemistry* **290**, 16723-16743
39. Zhang, X., and Cheng, X. (2003) Structure of the predominant protein arginine methyltransferase PRMT1 and analysis of its binding to substrate peptides. *Structure* **11**, 509-520
40. Weiss, V. H., McBride, A. E., Soriano, M. A., Filman, D. J., Silver, P. A., and Hogle, J. M. (2000) The structure and oligomerization of the yeast arginine methyltransferase, Hmt1. *Nat. Struct. Biol.* **7**, 1165-1171

41. Zhang, X., Zhou, L., and Cheng, X. (2000) Crystal structure of the conserved core of protein arginine methyltransferase PRMT3. *EMBO J.* **19**, 3509-3519
42. Troffer-Charlier, N., Cura, V., Hassenboehler, P., Moras, D., and Cavarelli, J. (2007) Functional insights from structures of coactivator-associated arginine methyltransferase 1 domains. *EMBO J.* **26**, 4391-4401
43. Cheng, Y., Frazier, M., Lu, F., Cao, X., and Redinbo, M. R. (2011) Crystal structure of the plant epigenetic protein arginine methyltransferase 10. *J. Mol. Biol.* **414**, 106-122
44. Sun, L., Wang, M., Lv, Z., Yang, N., Liu, Y., Bao, S., Gong, W., and Xu, R. M. (2011) Structural insights into protein arginine symmetric dimethylation by PRMT5. *Proc. Natl. Acad. Sci. U. S. A.* **108**, 20538-20543
45. Ho, M. C., Wilczek, C., Bonanno, J. B., Xing, L., Seznec, J., Matsui, T., Carter, L. G., Onikubo, T., Kumar, P. R., Chan, M. K., Brenowitz, M., Cheng, R. H., Reimer, U., Almo, S. C., and Shechter, D. (2013) Structure of the arginine methyltransferase PRMT5-MEP50 reveals a mechanism for substrate specificity. *PLoS One* **8**, e57008
46. Hasegawa, M., Toma-Fukai, S., Kim, J. D., Fukamizu, A., and Shimizu, T. (2014) Protein arginine methyltransferase 7 has a novel homodimer-like structure formed by tandem repeats. *FEBS Lett.* **588**, 1942-1948
47. Wang, C., Zhu, Y., Chen, J., Li, X., Peng, J., Chen, J., Zou, Y., Zhang, Z., Jin, H., Yang, P., Wu, J., Niu, L., Gong, Q., Teng, M., and Shi, Y. (2014) Crystal structure of arginine methyltransferase 6 from *Trypanosoma brucei*. *PLoS One* **9**, e87267
48. Cura, V., Troffer-Charlier, N., Wurtz, J. M., Bonnefond, L., and Cavarelli, J. (2014) Structural insight into arginine methylation by the mouse protein arginine methyltransferase 7: a zinc finger freezes the mimic of the dimeric state into a single active site. *Acta Crystallogr. D Biol. Crystallogr.* **70**, 2401-2412
49. Bonnefond, L., Stojko, J., Mailliot, J., Troffer-Charlier, N., Cura, V., Wurtz, J. M., Cianferani, S., and Cavarelli, J. (2015) Functional insights from high resolution structures of mouse protein arginine methyltransferase 6. *J. Struct. Biol.* **191**, 175-183
50. Wang, C., Zhu, Y., Caceres, T. B., Liu, L., Peng, J., Wang, J., Chen, J., Chen, X., Zhang, Z., Zuo, X., Gong, Q., Teng, M., Hevel, J. M., Wu, J., and Shi, Y. (2014) Structural determinants for the strict monomethylation activity by *trypanosoma brucei* protein arginine methyltransferase 7. *Structure* **22**, 756-768
51. Schubert, H. L., Blumenthal, R. M., and Cheng, X. (2003) Many paths to methyltransfer: a chronicle of convergence. *Trends Biochem. Sci.* **28**, 329-335

52. Gui, S., Wooderchak, W. L., Daly, M. P., Porter, P. J., Johnson, S. J., and Hevel, J. M. (2011) Investigation of the molecular origins of protein-arginine methyltransferase I (PRMT1) product specificity reveals a role for two conserved methionine residues. *The Journal of Biological Chemistry* **286**, 29118-29126
53. Gui, S., Gathiaka, S., Li, J., Qu, J., Acevedo, O., and Hevel, J. M. (2014) A Remodeled Protein Arginine Methyltransferase 1 (PRMT1) Generates Symmetric Dimethylarginine. *The Journal of Biological Chemistry*
54. Fuhrmann, J., Clancy, K. W., and Thompson, P. R. (2015) Chemical biology of protein arginine modifications in epigenetic regulation. *Chem. Rev.* **115**, 5413-5461
55. Antonysamy, S., Bonday, Z., Campbell, R. M., Doyle, B., Druzina, Z., Gheyi, T., Han, B., Jungheim, L. N., Qian, Y., Rauch, C., Russell, M., Sauder, J. M., Wasserman, S. R., Weichert, K., Willard, F. S., Zhang, A., and Emtage, S. (2012) Crystal structure of the human PRMT5:MEP50 complex. *Proceedings of the National Academy of Sciences* **109**, 17960-17965
56. Lee, D. Y., Ianculescu, I., Purcell, D., Zhang, X., Cheng, X., and Stallcup, M. R. (2007) Surface-scanning mutational analysis of protein arginine methyltransferase 1: roles of specific amino acids in methyltransferase substrate specificity, oligomerization, and coactivator function. *Mol. Endocrinol.* **21**, 1381-1393
57. Wooderchak, W. L., Zang, T., Zhou, Z. S., Acuna, M., Tahara, S. M., and Hevel, J. M. (2008) Substrate profiling of PRMT1 reveals amino acid sequences that extend beyond the "RGG" paradigm. *Biochemistry* **47**, 9456-9466
58. Bicker, K. L., Obiany, O., Rust, H. L., and Thompson, P. R. (2011) A combinatorial approach to characterize the substrate specificity of protein arginine methyltransferase 1. *Mol. Biosyst.* **7**, 48-51
59. Osborne, T. C., Obiany, O., Zhang, X., Cheng, X., and Thompson, P. R. (2007) Protein arginine methyltransferase 1: positively charged residues in substrate peptides distal to the site of methylation are important for substrate binding and catalysis. *Biochemistry* **46**, 13370-13381
60. Obiany, O., and Thompson, P. R. (2012) Kinetic mechanism of protein arginine methyltransferase 6 (PRMT6). *J. Biol. Chem.* **287**, 6062-6071
61. Obiany, O., Causey, C. P., Jones, J. E., and Thompson, P. R. (2011) Activity-based protein profiling of protein arginine methyltransferase 1. *ACS Chem. Biol.* **6**, 1127-1135
62. Feng, Y., Xie, N., Jin, M., Stahley, M. R., Stivers, J. T., and Zheng, Y. G. (2011) A transient kinetic analysis of PRMT1 catalysis. *Biochemistry* **50**, 7033-7044

63. Lakowski, T. M., and Frankel, A. (2009) Kinetic analysis of human protein arginine N-methyltransferase 2: formation of monomethyl- and asymmetric dimethyl-arginine residues on histone H4. *Biochem. J.* **421**, 253-261
64. Gui, S., Wooderchak-Donahue, W. L., Zang, T., Chen, D., Daly, M. P., Zhou, Z. S., and Hevel, J. M. (2013) Substrate-induced control of product formation by protein arginine methyltransferase 1. *Biochemistry* **52**, 199-209
65. Wilczek, C., Chitta, R., Woo, E., Shabanowitz, J., Chait, B. T., Hunt, D. F., and Shechter, D. (2011) Protein arginine methyltransferase Prmt5-Mep50 methylates histones H2A and H4 and the histone chaperone nucleoplasmin in *Xenopus laevis* eggs. *J. Biol. Chem.* **286**, 42221-42231
66. Robin-Lespinasse, Y., Sentis, S., Kolytcheff, C., Rostan, M. C., Corbo, L., and Le Romancer, M. (2007) hCAF1, a new regulator of PRMT1-dependent arginine methylation. *J. Cell Sci.* **120**, 638-647
67. Kerr, S. C., Azzouz, N., Fuchs, S. M., Collart, M. A., Strahl, B. D., Corbett, A. H., and Laribee, R. N. (2011) The Ccr4-Not complex interacts with the mRNA export machinery. *PLoS One* **6**, e18302
68. Burgos, E. S., Wilczek, C., Onikubo, T., Bonanno, J. B., Jansong, J., Reimer, U., and Shechter, D. (2015) Histone H2A and H4 N-terminal tails are positioned by the MEP50 WD repeat protein for efficient methylation by the PRMT5 arginine methyltransferase. *The Journal of Biological Chemistry* **290**, 9674-9689
69. Guo, A., Gu, H., Zhou, J., Mulhern, D., Wang, Y., Lee, K. A., Yang, V., Aguiar, M., Kornhauser, J., Jia, X., Ren, J., Beausoleil, S. A., Silva, J. C., Vemulapalli, V., Bedford, M. T., and Comb, M. J. (2014) Immunoaffinity enrichment and mass spectrometry analysis of protein methylation. *Mol. Cell. Proteomics* **13**, 372-387
70. Weimann, M., Grossmann, A., Woodsmith, J., Ozkan, Z., Birth, P., Meierhofer, D., Benlasfer, N., Valovka, T., Timmermann, B., Wanker, E. E., Sauer, S., and Stelzl, U. (2013) A Y2H-seq approach defines the human protein methyltransferase interactome. *Nat. Methods* **10**, 339-342
71. Baldwin, R. M., Bejide, M., Trinkle-Mulcahy, L., and Cote, J. (2015) Identification of the PRMT1v1 and PRMT1v2 specific interactomes by quantitative mass spectrometry in breast cancer cells. *Proteomics* **15**, 2187-2197
72. Lin, W. J., Gary, J. D., Yang, M. C., Clarke, S., and Herschman, H. R. (1996) The mammalian immediate-early TIS21 protein and the leukemia-associated BTG1 protein interact with a protein-arginine N-methyltransferase. *J. Biol. Chem.* **271**, 15034-15044

73. Lei, N. Z. (2009) A feedback regulatory loop between methyltransferase PRMT1 and orphan receptor TR3. *Nucleic Acids Res.* **37**, 832-848
74. Duong, F. H., Christen, V., Berke, J. M., Penna, S. H., Moradpour, D., and Heim, M. H. (2005) Upregulation of protein phosphatase 2Ac by hepatitis C virus modulates NS3 helicase activity through inhibition of protein arginine methyltransferase 1. *J. Virol.* **79**, 15342-15350
75. Inoue, K., Mizuno, T., Wada, K., and Hagiwara, M. (2000) Novel RING finger proteins, Air1p and Air2p, interact with Hmt1p and inhibit the arginine methylation of Npl3p. *The Journal of Biological Chemistry* **275**, 32793-32799
76. Singh, V., Miranda, T. B., Jiang, W., Frankel, A., Roemer, M. E., Robb, V. A., Gutmann, D. H., Herschman, H. R., Clarke, S., and Newsham, I. F. (2004) DAL-1/4.1B tumor suppressor interacts with protein arginine N-methyltransferase 3 (PRMT3) and inhibits its ability to methylate substrates in vitro and in vivo. *Oncogene* **23**, 7761-7771
77. Xu, W., Cho, H., Kadam, S., Banayo, E. M., Anderson, S., Yates, J. R., 3rd, Emerson, B. M., and Evans, R. M. (2004) A methylation-mediator complex in hormone signaling. *Genes Dev.* **18**, 144-156
78. Lacroix, M., El Messaoudi, S., Rodier, G., Le Cam, A., Sardet, C., and Fabbrizio, E. (2008) The histone-binding protein COPR5 is required for nuclear functions of the protein arginine methyltransferase PRMT5. *EMBO Rep* **9**, 452-458
79. Guderian, G., Peter, C., Wiesner, J., Sickmann, A., Schulze-Osthoff, K., Fischer, U., and Grimmler, M. (2011) RioK1, a new interactor of protein arginine methyltransferase 5 (PRMT5), competes with pICln for binding and modulates PRMT5 complex composition and substrate specificity. *The Journal of Biological Chemistry* **286**, 1976-1986
80. Aggarwal, P. (2010) Nuclear cyclin D1/CDK4 kinase regulates CUL4 expression and triggers neoplastic growth via activation of the PRMT5 methyltransferase. *Cancer Cell* **18**, 329-340
81. Chuang, T. W., Peng, P. J., and Tarn, W. Y. (2011) The exon junction complex component Y14 modulates the activity of the methylosome in biogenesis of spliceosomal small nuclear ribonucleoproteins. *The Journal of Biological Chemistry* **286**, 8722-8728
82. Jiang, W., Roemer, M. E., and Newsham, I. F. (2005) The tumor suppressor DAL-1/4.1B modulates protein arginine N-methyltransferase 5 activity in a substrate-specific manner. *Biochem. Biophys. Res. Commun.* **329**, 522-530

83. Lo Sardo, A., Altamura, S., Pegoraro, S., Maurizio, E., Sgarra, R., and Manfioletti, G. (2013) Identification and characterization of new molecular partners for the protein arginine methyltransferase 6 (PRMT6). *PLoS One* **8**, e53750
84. Jelinic, P., Stehle, J. C., and Shaw, P. (2006) The testis-specific factor CTCFL cooperates with the protein methyltransferase PRMT7 in H19 imprinting control region methylation. *PLoS Biol.* **4**, e355
85. Frankel, A. (2002) The novel human protein arginine N-methyltransferase PRMT6 is a nuclear enzyme displaying unique substrate specificity. *J. Biol. Chem.* **277**, 3537-3543
86. Kuhn, P. (2011) Automethylation of CARM1 allows coupling of transcription and mRNA splicing. *Nucleic Acids Res.* **39**, 2717-2726
87. Sayegh, J., Webb, K., Cheng, D., Bedford, M. T., and Clarke, S. G. (2007) Regulation of protein arginine methyltransferase 8 (PRMT8) activity by its N-terminal domain. *The Journal of biological chemistry* **282**, 36444-36453
88. Lakowski, T. M., t Hart, P., Ahern, C. A., Martin, N. I., and Frankel, A. (2010) Neta-substituted arginyl peptide inhibitors of protein arginine N-methyltransferases. *ACS Chem. Biol.* **5**, 1053-1063
89. Guo, H., Wang, R., Zheng, W., Chen, Y., Blum, G., Deng, H., and Luo, M. (2014) Profiling substrates of protein arginine N-methyltransferase 3 with S-adenosyl-L-methionine analogues. *ACS Chem. Biol.* **9**, 476-484
90. Feng, Y., Maity, R., Whitelegge, J. P., Hadjikyriacou, A., Li, Z., Zurita-Lopez, C., Al-Hadid, Q., Clark, A. T., Bedford, M. T., Masson, J. Y., and Clarke, S. G. (2013) Mammalian protein arginine methyltransferase 7 (PRMT7) specifically targets RXR sites in lysine- and arginine-rich regions. *The Journal of Biological Chemistry* **288**, 37010-37025
91. Wang, L., Charoensuksai, P., Watson, N. J., Wang, X., Zhao, Z., Coriano, C. G., Kerr, L. R., and Xu, W. (2013) CARM1 automethylation is controlled at the level of alternative splicing. *Nucleic Acids Res.* **41**, 6870-6880
92. Liu, F. (2011) JAK2V617F-mediated phosphorylation of PRMT5 downregulates its methyltransferase activity and promotes myeloproliferation. *Cancer cell* **19**, 283-294
93. Stopa, N., Krebs, J. E., and Shechter, D. (2015) The PRMT5 arginine methyltransferase: many roles in development, cancer and beyond. *Cell. Mol. Life Sci.* **72**, 2041-2059

94. Higashimoto, K., Kuhn, P., Desai, D., Cheng, X., and Xu, W. (2007) Phosphorylation-mediated inactivation of coactivator-associated arginine methyltransferase 1. *Proceedings of the National Academy of Sciences* **104**, 12318-12323
95. Feng, Q., He, B., Jung, S. Y., Song, Y., Qin, J., Tsai, S. Y., Tsai, M. J., and O'Malley, B. W. (2009) Biochemical control of CARM1 enzymatic activity by phosphorylation. *The Journal of Biological Chemistry* **284**, 36167-36174
96. Rust, H. L., Subramanian, V., West, G. M., Young, D. D., Schultz, P. G., and Thompson, P. R. (2014) Using Unnatural Amino Acid Mutagenesis To Probe the Regulation of PRMT1. *ACS Chem. Biol.*
97. Messier, V., Zenklusen, D., and Michnick, S. W. (2013) A nutrient-responsive pathway that determines M phase timing through control of B-cyclin mRNA stability. *Cell* **153**, 1080-1093
98. Pal, S., Vishwanath, S. N., Erdjument-Bromage, H., Tempst, P., and Sif, S. (2004) Human SWI/SNF-associated PRMT5 methylates histone H3 arginine 8 and negatively regulates expression of ST7 and NM23 tumor suppressor genes. *Molecular and cellular biology* **24**, 9630-9645
99. Rathert, P., Dhayalan, A., Murakami, M., Zhang, X., Tamas, R., Jurkowska, R., Komatsu, Y., Shinkai, Y., Cheng, X., and Jeltsch, A. (2008) Protein lysine methyltransferase G9a acts on non-histone targets. *Nat. Chem. Biol.* **4**, 344-346
100. Guccione, E. (2007) Methylation of histone H3R2 by PRMT6 and H3K4 by an MLL complex are mutually exclusive. *Nature* **449**, 933-937
101. Hyllus, D. (2007) PRMT6-mediated methylation of R2 in histone H3 antagonizes H3 K4 trimethylation. *Genes Dev.* **21**, 3369-3380
102. Feng, Y., Wang, J., Asher, S., Hoang, L., Guardiani, C., Ivanov, I., and Zheng, Y. G. (2011) Histone H4 acetylation differentially modulates arginine methylation by an in Cis mechanism. *The Journal of Biological Chemistry* **286**, 20323-20334
103. Scaramuzzino, C., Casci, I., Parodi, S., Lievens, P. M., Polanco, M. J., Milioto, C., Chivet, M., Monaghan, J., Mishra, A., Badders, N., Aggarwal, T., Grunseich, C., Sambataro, F., Basso, M., Fackelmayer, F. O., Taylor, J. P., Pandey, U. B., and Pennuto, M. (2015) Protein arginine methyltransferase 6 enhances polyglutamine-expanded androgen receptor function and toxicity in spinal and bulbar muscular atrophy. *Neuron* **85**, 88-100
104. Basso, M., and Pennuto, M. (2015) Serine phosphorylation and arginine methylation at the crossroads to neurodegeneration. *Exp. Neurol.* **271**, 77-83

105. Sims, R. J. (2011) The C-terminal domain of RNA polymerase II is modified by site-specific methylation. *Science* **332**, 99-103
106. Wang, Y., Wysocka, J., Sayegh, J., Lee, Y. H., Perlin, J. R., Leonelli, L., Sonbuchner, L. S., McDonald, C. H., Cook, R. G., Dou, Y., Roeder, R. G., Clarke, S., Stallcup, M. R., Allis, C. D., and Coonrod, S. A. (2004) Human PAD4 regulates histone arginine methylation levels via demethyliminination. *Science* **306**, 279-283
107. Cuthbert, G. L., Daujat, S., Snowden, A. W., Erdjument-Bromage, H., Hagiwara, T., Yamada, M., Schneider, R., Gregory, P. D., Tempst, P., Bannister, A. J., and Kouzarides, T. (2004) Histone deimination antagonizes arginine methylation. *Cell* **118**, 545-553
108. Raijmakers, R., Zendman, A. J., Egberts, W. V., Vossenaar, E. R., Raats, J., Soede-Huijbregts, C., Rutjes, F. P., van Veelen, P. A., Drijfhout, J. W., and Pruijn, G. J. (2007) Methylation of arginine residues interferes with citrullination by peptidylarginine deiminases in vitro. *J. Mol. Biol.* **367**, 1118-1129
109. Lee, Y. H., Coonrod, S. A., Kraus, W. L., Jelinek, M. A., and Stallcup, M. R. (2005) Regulation of coactivator complex assembly and function by protein arginine methylation and demethyliminination. *Proc. Natl Acad. Sci. USA* **102**, 3611-3616
110. Guo, Q., Bedford, M. T., and Fast, W. (2011) Discovery of peptidylarginine deiminase-4 substrates by protein array: antagonistic citrullination and methylation of human ribosomal protein S2. *Mol. Biosyst.* **7**, 2286-2295
111. Snijders, A. P., Hautbergue, G. M., Bloom, A., Williamson, J. C., Minshull, T. C., Phillips, H. L., Mihaylov, S. R., Gjerde, D. T., Hornby, D. P., Wilson, S. A., Hurd, P. J., and Dickman, M. J. (2015) Arginine methylation and citrullination of splicing factor proline- and glutamine-rich (SFPQ/PSF) regulates its association with mRNA. *RNA* **21**, 347-359
112. Thomas, D., Lakowski, T. M., Pak, M. L., Kim, J. J., and Frankel, A. (2010) Forster resonance energy transfer measurements of cofactor-dependent effects on protein arginine N-methyltransferase homodimerization. *Protein Sci.* **19**, 2141-2151
113. Herrmann, F., Lee, J., Bedford, M. T., and Fackelmayer, F. O. (2005) Dynamics of human protein arginine methyltransferase 1(PRMT1) in vivo. *The Journal of Biological Chemistry* **280**, 38005-38010
114. Morales, Y., Nitzel, D. V., Price, O. M., Gui, S., Li, J., Qu, J., and Hevel, J. M. (2015) Redox Control of Protein Arginine Methyltransferase 1 (PRMT1) Activity. *J. Biol. Chem.* **290**, 14915-14926

115. Lafleur, V. N., Richard, S., and Richard, D. E. (2014) Transcriptional repression of hypoxia-inducible factor-1 (HIF-1) by the protein arginine methyltransferase PRMT1. *Mol. Biol. Cell* **25**, 925-935
116. Pahlich, S., Zakaryan, R. P., and Gehring, H. (2006) Protein arginine methylation: Cellular functions and methods of analysis. *Biochim. Biophys. Acta* **1764**, 1890-1903
117. Ong, S. E., Mittler, G., and Mann, M. (2004) Identifying and quantifying in vivo methylation sites by heavy methyl SILAC. *Nat. Methods* **1**, 119-126
118. Sylvestersen, K. B., Horn, H., Jungmichel, S., Jensen, L. J., and Nielsen, M. L. (2014) Proteomic analysis of arginine methylation sites in human cells reveals dynamic regulation during transcriptional arrest. *Mol. Cell. Proteomics* **13**, 2072-2088
119. Lee, Y. H., and Stallcup, M. R. (2009) Minireview: protein arginine methylation of nonhistone proteins in transcriptional regulation. *Mol. Endocrinol.* **23**, 425-433
120. Kleinschmidt, M. A., Streubel, G., Samans, B., Krause, M., and Bauer, U. M. (2008) The protein arginine methyltransferases CARM1 and PRMT1 cooperate in gene regulation. *Nucleic Acids Res.* **36**, 3202-3213
121. Hou, Z. (2008) The LIM protein AJUBA recruits protein arginine methyltransferase 5 to mediate SNAIL-dependent transcriptional repression. *Mol. Cell. Biol.* **28**, 3198-3207
122. Wong, C. M., Tang, H. M., Kong, K. Y., Wong, G. W., Qiu, H., Jin, D. Y., and Hinnebusch, A. G. (2010) Yeast arginine methyltransferase Hmt1p regulates transcription elongation and termination by methylating Npl3p. *Nucleic Acids Res.* **38**, 2217-2228
123. Abramovich, C., Yakobson, B., Chebath, J., and Revel, M. (1997) A protein-arginine methyltransferase binds to the intracytoplasmic domain of the IFNAR1 chain in the type I interferon receptor. *EMBO J.* **16**, 260-266
124. Iwasaki, H. (2008) Involvement of PRMT1 in hnRNPQ activation and internalization of insulin receptor. *Biochem. Biophys. Res. Commun.* **372**, 314-319
125. Najbauer, J., Johnson, B. A., Young, A. L., and Aswad, D. W. (1993) Peptides with sequences similar to glycine, arginine-rich motifs in proteins interacting with RNA are efficiently recognized by methyltransferase(s) modifying arginine in numerous proteins. *J. Biol. Chem.* **268**, 10501-10509
126. Calnan, B. J., Tidor, B., Biancalana, S., Hudson, D., and Frankel, A. D. (1991) Arginine-mediated RNA recognition: the arginine fork. *Science* **252**, 1167-1171

127. Jones, S., Daley, D. T., Luscombe, N. M., Berman, H. M., and Thornton, J. M. (2001) Protein-RNA interactions: a structural analysis. *Nucleic Acids Res.* **29**, 943-954
128. Xu, C., Henry, P. A., Setya, A., and Henry, M. F. (2003) In vivo analysis of nucleolar proteins modified by the yeast arginine methyltransferase Hmt1/Rmt1p. *RNA* **9**, 746-759
129. McBride, A. E., Cook, J. T., Stemmler, E. A., Rutledge, K. L., McGrath, K. A., and Rubens, J. A. (2005) Arginine methylation of yeast mRNA-binding protein Npl3 directly affects its function, nuclear export, and intranuclear protein interactions. *J. Biol. Chem.* **280**, 30888-30898
130. Chen, Y. C., Milliman, E. J., Goulet, I., Cote, J., Jackson, C. A., Vollbracht, J. A., and Yu, M. C. (2010) Protein arginine methylation facilitates cotranscriptional recruitment of pre-mRNA splicing factors. *Mol. Cell. Biol.* **30**, 5245-5256
131. Yu, Z., Chen, T., Hebert, J., Li, E., and Richard, S. (2009) A mouse PRMT1 null allele defines an essential role for arginine methylation in genome maintenance and cell proliferation. *Mol. Cell. Biol.* **29**, 2982-2996
132. Yu, Z. (2012) The MRE11 GAR motif regulates DNA double-strand break processing & ATR activation. *Cell Res.* **22**, 305-320
133. Boisvert, F. M., Dery, U., Masson, J. Y., and Richard, S. (2005) Arginine methylation of MRE11 by PRMT1 is required for DNA damage checkpoint control. *Genes Dev.* **19**, 671-676
134. Adams, M. M., Wang, B., Xia, Z., Morales, J. C., Lu, X., Donehower, L. A., Bochar, D. A., Elledge, S. J., and Carpenter, P. B. (2005) 53BP1 oligomerization is independent of its methylation by PRMT1. *Cell Cycle* **4**, 1854-1861
135. Boisvert, F. M., Rhie, A., Richard, S., and Doherty, A. J. (2005) The GAR motif of 53BP1 is arginine methylated by PRMT1 and is necessary for 53BP1 DNA binding activity. *Cell Cycle* **4**, 1834-1841
136. Yoo, J. H., and Lee, S. C. (2001) Elevated levels of plasma homocyst(e)ine and asymmetric dimethylarginine in elderly patients with stroke. *Atherosclerosis* **158**, 425-430
137. Abedini, S., Meinitzer, A., Holme, I., Marz, W., Weihrauch, G., Fellstrom, B., Jardine, A., and Holdaas, H. (2010) Asymmetrical dimethylarginine is associated with renal and cardiovascular outcomes and all-cause mortality in renal transplant recipients. *Kidney Int.* **77**, 44-50

138. Tutarel, O., Denecke, A., Bode-Boger, S. M., Martens-Lobenhoffer, J., Lovric, S., Bauersachs, J., Schieffer, B., Westhoff-Bleck, M., and Kielstein, J. T. (2012) Asymmetrical dimethylarginine--more sensitive than NT-proBNP to diagnose heart failure in adults with congenital heart disease. *PLoS One* **7**, e33795
139. De Gennaro Colonna, V., Bianchi, M., Pascale, V., Ferrario, P., Morelli, F., Pascale, W., Tomasoni, L., and Turiel, M. (2009) Asymmetric dimethylarginine (ADMA): an endogenous inhibitor of nitric oxide synthase and a novel cardiovascular risk molecule. *Med. Sci. Monit.* **15**, RA91-101
140. Boger, R. H. (2003) The emerging role of asymmetric dimethylarginine as a novel cardiovascular risk factor. *Cardiovasc. Res.* **59**, 824-833
141. Chen, X., Niroomand, F., Liu, Z., Zankl, A., Katus, H. A., Jahn, L., and Tiefenbacher, C. P. (2006) Expression of nitric oxide related enzymes in coronary heart disease. *Basic Res. Cardiol.* **101**, 346-353
142. Rochette, L., Lorin, J., Zeller, M., Guillard, J. C., Lorgis, L., Cottin, Y., and Vergely, C. (2013) Nitric oxide synthase inhibition and oxidative stress in cardiovascular diseases: possible therapeutic targets? *Pharmacol. Ther.* **140**, 239-257
143. Matsuguma, K., Ueda, S., Yamagishi, S., Matsumoto, Y., Kaneyuki, U., Shibata, R., Fujimura, T., Matsuoka, H., Kimoto, M., Kato, S., Imaizumi, T., and Okuda, S. (2006) Molecular mechanism for elevation of asymmetric dimethylarginine and its role for hypertension in chronic kidney disease. *J. Am. Soc. Nephrol.* **17**, 2176-2183
144. Raptis, V., Kapoulas, S., and Grekas, D. (2013) Role of asymmetrical dimethylarginine in the progression of renal disease. *Nephrology (Carlton)* **18**, 11-21
145. Kielstein, J. T., Bode-Boger, S. M., Hesse, G., Martens-Lobenhoffer, J., Takacs, A., Fliser, D., and Hoepfer, M. M. (2005) Asymmetrical dimethylarginine in idiopathic pulmonary arterial hypertension. *Arterioscler. Thromb. Vasc. Biol.* **25**, 1414-1418
146. Zakrzewicz, D., and Eickelberg, O. (2009) From arginine methylation to ADMA: a novel mechanism with therapeutic potential in chronic lung diseases. *BMC Pulm. Med.* **9**, 5
147. Yang, Y., and Bedford, M. T. (2013) Protein arginine methyltransferases and cancer. *Nat. Rev. Cancer* **13**, 37-50

148. Cheung, N., Chan, L. C., Thompson, A., Cleary, M. L., and So, C. W. (2007) Protein arginine-methyltransferase-dependent oncogenesis. *Nature Cell Biol.* **9**, 1208-1215
149. Shia, W. J., Okumura, A. J., Yan, M., Sarkeshik, A., Lo, M. C., Matsuura, S., Komeno, Y., Zhao, X., Nimer, S. D., Yates, J. R., 3rd, and Zhang, D. E. (2012) PRMT1 interacts with AML1-ETO to promote its transcriptional activation and progenitor cell proliferative potential. *Blood* **119**, 4953-4962
150. Le Romancer, M. (2008) Regulation of estrogen rapid signaling through arginine methylation by PRMT1. *Mol. Cell* **31**, 212-221
151. Le Romancer, M., Treilleux, I., Bouchekioua-Bouzaghrou, K., Sentis, S., and Corbo, L. (2010) Methylation, a key step for nongenomic estrogen signaling in breast tumors. *Steroids* **75**, 560-564
152. Baldwin, R. M., Morettin, A., Paris, G., Goulet, I., and Cote, J. (2012) Alternatively spliced protein arginine methyltransferase 1 isoform PRMT1v2 promotes the survival and invasiveness of breast cancer cells. *Cell Cycle* **11**, 4597-4612
153. Mathioudaki, K., Scorilas, A., Ardavanis, A., Lymberi, P., Tsiambas, E., Devetzi, M., Apostolaki, A., and Talieri, M. (2011) Clinical evaluation of PRMT1 gene expression in breast cancer. *Tumour Biol.* **32**, 575-582
154. Hong, H., Kao, C., Jeng, M. H., Eble, J. N., Koch, M. O., Gardner, T. A., Zhang, S., Li, L., Pan, C. X., Hu, Z., MacLennan, G. T., and Cheng, L. (2004) Aberrant expression of CARM1, a transcriptional coactivator of androgen receptor, in the development of prostate carcinoma and androgen-independent status. *Cancer* **101**, 83-89
155. Seligson, D. B. (2005) Global histone modification patterns predict risk of prostate cancer recurrence. *Nature* **435**, 1262-1266
156. Mathioudaki, K. (2008) The PRMT1 gene expression pattern in colon cancer. *Br. J. Cancer* **99**, 2094-2099
157. Papadokostopoulou, A. (2009) Colon cancer and protein arginine methyltransferase 1 gene expression. *Anticancer Res.* **29**, 1361-1366
158. Elakoum, R., Gauchotte, G., Oussalah, A., Wissler, M. P., Clement-Duchene, C., Vignaud, J. M., Gueant, J. L., and Namour, F. (2014) CARM1 and PRMT1 are dysregulated in lung cancer without hierarchical features. *Biochimie* **97**, 210-218

159. Copeland, R. A., Solomon, M. E., and Richon, V. M. (2009) Protein methyltransferases as a target class for drug discovery. *Nat. Rev. Drug Discov.* **8**, 724-732
160. Boulanger, M. C., Liang, C., Russell, R. S., Lin, R., Bedford, M. T., Wainberg, M. A., and Richard, S. (2005) Methylation of Tat by PRMT6 regulates human immunodeficiency virus type 1 gene expression. *J. Virol.* **79**, 124-131
161. Li, Y. J., Stallcup, M. R., and Lai, M. M. (2004) Hepatitis delta virus antigen is methylated at arginine residues, and methylation regulates subcellular localization and RNA replication. *J. Virol.* **78**, 13325-13334
162. Bedford, M. T., and Richard, S. (2005) Arginine methylation an emerging regulator of protein function. *Mol. Cell* **18**, 263-272

CHAPTER 3

INVESTIGATING PRMT1: SUBSTRATE INTERACTIONS

ABSTRACT

Protein arginine methyltransferases (PRMTs) catalyze the methylation of terminal guanidino nitrogens of arginine residues in their protein substrates. PRMTs play a pivotal role in biology, yet much of the basic biochemistry for this class of enzymes remains unexplored. In particular, the molecular basis for substrate recognition by the PRMTs is poorly understood. The only current crystal structure of a PRMT1 with a substrate bound has very weak electron density around the substrate peptide side chains and therefore provides no information about what interactions are important for binding parts of the substrate besides the target arginine. Additionally, it remains unclear how a monomethylated peptide binds and is dimethylated by PRMT1. Herein, we aimed to co-crystallize PRMT1 with a monomethylated peptide substrate in order to understand how a monomethylated arginine is coordinated by the PRMT1 active site, and to learn how PRMT1 interacts with other parts of the peptide substrate. Many peptide containing crystals were screened, but no electron density for substrates was observed. A new strategy to use a protein substrate rather than a peptide also resulted in successful crystallization. Thus, detection of electron density of a suitable resolution has not been attained. Further trials are required to optimize crystal diffraction to produce better resolved data.

INTRODUCTION

Protein arginine methyltransferases (PRMTs) catalyze the transfer of methyl groups from the cofactor S-adenosyl-L-methionine (SAM or AdoMet) to the terminal guanidinium group of arginine residues in substrate proteins. Development, carcinogenesis, heart disease, and viral pathogenesis are among the processes influenced by the PRMT family of enzymes (1). Nine human PRMT isoforms (PRMT1-PRMT9) have been identified with homologues present in yeast, protozoa, *C. elegans*, *Drosophila melanogaster*, *Trypanosoma brucei*, plants, and fish, among others (2). PRMTs catalyze the methylation of arginine residues resulting in the formation of monomethylarginine (MMA), asymmetric dimethylarginine (ADMA), or symmetric dimethylarginine (SDMA) (Fig. 3-1). PRMTs can be classified into three distinct categories based on product formation: type I PRMTs monomethylate and asymmetrically dimethylate arginyl residues (PRMT1, PRMT2, PRMT3, PRMT4/CARM1, PRMT6, and PRMT8), type II PRMTs monomethylate and symmetrically dimethylate arginyl residues (PRMT5, and PRMT9), while type III PRMTs can only monomethylate arginine residues (PRMT7). PRMT methylation can alter protein-protein, protein-DNA, and protein-RNA interactions (2). PRMTs also regulate many cellular processes such as transcription, DNA repair, RNA processing and export, and cell differentiation (2,3). Intriguingly, MMA, ADMA, and SDMA can have opposing biological consequences (4,5).

Protein structures have been solved for many of the PRMTs from a variety of organisms and with a variety of cofactors. These structures include those of PRMT1 (6), PRMT3 (7), PRMT4/CARM1 (8), PRMT5 (9), PRMT6 (10), PRMT7 (11), and the plant

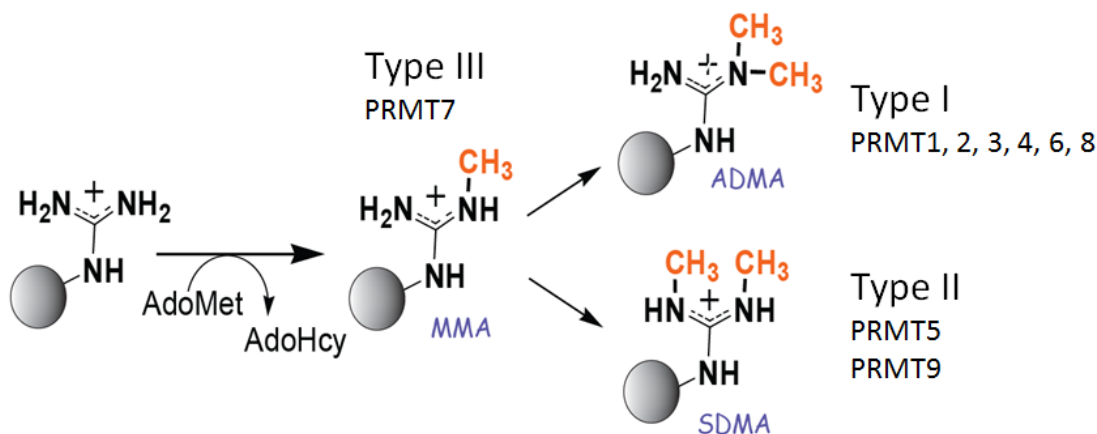


FIGURE 3-1. Reactions catalyzed by the mammalian protein arginine methyltransferases. PRMTs catalyze the transfer of a methyl group from AdoMet to a substrate arginine residue to form MMA, ADMA, or SDMA. Type I PRMTs (PRMT1, 2, 3, 4, 6, 8) can make MMA and ADMA. Type II PRMTs (PRMT5 and 9) can make MMA and SDMA. PRMT7, the only type III PRMT can only make MMA.

PRMT10 (12). These structures have provided a wealth of information regarding oligomerization, active site residues, and product specificity. PRMT1 is responsible for about 85% of arginine methylation in humans (13) and as the predominant PRMT *in vivo*, it is of particular interest. The rat PRMT1 homolog differs from human PRMT1 at only one residue (rH161 = hY161) and has high expression levels and activity, therefore making it an ideal model with which to study PRMT1. The crystal structure of rat PRMT1 was solved in 2003 with AdoHcy and R3, a 19 amino acid peptide substrate derived from fibrillarlin (GGRGGFGGRGGFGGRGGFG) (6). Because the peptide in this structure contains three potential methylation target arginines, it can be described as a slippery substrate; that is, one in which several parts of the substrate can be in the active site at any given time (Figure 3-2-A and B). The structure of the PRMT1-AdoHcy-R3 complex yielded electron densities revealing the location of bound peptide ligands. However, the

densities were broken into three separate peptide fragment binding sites and, except for the arginine in the active site, the side chain densities were not sufficiently resolved to allow clear identification of the amino acids (6). The three disconnected densities were suggested to represent a mixture of binding modes of the R3 peptide (Figure 3-2-C). The solved structure has been very valuable in identifying active site residues involved in binding and processing of the target arginine. However, it is still unclear how the monomethylated peptide binds and is dimethylated. Furthermore, because electron density was not observed for the peptide substrate side chains, little is known about what protein interactions are important with other parts of the substrate. Additionally, the observation of three different binding modes generated the possibility that various substrates may bind PRMT1 utilizing different binding grooves.

In order to better understand how PRMT1 binds its substrates, we set out to crystallize PRMT1 with a peptide containing only one monomethylated arginine. The target peptide chosen has two advantages: 1) it is not “slippery” and therefore should result in better electron density allowing visualization of the interactions between PRMT1 and the other parts of the substrate and 2) it would be the first monomethylated substrate crystallized with PRMT1, thus providing a better understanding of how a monomethylated species binds PRMT1 and is coordinated for a second catalytic step. Given that MMA and ADMA can produce different biological outcomes (5), knowing how PRMT1 is able to orient a monomethyl substrate is of great significance.

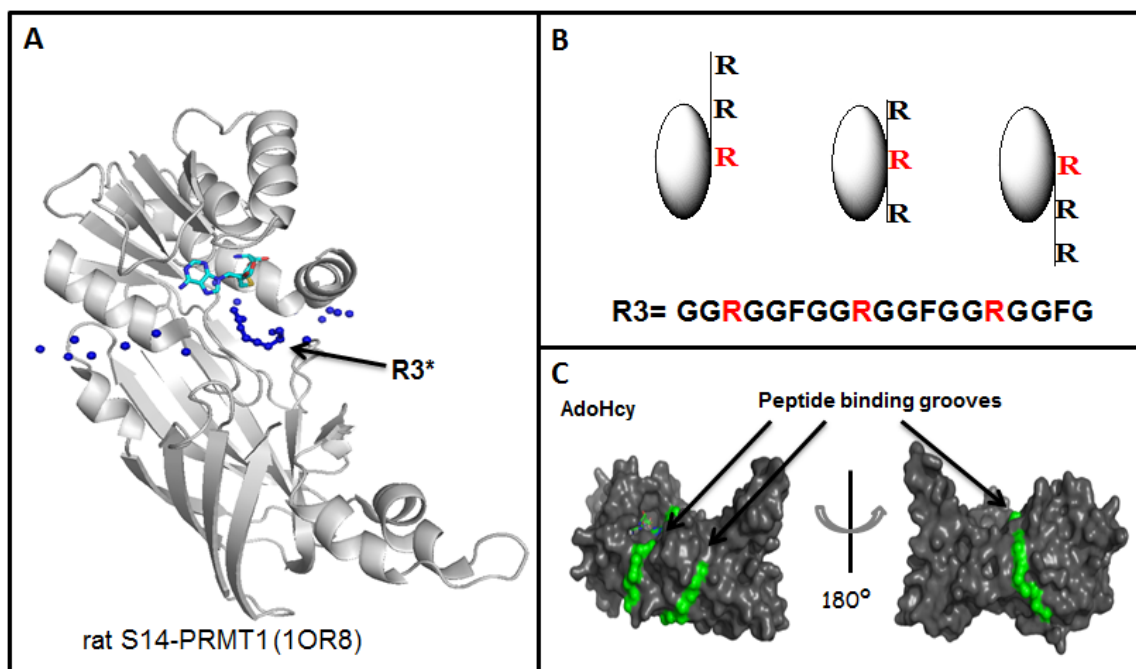


FIGURE 3-2. Structure of rat PRMT1 bound to R3 peptide (PDB: 1OR8). (A) PRMT1 (gray) was crystallized in the presence of AdoHcy (blue) and the R3 peptide substrate (blue). While most of the peptide backbone was observed, electron density was not observed for any of the peptide side chains, except for the active site arginine. (B) Representation of the three methylatable arginines in the R3 peptide each bound in the PRMT1 active site. (C) Surface representation of the PRMT1 monomer highlighting the three peptide binding grooves (green) where peptide backbone electron density was found.

Another goal of this work was to obtain a crystal structure containing PRMT1 and a full protein substrate. PRMT1 functions as a ring-like dimer arranged in head to tail fashion with a central cavity. This arrangement results in two active sites located on opposing ends of the central cavity. The substrate binding surface of PRMT1 is expected to be acidic because most PRMT1 substrates contain multiple positively charged arginines. The surface charge distribution of the dimer shows that acidic residues are enriched on the inner surface of the dimer ring and on the outer surface of the β barrel motif. While arginine substrates are commonly located on flexible loop regions of substrate proteins, how arginines in substrate proteins arrange into the PRMT1 dimer central cavity remains

unknown. In order to determine how a protein substrate is bound and methylated by PRMT1, we set out to choose a suitable protein substrate and solve a crystal structure of the proteins in complex.

For both goals, I have optimized purification protocols, created optimal constructs, and found various initial crystallization conditions. Further work should be done in order to optimize these conditions and obtain larger, better diffracting crystals.

EXPERIMENTAL PROCEDURES

Materials— AdoHcy was purchased from Sigma. All the peptides were synthesized by the Keck Institute and purified to $\geq 95\%$. The Matrix, Index, and Salt crystallization screens were purchased from Hampton Research, and the JCSG Core Suite screen was purchased from Qiagen.

Expression and Purification of S14-PRMT1— S14-PRMT1 (rat PRMT1v1 with first 13 residues removed) was expressed with a His₆ tag in *E. coli* BL21 cells at OD₆₀₀ of 0.4 with 0.5 mM IPTG for 18 hours at 22° C. The cells (~24 g) were lysed by sonication in lysis/wash buffer containing 50 mM sodium phosphate pH 7.5 and 20 mM imidazole at a 1 to 4 cell mass to buffer ratio. The soluble fraction was separated by centrifugation and allowed to incubate with 16 ml Ni-NTA Agarose (Qiagen) resin for 3 hours at 4° C. The Nickel resin was washed of impurities six times with four times the column volume using 50 mM sodium phosphate pH 7.5 and 70 mM imidazole (this was later corrected to 20 mM imidazole and two additional washes were added with 70 mM imidazole buffer to increase overall purification yield). The protein was eluted five times with one column volume of

50 mM sodium phosphate pH 7.5 and 250 mM imidazole. The protein was dialyzed overnight into 50 mM sodium phosphate pH 7.5 buffer and then loaded at a rate of 1 ml/min onto a HiTrap MonoQ (GE) column. The MonoQ column was run using a salt gradient with buffer A: 50 mM sodium phosphate pH 7.5 and buffer B: 50 mM sodium phosphate pH 7.5, 1 M NaCl. The gradient was run at 1 ml/min with step 1) 100% buffer A for 5 ml, step 2) increase to 20% buffer B over 15 ml, step 3) hold 20% buffer B for 5ml, step 4) increase to 40% buffer B over 15 ml, step 5) hold 40% buffer B for 5ml, step 6) increase to 100% buffer B over 20 ml, and step 7) hold 100% buffer B for 10 ml. Fractions containing protein (typically around 35% buffer B) were slowly concentrated to less than 1ml total volume using a 30 kDa cutoff centrifugal filter concentrator (Amicon). The protein was then loaded onto a 24 ml Superdex 200 gel filtration column equilibrated with 50 mM sodium phosphate, 300 mM NaCl pH 7.5, and run at 0.6 ml/min while collecting 2.5 ml fractions. Pure S14-PRMT1 was then buffer exchanged into 20 mM Tris pH 8.0, 250 mM NaCl, 1 mM EDTA, 0.1% β -mercaptoethanol, 5% glycerol and concentrated to ≥ 20 mg/ml prior to using for crystallization. AdoHcy was added to a final concentration of 600 μ M (concentration used for crystallization in paper) after the S14-PRMT1 was concentrated to ~ 20 mg/ml and prior to setting up crystallization trials. This step was slightly problematic due to the low solubility of AdoHcy in water. AdoHcy was made up in 1 M hydrochloric acid at a concentration of 120 mM and a small volume of this stock solution was added to the protein to a final concentration of 600 μ M AdoHcy. Because proteins tend to be less stable when very concentrated, the acidic addition often caused some of the protein to precipitate and become inviable for crystallization. If this occurred,

the solution was spun down and the soluble portion transferred to a new tube to use for crystal trials.

Expression and Purification of Hmt1 Constructs— *E. coli* BL21 cells expressing His₆-tagged Hmt1 were grown in Luria Broth media at 37° C to OD₆₀₀ reached 0.6, followed by induction with 0.5 mM IPTG at 22° C for 20 hours. Cell pellets were resuspended in two times cell volume lysis buffer (50 mM sodium phosphate pH 7.5, 100 mM NaCl, 20 mM imidazole, or 5 mM imidazole when purifying tagless constructs) and lysed using sonication. The cell lysate was clarified via centrifugation and incubated with Nickel resin (GoldBio) in a 1:1 cell mass: resin ratio for 1-2 hours at 4° C. The resin was washed eight times with eight column volumes of lysis buffer, followed by three washes with eight column volumes of wash buffer (50 mM sodium phosphate pH 7.5, 100 mM NaCl, 70 mM imidazole). The protein was then eluted off the resin five times with two column volumes of elution buffer (50 mM sodium phosphate pH 7.5, 100 mM NaCl, 250 mM imidazole). Elutions were pooled and dialyzed into 50 mM Hepes pH 7.5, 10% glycerol. The protein was then concentrated to ≥ 15 mg/ml and used immediately for crystallization trials.

Expression and Purification of Truncated Npl3 Proteins— His₆-tagged full length Npl3 was received from Ann McBride (pAM436). The pAM436 plasmid was generated by inserting an N-terminally His₆-tagged Npl3 into the pET24b+ vector using NdeI and SacI restriction sites. The His₆-TEV-T7 (HTT7) Npl3 constructs were all created in the Hevel lab as follows. An ultramer was synthesized by GenScript containing a 5' NdeI site followed by a 3 amino acid spacer, then a His₆ tag which was also followed by a 9 amino acid spacer prior to sequence for a TEV cleavage site. A NcoI site was next and

then a T7 affinity tag followed by a BamHI site. The ultramer then contained codon optimized Cterm Npl3 sequence (aa 284-414) and ended with a 3' KpnI site. This construct was received in a pUC57 vector. Because the 3' restriction site in the ordered sequence was mistakenly coding for a KpnI restriction site, instead of the desired SacI site, the entire sequence was PCR amplified using forward primers containing the 5' NdeI site and reverse primers matching the end of the Cterm Npl3 sequence and coding for a 3' SacI site. This PCR product was then ligated into a pAM436 plasmid that had been double digested with NdeI and SacI to remove all tags and Npl3 sequence. The resulting plasmid had a pET24b+ backbone and contained coding sequence for a His₆ tag, a TEV cleavage site, and a T7 tag; all flanked by NdeI and BamHI sites; this is referred to as the "HTT7" vector. Between the BamHI sites and the SacI site was the Cterm Npl3 codon optimized construct, which could be exchanged for any other sequence using the flanking restriction sites. These BamHI and SacI sites were then used to insert all other Npl3 constructs, into the "HTT7" plasmid.

E. coli BL21 NiCo21 (DE3) cells expressing His-TEV-T7 tagged Cterm Npl3 (residues 284-414) protein were grown in Luria Broth media at 37° C until OD₆₀₀ reached 0.6, followed by induction with 0.5 mM IPTG at 22° C for 20 hours. Cell pellets were resuspended in two times cell volume lysis buffer (50 mM sodium phosphate pH 7.5, 500 mM NaCl, 20 mM imidazole) and lysed using sonication. The cell lysate was clarified via centrifugation and incubated with Nickel resin (GoldBio) in a 2:1 cell mass to resin ratio for 1-2 hours at 4° C. The resin was washed eight times with eight column volumes of lysis buffer, followed by three washes with eight column volumes of wash buffer (50 mM sodium phosphate pH 7.5, 100 mM NaCl, 70 mM imidazole). The protein was then eluted off the resin five times with two column volumes of elution buffer (50 mM sodium

phosphate pH 7.5, 100 mM NaCl, 500 mM imidazole). Elutions were pooled, filtered and further purified using MonoQ and Heparin columns (GE) in tandem. Fractions containing Npl3 were pooled and dialyzed into 50 mM Hepes pH 7.5, 10% glycerol. The protein was then concentrated to ≥ 1 mg/ml, beaded in liquid nitrogen, and stored at -80° C. Note that all Npl3 constructs were expressed and purified as above.

Expression and co-purification of Hmt1 and Npl3 protein— *E. coli* BL21 cells expressing tagless Hmt1 were grown in Luria Broth media at 37° C to OD_{600} reached 0.6, followed by induction with 0.5 mM IPTG at 22° C for 20 hours. *E. coli* BL21 NiCo21 (DE3) cells expressing His-TEV-T7 tagged Cterm Npl3 (residues 284-414) protein were grown in Luria Broth media at 37° C to OD_{600} reached 0.6, followed by induction with 0.5 mM IPTG at 22° C for 20 hours. Seven grams of each cell pellet were weighed out and combined into 30 ml of lysis buffer (50 mM Hepes pH 7.5, 0.5 M NaCl, 20 mM imidazole) and lysed by sonication. The combined cell lysates was incubated with GoldBio Nickel-charged resin for 1 hour at 4° C. The Nickel resin was then washed twelve times with 5 column volumes of lysis buffer to remove any Hmt1 not complexed with HTT7 Cterm Npl3, as well as any nonspecific nucleic acids bound to the proteins. The resin was then washed twice with 5 column volumes of 50 mM Hepes pH 7.5, 0.1 M NaCl, 20 mM imidazole wash buffer, prior to eluting the protein complex six times with two column volumes of 50 mM Hepes pH 7.5, 0.1 M NaCl, 250 mM imidazole. The protein-complex containing elutions were pooled and dialyzed overnight into 50 mM Hepes pH 7.5 buffer to remove excess salt and imidazole. The proteins were then concentrated using a 30 kDa cutoff spin concentrator (Millipore) to ≥ 15 mg/ml and used for crystallization attempts.

Protein Interaction Determination— Initial attempts to map the interacting regions of Npl3 with Hmt1 using binding to T7 resin were unsuccessful due to strong nonspecific binding by Hmt1 to the T7 resin even in the absence of Npl3. Ultimately, protein interactions were probed by mixing lysates and co-purifying tagless Hmt1 with various HTT7-tagged Npl3 constructs over Nickel affinity resin. Positive interactions resulted in protein co-purification, while negative interactions resulted in most of the Hmt1 being present in the unbound fraction. Note that although tagless Hmt1 could also form nonspecific interactions with the Nickel resin, the amount of resin and protein present still allowed for clear distinction between true binding vs nonspecific binding. This was not the case when using T7 resin due to the small amount of both resin and protein used for these studies which required visualization by Western blotting in order to determine the presence of protein.

RESULTS

S14-PRMT1: Peptide Substrate Crystallization and Optimization— Initial attempts to solve a PRMT1 substrate bound structure were modeled closely after the published rat PRMT1 (rPRMT1) structure (6). The rPRMT1/R3 crystals were grown in mother liquor containing 100 mM Tris pH 9.0 and 1.6 M ammonium phosphate monobasic (final pH ~4.7). The concentration of peptide used, when present, was 1 mM and the protein was 20 mg/ml and contained 600 μ M AdoHcy (6). Our initial crystallization trials were set up on a 24 well sitting drop vapor diffusion hand tray in mother liquor containing 100 mM Tris pH 9.0 and varying the final ammonium phosphate monobasic concentration from 1.3

M to 1.8 M in 0.1 M increments. Using protein concentrated to 20 mg/ml or greater, drops were set up containing either 1.5 μ l protein: 1.5 μ l mother liquor, 2 μ L protein: 1 μ l mother liquor, or 1 μ l protein: 2 μ l mother liquor and the trays were placed in a 4° C crystallization chamber. Initial results indicated that using 2 μ l: 1 μ l protein to well solution ratio resulted in precipitation of the protein and not crystal formation. Small, needle shaped crystals were obtained when using a 1.5 μ l: 1.5 μ l protein to well solution ratio in the presence of 1.5 M to 1.8 M ammonium phosphate monobasic. Therefore, future crystallization conditions were based around these initial results. Many large batches of cells were grown, purified, and used in crystal trials. A summary of the most promising conditions that yielded crystals is depicted in Figure 3-3.

While conditions were optimized for production of crystals in the absence of peptide, any time monomethylated peptide was present in the crystallization attempts, either no crystals, or crystals of very small size formed. At this point, we turned to wider screening for any conditions that would yield crystals in the presence of peptide. Purified protein was taken to the lab of Dr. Chris Hill at the University of Utah where a Phenix crystallization robot was used to set up many conditions at once using much lower volumes of protein, effectively allowing us to screen hundreds of conditions using the same amount of protein needed to set up one 24 well hand tray. Two new conditions were obtained from this effort that yielded crystals in the presence of JMH1W-CH3 peptide (KGGFGGR(CH₃)GGFGGKW) (0.2 M magnesium acetate, 0.1 M sodium cacodylate pH 6.5, 30% (v/v) 2-methyl-2,4-pentanediol) (0.1 M bicine pH 9.0, 2% (v/v) 1,4 dioxane, 10% w/v PEG 20,000). Sitting drop vapor diffusion hand trays were then set up around these

S14-PRMT1 Initial Crystal Hit Summary				
Well Conditions	Protein to well ratio	[SAH]	[Protein]	Crystal Shape
0.1M Tris pH9.0, 1.5M ammonium phosphate monobasic	1.5 to 1.5	600 μ M	23.63mg/ml	needles
0.1M Tris pH9.0, 1.6M ammonium phosphate monobasic	1.5 to 1.5	600 μ M	23.63mg/ml	needles and rods
0.1M Tris pH9.0, 1.7M ammonium phosphate monobasic	1.5 to 1.5	600 μ M	23.63mg/ml	thick rods
0.1M Tris pH9.0, 1.8M ammonium phosphate monobasic	1.5 to 1.5	600 μ M	23.63mg/ml	small, thin rods
0.1M Tris pH9.0, 1.8M ammonium phosphate monobasic	2 to 1	600 μ M	23.63mg/ml	small, thin rods
0.1M Tris pH9.0, 1.6M ammonium phosphate monobasic	2 to 1	600 μ M	11.7mg/ml	small rods
0.1M Tris pH9.0, 1.7M ammonium phosphate monobasic	2 to 1	600 μ M	11.7mg/ml	small rods
0.1M Tris pH9.0, 1.7M ammonium phosphate monobasic	1.5 to 1.5	600 μ M SAH, 1mM JMH1WCH3 peptide	16.7mg/ml	small rods

FIGURE 3-3. Summary of initial S14-PRMT1 crystallization conditions. The initial conditions found to produce S14-PRMT1 crystals are described in detail, along with the concentration of protein and substrates present and the shape of the resulting crystals.

conditions, but unfortunately these crystals were salt, rather than protein crystals. We turned once again to trying to optimize the published crystallization conditions to grow crystals in the presence of peptide. Eventually, crystals containing S14-PRMT1- AdoHcy-eIF4A1-CH₃ (YIHRIGR(CH₃)GGR) were grown that produced good quality diffraction pattern when sent to the Stanford Synchrotron Radiation Lightsource. The structure was solved by molecular replacement using the existing PRMT1 structure (PDB: 1OR8) as a

search model. Unfortunately, although some density was present in the active site where peptide is expected to bind, it was not clear enough to build any peptide residues (Figure 3-4).

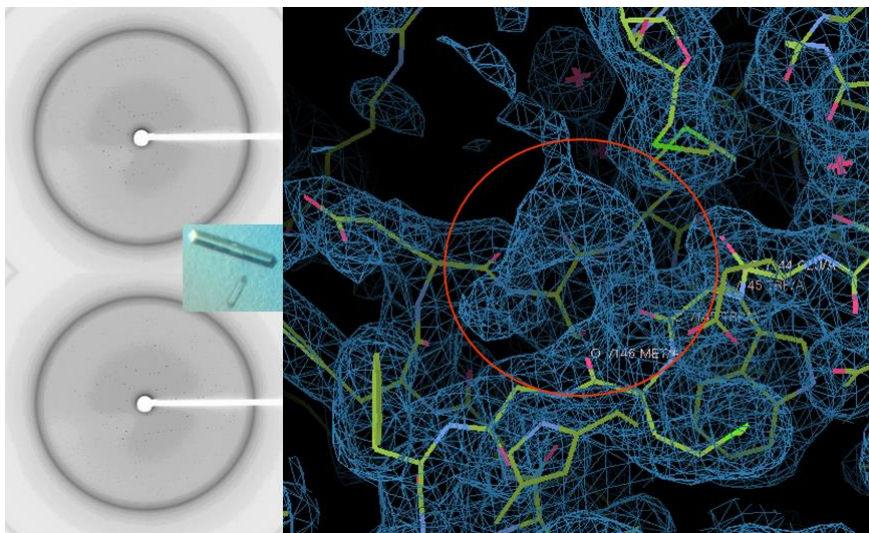


FIGURE 3-4. Diffraction pattern and electron density of PRMT1 crystal containing the eIF4A1-CH₃ peptide. A crystal of S14-PRMT1-AdoHcy-eIF4A1-CH₃ is shown along with two frames of a typical diffraction pattern that was used to solve the structure. However, there was not enough density visible in the active site to build the peptide substrate.

Given the lack of success in attaining a PRMT1 structure with a peptide substrate bound, a strategic decision was made to focus on attaining a structure with a protein substrate bound instead. The use of protein substrates is advantageous since these are the substrates PRMT1 methylates *in vivo*. Additionally, the length of a protein substrate is much greater than that of any peptide and a structure would yield a clearer picture of how substrate interactions far away from the PRMT1 active site contribute to determining whether a specific arginine-containing motif is a PRMT1 substrate. This is significant since

previous work in the Hevel lab showed that a single amino acid change in the helicase eIF4A1 (a PRMT1 protein substrate) from 'RGG' to 'RSG' (to mimic the sequence found in eIF4A3, which is not normally a PRMT1 substrate) abolished methylation by PRMT1. However, when the same RGG to RSG change was made in a peptide substrate methylation was retained, suggesting that sequences distant from the site of methylation are important in influencing the PRMT1 substrate specificity (14). For these reasons, all efforts were aimed at obtaining a structure of PRMT1 in complex with a protein substrate.

Hmt1: Protein Substrate Interaction Analysis— As previously mentioned, two PRMT1 crystals structures have thus far been solved, one from rat PRMT1, and one from yeast PRMT1, also called Hmt1 (heterogeneous nuclear ribonucleoprotein methyltransferase). Hmt1 is the major arginine methyltransferase in *Saccharomyces cerevisiae* and is the only known type I PRMT in this organism. Surprisingly, while mammalian *PRMT1* is essential for survival, yeast *HMT1* is not essential for normal yeast growth unless the *HMT1* knockouts are combined with mutations in the Npl3 protein (15). Npl3 is a major Hmt1 substrate that functions to shuttle mRNA between the nucleus and the cytoplasm (15). Functionally, inactivation of Hmt1 decreases the nuclear export of its major known substrates, Hrp1 and Npl3 (15), implicating arginine methylation in the regulation of mRNA and ribonucleoprotein (mRNP) export.

Npl3 is a heterogeneous nuclear ribonucleoprotein that contains a C-terminal domain rich in arginine and serine residues that are essential for its role in RNA transport. Methylation directly affects Npl3 export by weakening contacts with nuclear proteins (16). Efficient export does not require methylation, but unmethylated arginine residues lead to nuclear retention of hnRNPs and previous data has also shown that the C-terminal domain

of Npl3 alone (Cterm) can partially rescue RNA transport in Npl3-deficient cells (16). Given the importance of arginine methylation by Hmt1 on Npl3, these two proteins were chosen for our guided attempts at crystallization of Hmt1 in complex with a protein substrate.

The Npl3 protein is composed of a long, unstructured N-terminus, two RNA recognition motifs (RRMs), and a long arginine and serine (RS) rich C-terminal domain. While the RRM motifs have a conserved secondary structure (which has been solved by NMR (17)), the rest of the protein is predicted to be largely unstructured. Interestingly, the long C-terminal domain of Npl3 contains 15 RGG, 3RG, and 2RxR peptides (starting at R284 in Figure 3-5), all of which are potential methylation sites. Importantly, the RS-rich C-terminal domain of Npl3 alone has been shown to rescue growth of an $\Delta npl3$ strain, highlighting its importance for Npl3 function (18). Mass spectrometry studies have identified 16 arginine residues that are dimethylated *in vivo*, and one additional methylation site (16) (Figure 3-5). It was also noted that Npl3 function was greatly affected by lysine substitution at methylation sites. Notably, lysine substitutions in the four RGG tripeptides at the N-terminus of the RS domain had a greater influence on Npl3 function than mutating RGGs closer to the C-terminal end (16). The optimal Hmt1 co-crystallization partner should: 1) form a stable complex with Hmt1 and be easily purified, 2) provide enough steric bulk to limit binding modes in the crystal, and 3) form quality diffracting crystals. With all of this in mind, we set out to create the best possible construct of Npl3 to co-crystallize with Hmt1 in order to decipher how Hmt1 binds and methylates protein substrates.

```

1  MSEAQETHVE QLPESVVDAP VEEQHQEPPQ APDAPQEPQV PQESAPQESA PQEPPAPQEQ
61  NDVPPPSNAP IYEGEESHVS QDYQEAHQHH QPPEPQPYYP PPPPGEHMHG RPPMHRQEG
121 ELSNTRLFVR PFPLDVQESE LNEIFGPFGP MKEVKILNGF AFVEFEEAES AAKAIEEVHG
181 KSFANQPLEV VYSKLPKRY RITMKNLPEG CSWDLKDLA RENSLETTFS SVNTRDFDGT
241 GALEFPSEEI LVEALERLNN IEFRGSVITV ERDDNPPPIR RSN○RGG○FR○GR○ GG○FRGG○FRGG○
      R284 R290 R294 R298
301 FRGG○FRGG○FRGG○FRGG○ GGPRGG○FGGP○ RGGYGGYS○RG○ GYGGYS○RGGY○ GGSRGGYD○SP○ RGGYD○SP○RGG○
      R302 R307 R314
361 YSRGGYGGPR NDYGP○PRGSY○ GGSRGGYDGP○ RGDYGPPRDA YRTRDAPRER SPTR

```

FIGURE 3-5. Npl3 sequence and arginine methylation sites. The sequence of the Npl3 protein is shown, the two RNA recognition motifs (RRMs) are colored in light blue, while the long C-terminal tail is colored in dark blue. Arginines found exclusively dimethylated are marked with a filled circle, while those found monomethylated and dimethylated are marked with open circles.

Npl3 Construct Design— Hmt1 constructs were designed both with a His₆-tag and without any affinity tags in order to study the interaction between Hmt1 and truncated parts of Npl3. The design of Npl3 constructs required either the absence or presence of a His₆-tag, which could be cleaved in order to quickly assess Hmt1: Npl3 interaction. All Npl3 constructs were generated containing an N-terminal His₆-tag, followed by a TEV cleavage site and a T7 short affinity tag, which is collectively referred to as an HTT7 tag. This design allowed us to take advantage of the His₆-tag for quick purification, or to cleave the His₆-tag and study Npl3 interaction with Hmt1 via pull-down studies binding Npl3 to a T7 resin. Attempts to study the interaction between Hmt1 and Npl3 bound to T7 resin was unsuccessful due to the ability of Hmt1 to bind to the T7 resin in a nonspecific fashion (data not shown). Subsequent interaction studies were done by binding HTT7-Npl3 (various constructs) to Nickel resin and determining whether tagless Hmt1 could be co-purified.

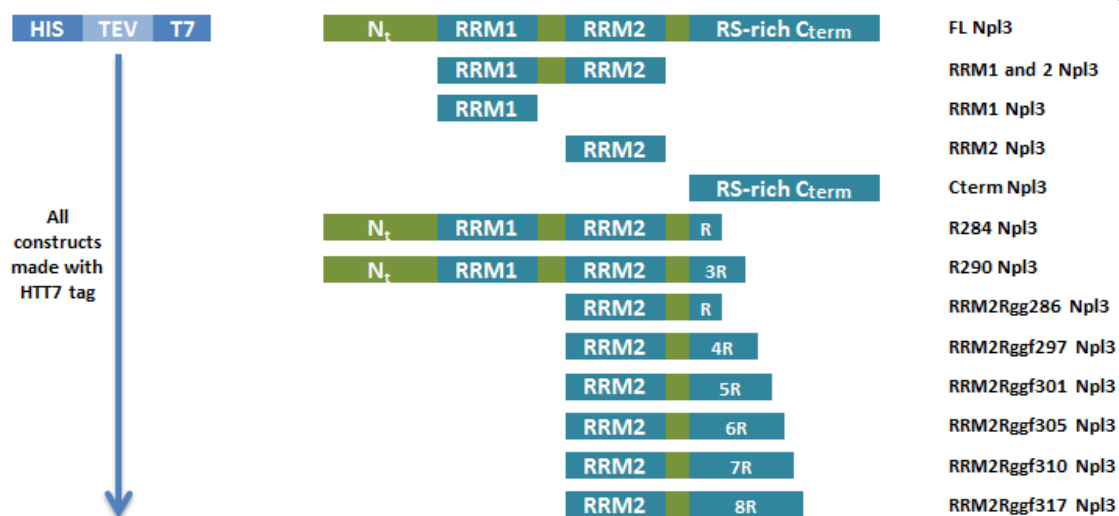


FIGURE 3-6. Npl3 constructs designed. Npl3 constructs were designed with an N-terminal His₆-TEV-T7 tag for purification and interaction studies. Constructs were designed to isolate each domain in Npl3 and to test the minimal region and number of arginines required for arginine methylation to occur.

While it is known that the Npl3 methylation sites are contained within the C-terminal tail, it was unknown whether additional regions of the Npl3 protein were required for Hmt1 recognition. Therefore, constructs were created containing only RRM1, only RRM2, RRM1 and 2, the C-terminal domain only (Cterm), or RRM2 with various lengths of C-terminal domain (see Figure 3-6 and table 3-1) in order to minimize the possible binding modes while maintaining steric bulk for crystallization.

The Npl3 constructs were tested for their ability to co-purify tagless Hmt1, and to be methylated. Although all constructs presented in Table 3-1 were created, many remain to be tested. Ultimately, while work continued to produce an optimal, minimal construct which could be methylated and stably bind Hmt1, the Cterm Npl3 construct was used in efforts to solve a structure of Hmt1 and a substrate protein complex.

Table 3-1. Npl3 construct interaction with Hmt1

Npl3 construct	Residues	Able to pull down Hmt1?	Methylated?
Full Length Npl3	1 - 414	yes	yes
RRM1 Npl3	121 - 194	no	no
RRM2 Npl3	199 - 273	no	no
RRM1 and 2 Npl3	121 - 273	no	no
Cterm Npl3	284 - 414	yes	yes
R284 Npl3	1 - 284	no	no
RRM2Rgg286 Npl3	199 - 286	no	no
R290 Npl3	1 - 290	no	N/A
RRM2 Rggf297 Npl3	199 - 297	N/A	N/A
RRM2 Rggf301 Npl3	199 - 301	N/A	N/A
RRM2 Rggf305 Npl3	199 - 305	N/A	N/A
RRM2 Rggf310 Npl3	199 - 310	N/A	N/A
RRM2 Rggf317 Npl3	199 - 317	N/A	N/A

Hmt1: Protein Substrate Crystallization and Optimization— For crystallization attempts, HTT7 Cterm Npl3 (R284 - 414) and excess tagless Hmt1 cells were mixed and purified in tandem. The His₆-tag on the Npl3 construct was used to bind to Nickel resin and any tagless Hmt1 not in complex with Npl3 was removed during the Nickel resin washing steps, assuring that only stable complex was purified. Additionally, because it is known that both Npl3 and Hmt1 bind nucleic acids, the lysis and initial wash buffers contained 500 mM NaCl in order to break up any weak nucleic acid interactions. After the Nickel purification step, the complex was dialyzed to remove excess imidazole and subsequently concentrated prior to setting up crystallization trials. The concentration step used a 30 kDa cutoff concentrator in order to assure protein complex formation; since the Cterm Npl3 construct has a molecular weight of about 15 kDa, any protein not in complex

with Hmt1 should flow through the concentrator membrane, assuring that only the larger molecular weight complex was used for crystallization.

Crystallization attempts were first tried at a complex concentration of 16.3 mg/ml or 26.86 mg/ml. Crystallization conditions were screened using commercially available kits (Natrix, Index, Salt [Hampton Research], and JCSG Core Suites [Qiagen]) by the sitting drop vapor diffusion method in 96-well three drop plates, and employing a Gryphon crystallization robot (Art Robbins Instruments) with 100 nl protein solution + 300 nl mother liquor drops, 200 nl protein solution + 200 nl mother liquor drops, and 300 nl protein solution + 100 nl mother liquor drops. The plates were placed in a 4° C crystallization chamber and monitored periodically. Initial crystal hits were followed up by hand with larger volume crystallization trays using the hanging drop vapor diffusion method. A representative summary of the crystal hits found is shown in Figure 3-7.

As shown in Figure 3-7, most conditions yielding crystals preferentially crystallized one protein or the other and only one condition contained both Hmt1 and Cterm Npl3. Additionally, these initial crystal hits diffracted poorly with the best crystals reaching only about 15 Å resolution. Further optimization of these crystallization conditions, with special focus on the condition yielding the protein complex should be able to improve the crystal diffraction.

DISCUSSION

While much biochemical work has been done to probe the parameters guiding PRMT1 substrate specificity (14,19,20), the field has been largely constrained by

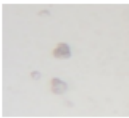

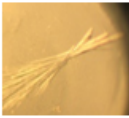

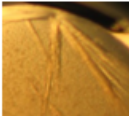





Hmt1 and Cterm Npl3 Crystal Hit Summary Table					
Protein Crystallized	Screen	Condition	Prot to well ratio	Crystal	Gel
Npl3 only	Natrix G7	0.7M Ammonium tartrate dibasic, 0.1M Sodium acetate trihydrate pH4.6	3 to 1		 *
Hmt1 only	Qiagen D2	0.2M KCl, 20% (w/v) PEG 3350	3 to 1		 +
Hmt1 only	Natrix G8	0.04M LiCl, 0.08M Strontium chloride hexahydrate, 0.04M Na cacodylate trihydrate pH7.0, 30% v/v MPD, 0.012M Spermine tetrahydrochloride	2 to 2		 +
Hmt1 only	Natrix F9	0.012M NaCl, 0.08M KCl, 0.04M Na cacodylate pH6.0, 50% MPD, 0.012M Spermine tetrahydrochloride	2 to 1		 +
Hmt1 and Npl3	SaltRx B11	0.4M Magnesium formate dihydrate, 0.1M Sodium Acetate trihydrate pH4.6	2 to 2		 + *

FIGURE 3-7. Summary of Hmt1 and Cterm Npl3 crystallization conditions. The conditions found to produce Hmt1, Cterm Npl3, or Hmt1-Cterm Npl3 complex crystals are described. Crystal shapes and the proteins present in each crystal are also shown.

the absence of a crystal structure clearly detailing the molecular interactions between PRMT1 and its substrates. The work reported here aimed to fill this knowledge gap by first attempting to solve a structure of PRMT1 in complex with a peptide substrate, and later with a protein substrate.

The basic strategy outlined by the only available structure of PRMT1 with a substrate (PDB ID: 1OR8) was modified in an attempt to solve a similar structure with a

monomethylated peptide substrate. Although unsuccessful in attaining additional information about substrate binding, the work summarized in this chapter has helped in solving the structure of a PRMT1 variant (21), and should serve as a guide for future attempts at solving a seemingly elusive substrate bound PRMT1 structure. In hindsight, the use of phosphate buffer in purifying the rat PRMT1 protein was likely responsible for the many salt crystals obtained during the initial screening phase and should be avoided for any future crystallization attempts. Hepes buffers were used in the second phase of this work (Hmt1/Npl3) and there was a steep decline in the number of salt crystals obtained from initial crystallization screens. Since this work was done we have also learned that PRMT1 is under redox control and is susceptible to oxidation in air (22). Any future PRMT1 crystallization attempts should maintain reductant in all steps of purification in order to minimize protein heterogeneity.

The choice of substrate for co-crystallization is also critical in obtaining a complex with clear substrate density. A peptide substrate containing a single methylatable arginine should be targeted to avoid the shifting observed with the R3 substrate, and the sequence and K_D of the peptide also need to be considered when choosing the optimal crystallization partner. Work by Osborne *et al.* using variants of the H4-21 peptide (Ac-SGRGKGGKGLGKGGAKEHRKV) showed that C-terminal basic residues are important for substrate recognition (20). For this reason, it will be important to maintain a positive patch in the peptide sequence for PRMT1. The dissociation constant (K_D) of most peptide substrates have been reported in the low micromolar range and may limit the success of solving a structure of PRMT1 in complex with a peptide. For example, the K_D determined by Dr. Gui in our lab for the eIF4A1-CH3 peptide which could not be observed in the

previously mentioned structure is $2.61 \pm 0.20 \mu\text{M}$, while the K_D for the H4-21 peptide is $0.080 \pm 0.018 \mu\text{M}$ (data generated by Dr. Laurel Gui in Hevel lab), indicating this peptide is much better suited for co-crystallization. In fact, and as will be discussed later, structures of other PRMT isoforms have been solved recently with the H4-21 peptide bound. While the H4-21 peptide associates strongly with PRMT1, the K_D of the monomethylated version is $1.33 \pm 0.12 \mu\text{M}$, making it a less suitable substrate for co-crystallization. Although a K_D for a protein substrate has not been reported, a variety of substrate proteins are able to precipitate with PRMT1, indicating that PRMT1 forms stronger interaction with protein substrates; making the use of a protein substrate likely a more successful strategy for co-crystallization attempts.

The structures of human PRMT5 (hPRMT5) and *Trypanosoma brucei* PRMT7 (TbPRMT7) containing portions of histone H4 substrate peptide have been published. Although the substrate bound structure of these type II and type III, PRMTs have helped identify how the histone H4 peptide substrate is bound by each of these isoforms, progress has not been made in deciphering the PRMT1 substrate binding mechanism. However, the differences and similarities in binding modes between the hPRMT5 and TbPRMT7 structures may help indicate what features may be specific to each isoform, or conserved among the PRMTs. The substrate arginine is projected into the active site of hPRMT5 at the tip of a sharp β -turn in the peptide substrate. In contrast, the peptide substrate TbPRMT7 forms a wide turn on the surface of the active site (9,23). These differences seem to indicate that hPRMT5 requires flexibility in the substrate sequence immediately surrounding the target arginine in order to form a sharp β -turn, whereas no such constraints seem necessary for TbPRMT7 substrates to bind into the active site. However, these generalizations are

speculative since only one substrate bound structure has emerged for each isoform and different binding modes may likely exist for different substrates, a possibility suggested by the current PRMT1 substrate bound structure (6). The R3 (GGRGGFGGRGGFGGRGGFG) peptide substrate co-crystallized with rat PRMT1 was mapped onto the PRMT1 core as patches of backbone density along three possible peptide binding grooves with only an arginine residue clearly identifiable in the active site. The presence of the three binding grooves led to the theory that different PRMT1 substrates might interact with PRMT1 using different binding modes through different binding grooves. In support of this theory, biochemical manipulation of a residue on one of these grooves resulted in an altered pattern of PRMT1 methylation on hypomethylated cell extracts, inhibiting the methylation of some proteins while leaving the methylation of others unchanged (24).

Similar to what was observed in the hPRMT5 and TbPRMT7 structures, binding of the R3 peptide to rPRMT1 seems to occur mainly through backbone interactions. This observation is also supported by substrate profiling studies which have shown little to no consensus sequence for substrate recognition by PRMT1 (14,19), (although there is a prevalence of 'RGG', 'RXR', and 'RG' sequences observed *in vivo*). The presence of glycine around the targeted arginine builds conformational flexibility into the region of methylation that may be a requirement of specific binding modes. Alternatively, the prevalence of glycine could reflect the physical contortions that substrates must commit to in order to access an active site situated in the rim of the dimeric structure. Additional PRMT structures with various substrates are critical to be able to answer many of these questions and should be the focus of future work.

This chapter has summarized crystallization efforts aimed at determining the molecular details of how PRMT1 is able to interact with substrates. Although a structure was not achieved, this work was able to narrow down several crystallization conditions that can serve as a road map for future crystallization attempts. The recently obtained structures of hPRMT7 and TbPRMT7 bound to H4 peptide substrates highlight the need for substrate bound PRMT structures.

REFERENCES

1. Pawlak, M. R., Scherer, C. A., Chen, J., Roshon, M. J., and Ruley, H. E. (2000) Arginine N-methyltransferase 1 is required for early postimplantation mouse development, but cells deficient in the enzyme are viable. *Molecular and cellular biology* **20**, 4859-4869
2. Bedford, M. T., and Richard, S. (2005) Arginine methylation an emerging regulator of protein function. *Mol. Cell* **18**, 263-272
3. Bedford, M. T., and Clarke, S. G. (2009) Protein arginine methylation in mammals: who, what, and why. *Mol. Cell* **33**, 1-13
4. Jung, C. S., Oldfield, E. H., Harvey-White, J., Espey, M. G., Zimmermann, M., Seifert, V., and Pluta, R. M. (2007) Association of an endogenous inhibitor of nitric oxide synthase with cerebral vasospasm in patients with aneurysmal subarachnoid hemorrhage. *J. Neurosurg.* **107**, 945-950
5. Kirmizis, A., Santos-Rosa, H., Penkett, C. J., Singer, M. A., Green, R. D., and Kouzarides, T. (2009) Distinct transcriptional outputs associated with mono- and dimethylated histone H3 arginine 2. *Nat. Struct. Mol. Biol.* **16**, 449-451
6. Zhang, X., and Cheng, X. (2003) Structure of the predominant protein arginine methyltransferase PRMT1 and analysis of its binding to substrate peptides. *Structure* **11**, 509-520
7. Zhang, X., Zhou, L., and Cheng, X. (2000) Crystal structure of the conserved core of protein arginine methyltransferase PRMT3. *EMBO J.* **19**, 3509-3519

8. Troffer-Charlier, N., Cura, V., Hassenboehler, P., Moras, D., and Cavarelli, J. (2007) Functional insights from structures of coactivator-associated arginine methyltransferase 1 domains. *EMBO J.* **26**, 4391-4401
9. Antonysamy, S., Bonday, Z., Campbell, R. M., Doyle, B., Druzina, Z., Gheyi, T., Han, B., Jungheim, L. N., Qian, Y., Rauch, C., Russell, M., Sauder, J. M., Wasserman, S. R., Weichert, K., Willard, F. S., Zhang, A., and Emtage, S. (2012) Crystal structure of the human PRMT5:MEP50 complex. *Proceedings of the National Academy of Sciences* **109**, 17960-17965
10. Wang, C., Zhu, Y., Chen, J., Li, X., Peng, J., Chen, J., Zou, Y., Zhang, Z., Jin, H., Yang, P., Wu, J., Niu, L., Gong, Q., Teng, M., and Shi, Y. (2014) Crystal structure of arginine methyltransferase 6 from *Trypanosoma brucei*. *PLoS One* **9**, e87267
11. Hasegawa, M., Toma-Fukai, S., Kim, J. D., Fukamizu, A., and Shimizu, T. (2014) Protein arginine methyltransferase 7 has a novel homodimer-like structure formed by tandem repeats. *FEBS Lett.* **588**, 1942-1948
12. Cheng, Y., Frazier, M., Lu, F., Cao, X., and Redinbo, M. R. (2011) Crystal structure of the plant epigenetic protein arginine methyltransferase 10. *J. Mol. Biol.* **414**, 106-122
13. Tang, J., Frankel, A., Cook, R. J., Kim, S., Paik, W. K., Williams, K. R., Clarke, S., and Herschman, H. R. (2000) PRMT1 is the predominant type I protein arginine methyltransferase in mammalian cells. *J. Biol. Chem.* **275**, 7723-7730
14. Wooderchak, W. L., Zang, T., Zhou, Z. S., Acuna, M., Tahara, S. M., and Hevel, J. M. (2008) Substrate profiling of PRMT1 reveals amino acid sequences that extend beyond the "RGG" paradigm. *Biochemistry* **47**, 9456-9466
15. Shen, E. C., Henry, M. F., Weiss, V. H., Valentini, S. R., Silver, P. A., and Lee, M. S. (1998) Arginine methylation facilitates the nuclear export of hnRNP proteins. *Genes Dev.* **12**, 679-691
16. McBride, A. E., Cook, J. T., Stemmler, E. A., Rutledge, K. L., McGrath, K. A., and Rubens, J. A. (2005) Arginine methylation of yeast mRNA-binding protein Npl3 directly affects its function, nuclear export, and intranuclear protein interactions. *J. Biol. Chem.* **280**, 30888-30898
17. Deka, P., Bucheli, M. E., Moore, C., Buratowski, S., and Varani, G. (2008) Structure of the yeast SR protein Npl3 and Interaction with mRNA 3'-end processing signals. *J. Mol. Biol.* **375**, 136-150

18. McBride, A. E., Conboy, A. K., Brown, S. P., Ariyachet, C., and Rutledge, K. L. (2009) Specific sequences within arginine-glycine-rich domains affect mRNA-binding protein function. *Nucleic Acids Res.* **37**, 4322-4330
19. Bicker, K. L., Obianyo, O., Rust, H. L., and Thompson, P. R. (2011) A combinatorial approach to characterize the substrate specificity of protein arginine methyltransferase 1. *Mol. Biosyst.* **7**, 48-51
20. Osborne, T. C., Obianyo, O., Zhang, X., Cheng, X., and Thompson, P. R. (2007) Protein arginine methyltransferase 1: positively charged residues in substrate peptides distal to the site of methylation are important for substrate binding and catalysis. *Biochemistry* **46**, 13370-13381
21. Gui, S., Wooderchak, W. L., Daly, M. P., Porter, P. J., Johnson, S. J., and Hevel, J. M. (2011) Investigation of the molecular origins of protein-arginine methyltransferase I (PRMT1) product specificity reveals a role for two conserved methionine residues. *The Journal of Biological Chemistry* **286**, 29118-29126
22. Morales, Y., Nitzel, D. V., Price, O. M., Gui, S., Li, J., Qu, J., and Hevel, J. M. (2015) Redox Control of Protein Arginine Methyltransferase 1 (PRMT1) Activity. *J. Biol. Chem.* **290**, 14915-14926
23. Wang, C., Zhu, Y., Caceres, T. B., Liu, L., Peng, J., Wang, J., Chen, J., Chen, X., Zhang, Z., Zuo, X., Gong, Q., Teng, M., Hevel, J. M., Wu, J., and Shi, Y. (2014) Structural determinants for the strict monomethylation activity by trypanosoma brucei protein arginine methyltransferase 7. *Structure* **22**, 756-768
24. Lee, D. Y., Ianculescu, I., Purcell, D., Zhang, X., Cheng, X., and Stallcup, M. R. (2007) Surface-scanning mutational analysis of protein arginine methyltransferase 1: roles of specific amino acids in methyltransferase substrate specificity, oligomerization, and coactivator function. *Mol. Endocrinol.* **21**, 1381-1393

CHAPTER 4

HMT1 REGULATION BY THE AIR1/2 PROTEINS

ABSTRACT

PRMTs are crucial enzymes that affect a multitude of biological processes and pathways by posttranslationally methylating protein arginine residues. However, despite the knowledge that dysregulation of PRMTs leads to disease, very little is currently known about how the PRMT proteins are regulated. Evidence suggests the Air1/2 proteins may regulate Hmt1 (yeast PRMT1) activity, but the mechanism of regulation is unknown. Here we provide the first data to show that while Air1 is a regulator of Hmt1 activity, the Air2 protein does not have a significant effect on methyltransferase activity. We have determined that a ~60 amino acid region of the Air1 protein is sufficient for the inhibition of Hmt1 activity. Interestingly, this same region of Air1 is necessary for interactions with Trf4, a member of the nuclear RNA surveillance TRAMP complex. We also present conditions used to generate a crystal containing an Air2-Hmt1 complex that has produced 3.2 Å quality data that will be used to solve the structure of this complex. This could be the first structure showing how a protein interacts with any of the PRMTs and could lead to insights on how Air2 binds and interacts with Hmt1.

INTRODUCTION

Protein arginine methyltransferase (PRMT) activity has emerged as an important player in numerous essential biological processes (1,2). Several disease states have been linked to dysregulation of arginine methyltransferase activity (3-10), marking PRMTs an important potential drug targets (11). However, before significant progress can be made in this area, the general knowledge of the regulation of PRMTs needs to be dramatically increased. In fact, despite the large number of pathways known to be affected by arginine methylation, very little is currently known about how arginine methyltransferase activity is affected by protein regulators.

Nine PRMT isoforms have been described in humans, and four have been described in *Saccharomyces cerevisiae* (Rmt2, Hsl7, Sfm1, and Hmt1)(12). Each of the yeast PRMTs exhibits unique product specificity (Figure 4-1). Rmt2 is a type IV PRMT that methylates the δ -nitrogen of arginine, an activity currently observed only in yeast (13). Hsl7 is a type II PRMT capable of forming monomethylarginine (MMA) and symmetric dimethylarginine (sDMA) (14). Sfm1 is a SPOUT methyltransferase family member tentatively classified as a type III PRMT, since only MMA formation has been observed (15). Hmt1, the predominant *S. cerevisiae* arginine methyltransferase, is a type I PRMT capable of both MMA and asymmetric dimethylarginine (aDMA) formation. Hmt1, like its human homolog PRMT1, is responsible for most PRMT activity in *S. cerevisiae*, accounting for about 66% of all MMA and 89% of all ADMA formed *in vivo* (16,17). While the number of identified Hmt1 substrates continues to grow (18), the best characterized substrates are RNA binding proteins such as Npl3 and Hrp1. Although the full effect of methylation on such proteins is still unclear, Hmt1 activity has been shown to

facilitate the export of mRNA-shuttling proteins from the nucleus, thus implicating Hmt1 methylation in nucleocytoplasmic RNA transport (19). Given that Hmt1 is the only known type I PRMT in *S. cerevisiae* and seems to function as the work horse of yeast arginine methylation, Hmt1 serves as a good model on which to study how other proteins are able to regulate PRMT activity. In all organisms, only a handful of proteins have been reported to modulate PRMT1 activity. In *S. cerevisiae*, the Air1 protein is the only protein to have a proven role in regulating yeast arginine methylation (20).

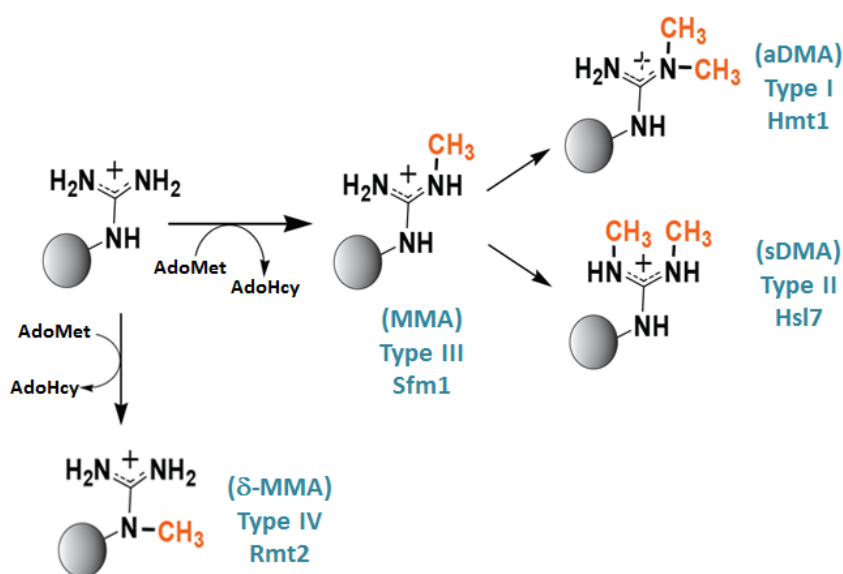


FIGURE 4-1. Reactions catalyzed by yeast protein arginine methyltransferases. Four types of PRMTs are present in yeast and are classified by the products formed. The type I PRMT, Hmt1 can form MMA and aDMA. The type II Hsl7 can form MMA and sDMA. The Sfm1 protein has only been found to catalyze MMA formation and is classified as a type III. The type IV Rmt2 catalyzes the monomethylation of the δ -nitrogen of arginine, making δ -MMA.

Air1 and Air2, or Arginine methyltransferase-interacting RING finger proteins 1 and 2, were discovered in 2000 by Inoue *et al.* in a study aimed at finding Hmt1-interacting proteins in *S. cerevisiae* (20). This report went on to show that Air1 can inhibit Hmt1 methylation of the Npl3 protein, both *in vivo* and *in vitro* (20). Although not specifically tested, the high degree of similarity between Air1 and Air2, along with functional overlap suggested from single and double knockout experiments in which severe growth defect was observed only when both proteins were absent, led to the suggestion that Air1 and Air2 may both regulate Hmt1 activity (20). Even though this discovery occurred over a decade ago, the interaction has not been explored further until now.

The primary function of the Air1/2 proteins is within the TRAMP (Trf5(4)/Air1(2)/Mtr4 polyadenylation) complex. The TRAMP complex is an essential exosome cofactor that is able to recognize a wide variety of RNA substrates including aberrant forms of tRNAs, rRNA processing intermediates, snoRNAs, and cryptic unstable transcripts (21-24). The TRAMP complex recognizes a particular RNA substrate and adds a short poly-adenylate tail to the 3' end of the RNA, stimulating it for degradation by the nuclear exosome (Figure 4-2) (23,25).

The nuclear exosome is conserved in eukaryotes from yeast to humans, and homologs of TRAMP components are found in many organisms as well, including humans (26,27). In the TRAMP complex, Mtr4 is a helicase which unwinds substrate RNA secondary structure before delivery to the exosome. Trf5 and Trf4 are RNA specific poly(A) polymerases that add short (4-5) poly(A) tails to the 3' end of the RNA substrate which targets the RNA for degradation; either one can be found as part of the TRAMP

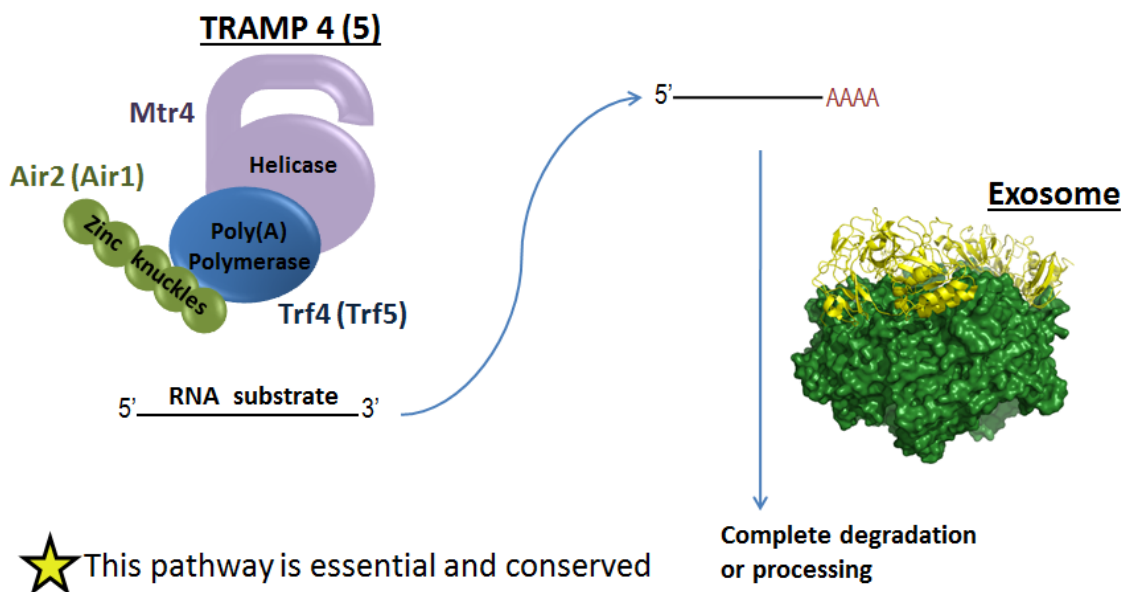


FIGURE 4-2. The TRAMP complex is an essential nuclear exosome cofactor. The TRAMP complex is composed of Trf4/5, Air1/2, and the Mtr4 helicase. TRAMP adds short poly(A) tails to the 3' end of substrate RNA, which targets the RNA for degradation by the exosome.

complex. The homologs Air1 and Air2 are putative RNA binding proteins with 45% sequence similarity, each composed of a core (68% sequence identity in core) containing five zinc knuckle motifs (C-X₂-C-X₄-H-X₄-C) flanked by extended N- and C-terminal sequences which are predicted to be largely unstructured (Figure 4-3). The zinc knuckle (also commonly called zinc finger) motifs are typically found to fold into reverse turns, coordinating a zinc ion using one histidine and three cysteine residues, and are known for their ability to bind RNA (28,29), although these motifs have been shown to bind DNA and proteins as well (30-32). Either Air1 or Air2 can be found as part of the TRAMP complex, suggesting they may be functionally redundant in this complex. One of the most intriguing questions regarding the TRAMP complex is how it is capable of identifying a

vast number of RNA targets which have no obvious sequence or secondary structure in common. The Trf4/5 proteins lack a recognizable RNA binding motif, suggesting that it is the Air1/2 proteins that provide RNA binding function, likely through the use of the zinc knuckle motifs. Recently, a crystal structure of the catalytic core of Trf4 and a fragment of Air2 (zinc knuckles 4 and 5) showed that these two zinc knuckles serve in the interaction of Air2 with Trf4 (32). This study was also able to demonstrate that *in vitro*, zinc knuckle one of Air2 enhances polyadenylation of some tRNAs by Trf4. This is the only report that has shown any part of Air2 being involved in substrate discrimination. Presumably, Air1 would interact with Trf5 in a very similar manner. While the role Air1/2 play in substrate recognition as part of the TRAMP complex is still not fully understood, the regulation of Hmt1 by the Air1/2 proteins creates an interesting link between nuclear RNA surveillance and Hmt1 methylation. Therefore, understanding how the Air1/2 proteins function to regulate Hmt1 activity will not only yield valuable information regarding PRMT regulatory mechanisms, but given the role of Hmt1 in facilitating mRNA export, regulation by the Air proteins which have an established role in RNA surveillance hints at a functional role for Hmt1 in the RNA regulation of *S. cerevisiae*.

In order to understand Hmt1 regulation by the Air1/2 proteins, I have worked in collaboration with the Johnson lab (Utah State University) whose main research focus is the TRAMP complex, to express and purify recombinant Air1 and Air2 for methyltransferase inhibition studies. Several constructs of both Air1 and Air2 were created to map the areas of interaction with Hmt1, and to determine the minimal region necessary for Hmt1 inhibition. The solubility and stability of the Air proteins proved to be the limiting

A

```

AIR1      MSTLLSEVESIDTLPYVKDTPPTGSDSSSFNKLAPSIEDVDANPEELRTLRLGQGRYFGI 60
AIR2      -----MEKNTAPFVVDTAPTTP-----DKLVAPSIEEVNSNPNELRALRGQGRYFGV 48
           . * *:* *:* *:* * * * * * * * * * * * * * * * * * * * * * * * * *
           : * *:* *:* *:* * * * * * * * * * * * * * * * * * * * * * * * * *

AIR1      TDYDSNGAIMEAEPKCNNCSQRGHLKRNCEHVICTYCGFMDDHYSQHCKAIICTNCNAN 120
AIR2      SDDDDK-AIKEAAPKCNNCSQRGHLKRDCEHIICSYCGATDDHYSRHCCKAICCSKCDEV 107
           : * * * * * * * * * * * * * * * * * * * * * * * * * * * * * * * *
           : * * * * * * * * * * * * * * * * * * * * * * * * * * * * * * * *

AIR1      GHYKSCCPHKWKKVFCCLCNPKRHSRERCESIWRSYLLKTKD--ANQGFDFQTFVSYNC 178
AIR2      GHYRSCCPHKWKKVFCCLCNPKRHSRERCESIWRSYLLKTKD--ANQGFDFQTFVSYNC 167
           * * * * * * * * * * * * * * * * * * * * * * * * * * * * * * * *
           * * * * * * * * * * * * * * * * * * * * * * * * * * * * * * * *

AIR1      GNAGHFGDDCAERRSSRPVNTDGSFACDNLATKFKQHYFNQLKDYKREASQRQHFNDNEH 238
AIR2      GKGHFGDDCAEKRSSRPVNTDGSFACDNLATKFKQHYFNQLKDYKREASQRQHFNDNEH 218
           * . * * * * * * * * * * * * * * * * * * * * * * * * * * * * * * *
           * . * * * * * * * * * * * * * * * * * * * * * * * * * * * * * * *

AIR1      EFNLLDYEYNDDAYDLPGSRTYRDKMKWKGKQVSTRKNSSNNRYESSNNRK--KKS PFS 296
AIR2      DYQFSES IYDEDPLRPSHKRHSQNDHSHSGRNKRASNFHPPPYQKSNVIQPTIRGETL 278
           : : : : * : : * . * : : : : : : : : : : : . * . * * * * * : :

AIR1      AQNYKVTNKRKRVQTHPLDFPSSQNNRNTDYSSQFSYNRDDFFKGPKNKRGRSSS-NKSQ 355
AIR2      SLNNNISKNRYQNTKVNVSISSENMYGSRYNPSTYVDNNSISNSNSNYRNYNSYQPYRSG 338
           : * : : * * * * * . : : : . * * * . * * * . : : : : : : : . * . : *

AIR1      RNGRY- 360      Zinc knuckle = Cys-X1-2-Cys-X4-6-His-X4-Cys
AIR2      TLGKRR 344
           * :

```

B



FIGURE 4-3. Air1 and Air2 sequence alignment. Both Air1 and Air2 contain five zinc knuckle motifs within their core region. These are flanked by N-terminal and C-terminal sequences predicted to be primarily unstructured.

factor for these studies, and therefore a full characterization of the mode of inhibition could not be attained. However, attempts to determine the molecular level details of the interaction between Hmt1 and the Air proteins via co-crystallization have shown significant promise and will be the focus of future efforts.

EXPERIMENTAL PROCEDURES

Materials— AdoMet was purchased from Sigma as a chloride salt ($\geq 80\%$, from yeast). [^3H]AdoMet (83.1 Ci/mmol) was purchased from Perkin Elmer. ZipTip[®]_{C4/C18} pipette tips were purchased from Millipore. The R3 (acGGRGGFGRGGFGRGGRG),

JMH1W (KGGFGGRGGFGGKW), and RKK (GGRGGFGGKGGFGGKW) peptides were synthesized by the Keck Institute (Yale University) and purified to $\geq 95\%$.

Expression and Purification of Hmt1— *E. coli* BL21 cells expressing His₆-tagged Hmt1 were grown in Luria Broth media at 37° C to OD₆₀₀ reached 0.6, followed by induction with 0.5mM IPTG at 22° C for 20 hours. Cell pellets were resuspended in two times cell volume lysis buffer (50 mM sodium phosphate pH 7.5, 100 mM NaCl, 20 mM imidazole) and lysed using sonication. The cell lysate was clarified via centrifugation and incubated with Nickel resin (GoldBio) in a 1:1 cell mass: resin ratio for 1-2 hours at 4° C. The resin was washed eight times with eight column volumes of lysis buffer modified to contain 500 mM NaCl, followed by three washes with eight column volumes of wash buffer (50 mM sodium phosphate pH 7.5, 100 mM NaCl, 70 mM imidazole). The protein was then eluted off the resin five times with two column volumes of elution buffer (50 mM sodium phosphate pH 7.5, 100 mM NaCl, 250 mM imidazole). Elutions were pooled and dialyzed into 50 mM Hepes pH 7.5, 10% glycerol. The protein was then concentrated, aliquoted, and flash frozen in liquid nitrogen prior to storage at -80° C.

Expression and Purification of Air Proteins (Done by Johnson lab)— Air1 and Air2 constructs were created, expressed, and purified in the Johnson Lab as previously described (33). In brief, His₆-tagged and His₆_TEV_FLAG-tagged (HTFlag) codon optimized Air1 and Air2 constructs were created. Expression constructs were transformed into in BL21 (DE3) codon+ RIL *E. coli* cells (Agilent Technologies). Overnight starter cultures were grown at 37° C in 30 ml LB media supplemented with 250 μ M ZnSO₄ and appropriate antibiotics. Approximately 5 ml starter culture was used to inoculate each 500

ml LB growth flask that had also been supplemented with 250 μM ZnSO_4 and appropriate antibiotics. The cell growths were incubated at 37° C until OD_{600} reached 0.6-0.8, at which point protein expression was induced with the addition of 0.3 mM IPTG. The cultures were then incubated at room temperature for 16 hours, harvested by centrifugation, and dry cell pellets were stored at -80° C until used.

To purify the Air1/2 protein constructs, cells were resuspended in lysis buffer (50 mM Hepes pH 7.5, 500 mM NaCl, 2 mM β -mercaptoethanol, 200 μM ZnSO_4 , 10% glycerol, 10 mM imidazole, 1 $\mu\text{g/ml}$ aprotinin, 1.4 $\mu\text{g/ml}$ pepstatin, 1 $\mu\text{g/ml}$ leupeptin, and 0.2 mg/ml lysozyme), using 3 ml of buffer for every gram of cells. Cells were lysed by sonication and cleared lysate was incubated with 5 ml GoldBio or GE Nickel affinity resin for 1 hour at 4° C. The Nickel resin was then washed with 700 ml lysis buffer (without protease inhibitors or lysozyme), followed by 200 ml of high salt buffer (50 mM Hepes pH 7.5, 1 M NaCl, 2 mM β -mercaptoethanol, 200 μM ZnSO_4 , 10% glycerol) and then low salt buffer (100 ml of 50 mM Hepes pH 7.5, 150 mM NaCl, 2 mM β -mercaptoethanol, 200 μM ZnSO_4 , 10% glycerol). The protein was then eluted from the resin three times with 20 ml of 50 mM Hepes pH 7.5, 150 mM NaCl, 2 mM β -mercaptoethanol, 200 μM ZnSO_4 , 10% glycerol, 500 mM imidazole, allowing the elution buffer to incubate with the resin for 5 minutes prior to elution. The three Nickel elutions were then pooled and loaded onto a 5 ml Heparin column (GE), which was then run using a 100 ml gradient from 0 to 100% low salt to high salt buffer as used in the Nickel step, except without ZnSO_4 present. For inhibition studies, the protein peaks were then collected, concentrated and buffer exchanged in a 10kDa cutoff concentrator (Millipore) to the low salt buffer. The

concentrated to protein (~ 0.5 mg/ml) were then be aliquoted and flash frozen in liquid nitrogen prior to storage at -80° C.

For the constructs Air2 N-ZnK5, Air2 N-ZnK3, and Air1 ZnK4-5, the proteins were purified on Nickel resin as noted above, but then loaded onto a 5 ml MonoQ column (GE) instead of Heparin. The contaminants would bind to the column while these constructs would not. Therefore, the flow through would be collected, concentrated, buffer exchanged, and frozen as described above.

It should also be noted that all Air1/2 inhibition data shown in this chapter corresponds to His₆-tagged Air1/2 constructs. HTFlag constructs were used for binding studies and were also tested for inhibition but no effect was detected with any HTFlag Air1 constructs, indicating this longer tag was somehow able disrupt the Air1 inhibition of Hmt1.

Expression and Purification of Npl3— His₆-tagged full length Npl3 (pAM436) was a generous gift from Dr. Ann McBride (Bowdoin University). *E. coli* BL21 NiCo21 (DE3) cells expressing His₆-Npl3 protein were grown in Luria Broth media at 37° C until OD₆₀₀ reached 0.6, followed by induction with 0.5 mM IPTG at 22° C for 20 hours. Cell pellets were resuspended in two times cell volume lysis buffer (50 mM sodium phosphate pH 7.5, 500 mM NaCl, 20 mM imidazole) and lysed by sonication. The cell lysate was clarified via centrifugation and incubated with Nickel resin (GoldBio) in a 2:1 cell mass to resin ratio for 1-2 hours at 4° C. The resin was washed eight times with eight column volumes of lysis buffer, followed by three washes with eight column volumes of wash buffer (50 mM sodium phosphate pH 7.5, 100 mM NaCl, 70 mM imidazole). The protein

was then eluted off the resin five times with two column volumes of elution buffer (50 mM sodium phosphate pH 7.5, 100 mM NaCl, 500 mM imidazole). Elutions were pooled, filtered and further purified using MonoQ and Heparin columns (GE) in tandem. Fractions containing Npl3 were pooled and dialyzed into 50 mM Hepes pH 7.5, 10% glycerol. The protein was then concentrated to ≥ 1 mg/ml, beaded in liquid nitrogen, and stored at -80° C.

Methyltransferase Activity Assay— A quantitative methylation assay using ZipTip_{C4/C18} pipette tips was used in testing the enzymatic activity under steady-state conditions (34). Briefly, methyltransferase activity was tested with 100 nM Hmt1, 2 μ M AdoMet (1 μ M [³H]AdoMet), 380 nM BSA, and 10 nM MTAN (5'-methylthioadenosine /S-adenosylhomocysteine nucleosidase) in 50 mM sodium phosphate (pH 8.0), initiated with 500 nM Npl3 protein substrate at 30° C. When present, 500 nM Air1/2 (various constructs) was added to the reaction mixture and allowed to incubate for 10 minutes on ice prior to initiation with substrate. When used, EDTA was present at a 1 mM final concentration and RNase at 15 μ g/ml. At different time points, 5 μ l samples were removed from reactions, quenched to stop the reaction, and processed with ZipTip_{C4/C18} pipette tips to separate the unreacted [³H]AdoMet from the radiolabeled product.

Co-expression and Purification of His₆ Air2 and Δ N22+2 Hmt1— A pETDuet construct containing codon optimized Air2 N-ZnK5 in cloning site 1 (His₆-tag) and untagged Hmt1K13S in cloning site 2 was obtained from the Johnson lab. The Hmt1K13S protein was removed from cloning site 2 using the NdeI and XhoI restriction sites. A Δ N22+2 Hmt1 construct was received from Dr. Anne McBride (Bowdoin University) and was used as a template for PCR amplification with primers containing a 5' NdeI site and a

3' XhoI site. This PCR product was ligated into the pETDuet cloning site 2 to create a pETDuet vector which co-expressed His₆-Air2 N-ZnK5 and untagged Δ N22+2Hmt1.

The Air2- Δ Hmt1 construct was transformed into BL21 (DE3) codon+ RIL *E.coli* cells. A single colony from a fresh transformation plate was used to inoculate a 50 ml LB overnight culture supplemented with 250 μ M ZnSO₄ and antibiotics (ampicillin and chloramphenicol). Approximately 5 ml of the starter culture was used to inoculate each of six 500 mL cultures of LB media (also containing 250 μ M ZnSO₄) in 2.5 L baffled flasks. The cell cultures were incubated at 37° C at 300 rpm until an OD₆₀₀ of 0.3 was reached. Protein expression was induced by adding 0.05 mM IPTG. The cultures were then moved to a room temperature shaker and adjusted to 200 rpm for 20 hours. The cells were then harvested by centrifugation and stored at -80° C until used.

About 21 g of cells were resuspended in 63 ml of lysis buffer containing 50 mM Tris pH 7.5, 50 mM NaCl, 200 μ M ZnSO₄, 1 μ g/ml aprotinin, 1.4 μ g/ml pepstatin, 1 μ g/ml leupeptin, and 0.2 mg/ml lysozyme. The cells were lysed by sonicating at 6/80 four times for 20 pulses with 30 second rest on ice in between. The cleared lysate was incubated with 12 ml Nickel resin in six 15 ml conical tubes (GoldBio) which had been previously equilibrated with buffer 1 (50 mM Tris pH 7.5, 50 mM NaCl, 200 μ M ZnSO₄) for 1 hour at 4° C. The resin was then washed fourteen times with 7 ml buffer 1 per tube. Two washes were done with 5 ml per tube of 50 mM Tris pH 7.5, 150 mM NaCl, 200 μ M ZnSO₄, 5 mM imidazole. The protein complex was finally eluted with 3 ml per tube of elution buffer (50 mM Tris pH 7.5, 50 mM NaCl, 200 μ M ZnSO₄, 250 mM imidazole, 5 mM β -mercaptoethanol). The elutions were filtered and loaded onto a 5 ml Heparin column (GE) at 3 ml/min. Although some Air2 protein stuck to the Heparin column, the complex was

found in the unbound fraction which was concentrated down to 5 ml total volume using a 30 kDa cutoff concentrator (Millipore). The 5 ml of concentrated Air2/ Δ Hmt1 complex was loaded onto a 120 ml size exclusion column (HiLoadTM 16/60 SuperdexTM 75 prep grade (Amersham)) equilibrated with 50 mM Tris pH 7.5, 50 mM NaCl, 200 μ M ZnSO₄, 5 mM β -mercaptoethanol, 10% glycerol and run at 1 ml/min for 270 minutes while collecting 3 ml fractions. Fractions 18, 17, and a combination of 14-16 and 19-20 were each separately concentrated to \geq 20 mg/ml (F17 seemed to have a 2:1 Hmt1 to Air2 ratio; F18 had an approximately 1:1 ratio). Final concentrations were: F17 = 27.44 mg/ml, F18 = 23.7 mg/ml, and the mixed fractions = 22.3 mg/ml. Each was used to set up crystal trays immediately upon concentrating and the leftover protein was flash frozen in 200 μ l aliquots and stored at -80° C. Attempts to optimize crystallization conditions used frozen protein from each batch. No significant difference was observed in the ability to form crystals between the three batches of protein. Prior freezing of the protein complex also did not seem to deter crystal formation or crystal quality.

Crystallization, Crystal Optimization, and Data Collection of Air2/ Δ Hmt1 Complex— Concentrated Air2 (N-ZnK5) and Δ N22+2 Hmt1 described above was used for sitting-drop vapor diffusion crystallization screening trials using an Art Robbins Gryphon LCP Crystallization Robot (Art Robbins Instruments) located in the Johnson lab. Intelli-plate 96-well crystallization plates (Art Robbins Instruments) were used for crystallization trials. Five different crystallization screens each containing 96 individual crystallization solutions were used to set up five 96-well crystallization plates for each concentrated complex fraction. The crystallization screens used were the MCSG suite (Microlytic) which consist of four different screens (MCSG 1-4), and the Index screen

(Hampton Research). Crystallization plates were incubated at 4° C. After one week protein crystals were observed in many crystallization conditions and the best looking crystals were analyzed for diffraction quality using a home-source X-ray generator (MicroMax-007HF) and detector (Rigaku R-Axis IV++), as well as being subjected to washing with crystallization solution, run on an SDS-PAGE gel and stained with SYPRO Ruby (Sigma) to determine the presence of both proteins in the crystal. Several analyzed crystals were salt, but the majority were poor diffracting ($> 15 \text{ \AA}$) protein crystals. One condition from the Index screen, position H7 (0.15 M D, L-Malic Acid pH 7.0, 20% PEG3350) showed the best diffraction quality ($\sim 10 \text{ \AA}$) and contained both proteins as shown by gel analysis.

Additional 24-well hanging drop trays were set up to screen around this condition: (D, L Malic Acid pH 7.0 was varied from 0.1 M to 0.225 M; the pH was also varied to 6.5, 7.5, and 8.2; PEG 3350 concentrations were varied from 19% to 20.5%). In addition, two hanging drop hand trays were set up with the original Index H7 condition to test the effect of additives. Using the F18 protein complex in a 1:3 and 2:2 protein to well solution ratio with a total drop volume of 4.5 μl which included 0.5 μl of additive from the Hampton Research Additive Screen (HR2-428), four drops were set up per well containing 500 μl of 0.15 M D, L-Malic Acid pH 7.0, 20% PEG 3350. These trays were placed at 4° C and crystals were noted after two days. Two additive conditions in the 1:3 ratio tray produced large crystals which were analyzed for diffraction quality. The addition of 1 M tri sodium citrate yielded crystals diffracting to 8 \AA , while the addition of 1 M NDSB-256 improved diffraction to $\sim 5 \text{ \AA}$. Another hanging drop vapor diffusion tray was set up using 0.15 M D, L-Malic Acid pH 7.0, 20% PEG 3350 as the well solution with both 1 M tri sodium citrate and 1 M NDSB-256 additives in varying ratios, along with different drop ratios and

different well solution volumes. Since most of these conditions produced crystals, the best from each were flash frozen in a cryo buffer supplemented with 7.5% glycerol and were sent to the Stanford Synchrotron Radiation Lightsource (SSRL) for data collection. Ultimately, a 3.2 Å resolution dataset was collected from a crystal grown for 2 days at 4°C in a 4.5 µl drop containing 1 µl protein complex (F18 fraction), 3 µl 0.15 M D, L-Malic Acid pH 7.0, 20% PEG 3350, and 0.5 µl 2 M NDSB-256 additive. Additionally, an X-ray excitation scan was conducted on this crystal at SSRL which detected the presence zinc ions, suggesting that the crystal contained Air2 zinc knuckles. Molecular replacement was performed using Phaser (35) from the Phenix program suite (36). The search model used was Δ N22+2 Hmt1 hexamer (Protein Data Bank entry 1G6Q).

RESULTS

Air1 and Air2 Interact With Hmt1— The only report of the interaction between the Air1/2 proteins and Hmt1 found that Air1 binds directly with Hmt1 and at least the first 56 amino acids of Hmt1 are essential for the binding of Air1 (20). However, the regions of Air1 necessary for binding Hmt1 were not indicated. Additionally, although it was suggested that Air2 would likely function in a manner similar to Air1, Hmt1 inhibition or binding by the Air2 protein was never proven. Therefore, a partnership was established with the Johnson lab at Utah State University in order to identify the regions of Air1, and possibly Air2, required for Hmt1 binding. Using the few predicted structural features of Air1/2 as a guide (ZnK), several truncated Air1 and Air2 constructs were created and tested for their ability to complex with Hmt1 (Figure 4-4-A). It was first established that without

the extended C-terminal region, both Air1 and Air2 are able to form a stable complex with Hmt1. The Johnson lab was able to perform *in vitro* pull-down experiments to show that truncated Air1 constructs are able to bind Hmt1 (Figure 4-4-B). Notably, the Air1 protein region spanning zinc knuckles 4 through 5 is enough to form a stable complex with Hmt1, although this does not discount binding by other regions of Air1. Size exclusion chromatography studies further established that an Air2 N-ZnK3 construct is sufficient to form a stable complex with Hmt1 *in vitro* (Figure 4-4-C), indicating that while Air2 region spanning zinc knuckles 4 through 5 may interact with Hmt1, this region is not necessary for stable complex formation. Due to protein availability, it has not been possible to determine whether this region alone is able to bind Hmt1. Future studies should attempt to clarify whether Air1 and Air2 indeed utilize the same regions for Hmt1 binding. Additionally, isolating minimal binding regions of the Air1/2 proteins would facilitate quantitative analyses of the binding interactions (as well as potentially enable further characterization of the mechanism of Hmt1 inhibition), and may prove promising for use in crystallization trials to determine exactly how Air1/2 and Hmt1 interact at the molecular level.

Characterization of the Differential Effects of Air1 and Air2 on Hmt1 Activity—

Although full length Air1 was previously confirmed to inhibit Hmt1 methylation of Npl3 both *in vitro* and *in vivo* (20), the suggested regulatory role of Air2 on methyltransferase activity was never verified. C-terminal truncated constructs of Air1 and Air2 generated by the Johnson lab were used in conjunction with an *in vitro* methyltransferase assay developed in the Hevel lab to test their effect on the Hmt1 methylation of Npl3. As depicted

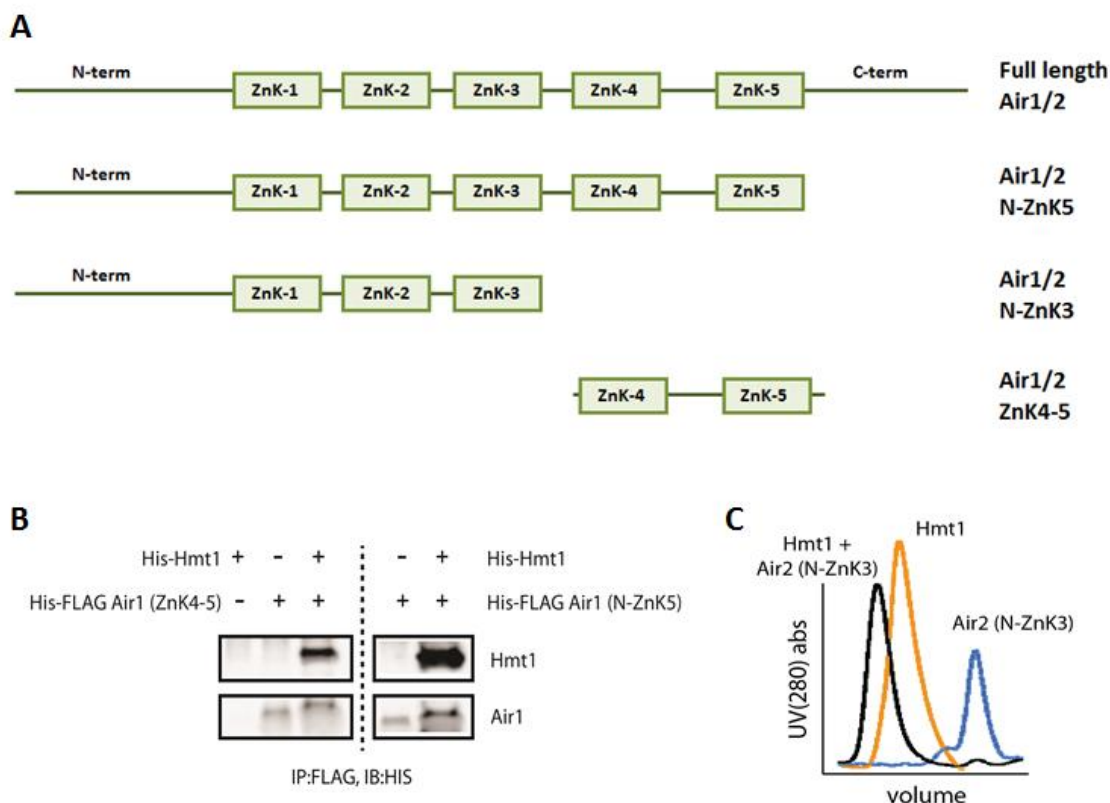


FIGURE 4-4. Air1 and Air2 truncated constructs used to test binding to Hmt1 and the ability to inhibit Hmt1 activity. (A) Air1 and Air2 truncated constructs are shown. All were made with both His₆ and His₆-TEV-FLAG tags. (B) FLAG-tagged Air1 N-ZnK5 and Air1 ZnK4-5 pull down Hmt1 on FLAG resin. Samples were run on SDS-PAGE and visualized by anti-His antibody. (C) Purified Hmt1 and Air2 N-ZnK3 co-elute on a size exclusion column, forming a complex with apparent 1:1 stoichiometry.

in Figure 4-5, we were able to show that Air1 N-ZnK5, even without the C-terminal region is able to inhibit Npl3 methylation by Hmt1. In contrast, the Air2 N-ZnK5 construct has no significant effect on the ability of Hmt1 to methylate Npl3 (Figure 4-5). This result highlights a clear functional difference between the Air proteins.

Characterization of Air1 Inhibition of Hmt1 Activity— Once Air1 regulation of Hmt1 was confirmed, the next step was to characterize what features of Air1 are needed

for inhibition of Hmt1. Air1 has no predicted secondary structure, other than the five zinc knuckle motifs which are thought to primarily enable Air1 to bind RNA (37,38). Zinc knuckles 4 and 5 of Air2 have also been shown to participate in protein-protein binding interactions with Trf4, and are believed to also mediate Air1 interactions with Trf5 (32). We therefore set out to determine whether RNA-binding or zinc-binding by the Air1 protein are necessary for Hmt1 inhibition. Our preliminary results (Figure 4-6) show that treatment with RNase has no significant effect on the regulation of Hmt1 activity by Air1. However, treatment with EDTA to remove the zinc coordinated by the zinc knuckle motifs completely abolished the ability of the Air1 protein to inhibit methyltransferase activity (Figure 4-6). Therefore, we conclude that while RNA binding is not important for Air1 regulatory function, intact zinc knuckle motifs are required for Air1 to inhibit Hmt1 methylation of Npl3.

Given the significance of the Air1 zinc knuckle motifs for the regulation of Hmt1, we next set out to determine which zinc knuckles are necessary for this effect. Air1 constructs containing Air1 N-ZnK3 were unable to affect Hmt1 activity, while Air1 N-ZnK5 and, importantly, Air1 ZnK4-5 constructs were able to inhibit methylation of Npl3 (Figure 4-7). These results indicate that the minimal region of Air1 required for Hmt1 regulation lies within the ~60 amino acid region between zinc knuckles 4 and 5. Significantly, this is the same region known to regulate the interaction of Air2 with Trf4 (32). *In vivo*, Air1 and Air2 are predicted to be the limiting components of the TRAMP complex (39). Therefore, the revelation that the same region of Air1 necessary to inhibit Hmt1 activity is seemingly required for interaction with Trf5 are puzzling, especially with

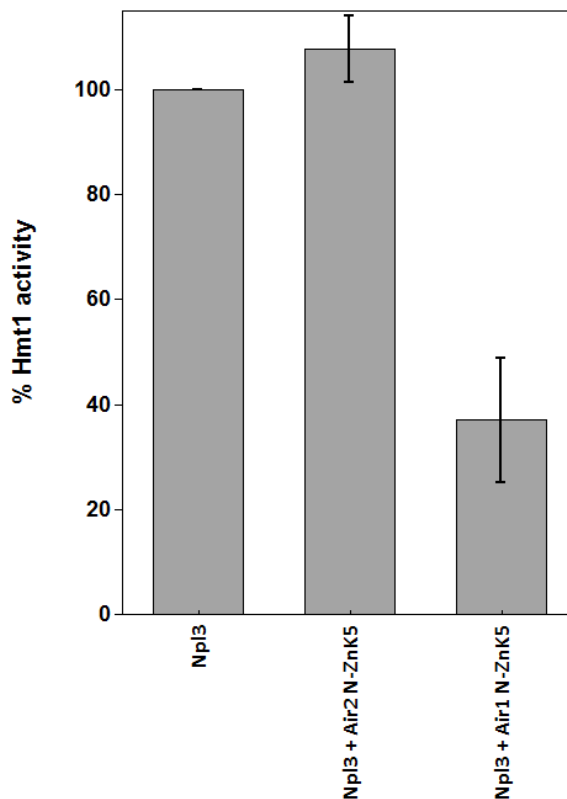


FIGURE 4-5. Effect of Air2 and Air1 on the methylation of Npl3 by Hmt1. The rate of Hmt1 activity on Npl3 was normalized to 100%. The addition of Air2 N-ZnK5 slightly enhanced the rate of Npl3 methylation, but only as typically observed upon the addition of more total protein (same as BSA addition, data not shown). The addition of Air1 N-ZnK5 inhibited activity of Hmt1 on Npl3. Data shown is average of minimum two replicates.

no known evidence that either Air1 or Air2 may exist independently of Trf5 or Trf4 in the cell. The potential puzzle aside, the results discovered here may provide an opportunity to further narrow the regions of Air1 required for Hmt1 inhibition. Since Air2 does not inhibit Hmt1, the residues between zinc knuckles 4 and 5 of Air1 that are not conserved in Air2 and that are not Trf4/5 binding residues are likely to be the ones responsible for the inhibition of Hmt1 (Figure 4-8). Future studies should target these residues. Through either

alanine scanning, or the construction of chimeric Air1/2 proteins, it should be possible to define the sequences required for Hmt1 inhibition.

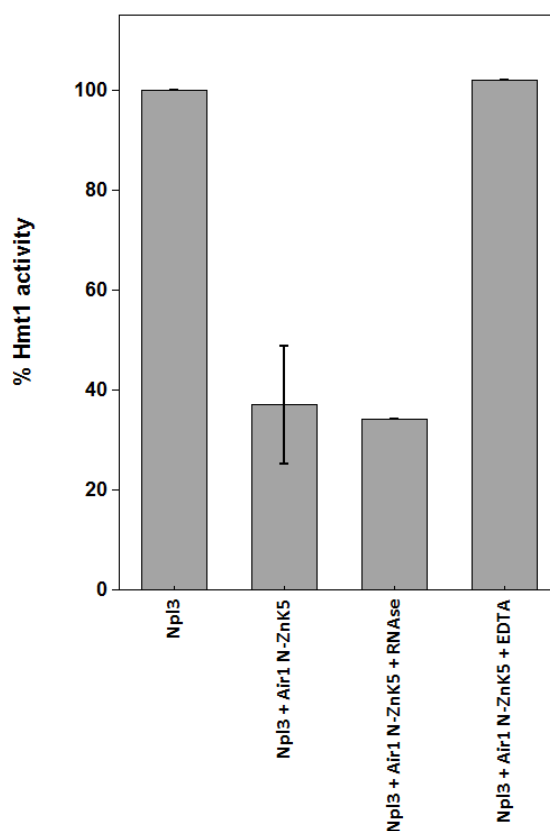


FIGURE 4-6. Air1 zinc binding is required for inhibitory effect on Hmt1. The percent inhibition by Air1 N-ZnK5 on Hmt1 activity is unchanged by the addition of 15 μ g RNase. The addition of 1 mM EDTA chelates the zinc from the Air1 protein and abolishes inhibition of Hmt1 activity. Single activity measurements shown for the addition of RNase and EDTA.

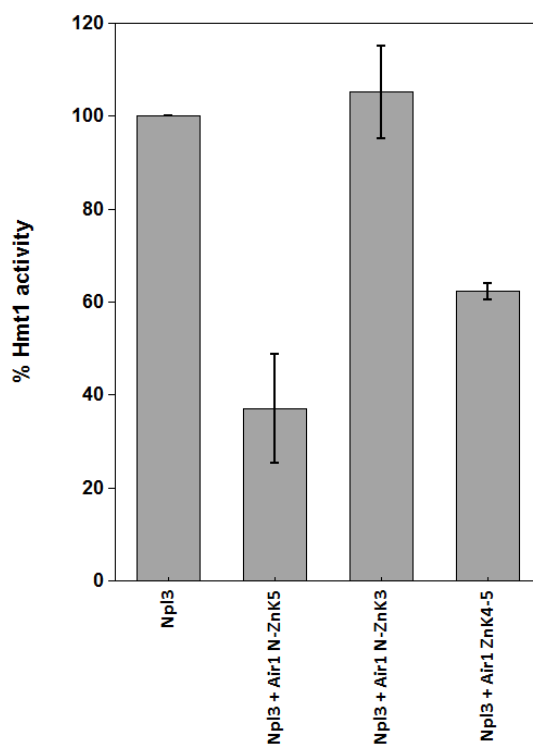


FIGURE 4-7. Air1 zinc knuckles 4 and 5 are required for Hmt1 inhibition. An Air1 construct missing zinc knuckles 4 and 5 (Air1 N-ZnK3) is unable to inhibit Hmt1 activity, while ~60 amino acid region containing Air1 ZnK4-5 alone is shown to retain the inhibitory effect.



FIGURE 4-8. Sequence alignment of Air2 and Air1 zinc knuckles 4 through 5. Strictly conserved residues are colored in blue while semi-conserved residues are in light blue. Dark blue triangles above indicate Air2 residues shown to interact with Trf4 (PDB: 3NYB). Red arrows indicate residues that are not conserved between Air1 and Air2, or required for interaction with Trf4 which should be targeted for mutagenesis.

Characterization of the Hmt1-Air Interaction Through Crystallography— A

crystallographic approach was also pursued to determine the molecular details of the interaction between the Air proteins and Hmt1. The Hmt1 protein has been previously crystallized with an N-terminal truncation shown to improve crystal formation and diffraction (40). The Johnson lab created several constructs for the co-expression of Air2 and full-length Hmt1 and were successful in obtaining crystals of the complex. However, these crystals had poor diffraction quality and could not be used to solve a structure of the complex (33). Using the Johnson lab constructs, purification strategy, and crystallization conditions as a guide, I attempted to improve upon their efforts by using the N-terminally truncated Hmt1 construct that had been previously crystallized in order to enhance crystal diffraction.

A His₆-tagged Air2 N-ZnK5 construct was co-expressed with the Δ N22+2 Hmt1 construct that had been previously crystallized. Following the Johnson lab optimized purification strategy as a guide, $\geq 95\%$ clean Air2-Hmt1 complex was purified and used for crystallization trials. Hundreds of new conditions were screened for their ability to crystallize this complex, and while several resulted in protein crystals, none provided usable X-ray diffraction. We then turned to the crystallization condition previously used by the Johnson lab to generate 7 Å diffraction patterns and were able to get crystals that contained both proteins (Figure 4-9-A) and that diffracted out to about 10 Å (Figure 4-9-B). We then set out to optimize this condition to improve the diffraction quality. Ratios of reagents were varied without much improvement. Through the use of an additive screen (Hampton Research) we were finally able to produce crystals that diffracted at our home X-ray source out to 5 Å (condition: 1 μ l Air2/ Δ Hmt1 complex, + 3 μ l well solution (0.15

M D, L-Malic Acid pH 7.0, 20% PEG 3350) + 0.5 μ l additive (1 M NDBS-256)). Several crystals grown under these optimized conditions were then sent to the Stanford Synchrotron Radiation Lightsource (SSRL) where we were able to collect usable diffraction data out to 3.2 Å (Figure 4-9-C).

We have been able to solve a partial structure using molecular replacement to place six Δ N22+2 Hmt1 molecules into an electron density map. The previously solved Δ N22+2 Hmt1 structure was also a hexamer (40). As it stands, no Air2 has yet been built into the structure, but there are many areas of open density remaining where Air2 may be built. Of slight concern is the fact that the majority of the remaining density appears to have secondary structural features not expected to occur in Air2 (Figure 4-10). However, an X-ray excitation scan was conducted on the crystal at SSRL which detected the presence of zinc ions within the crystal. This, along with the previous detection of both Air2 and Hmt1 in a crystal under this condition (Figure 4-9-A), suggests that Air2 is present. Further work will be done to build Air2 into the existing electron density and finally decipher how Air2 interacts with Hmt1 at the molecular level.

Additional work currently underway in the Hevel lab will focus on using a similar strategy to solve the structure of Air1 N-ZnK5 or Air1 ZnK4-5 in complex with Δ N22+2 Hmt1. Such a structure will represent the first depiction of how Hmt1 is able to interact with another protein and will also provide the first molecular details of how Hmt1 can be regulated.

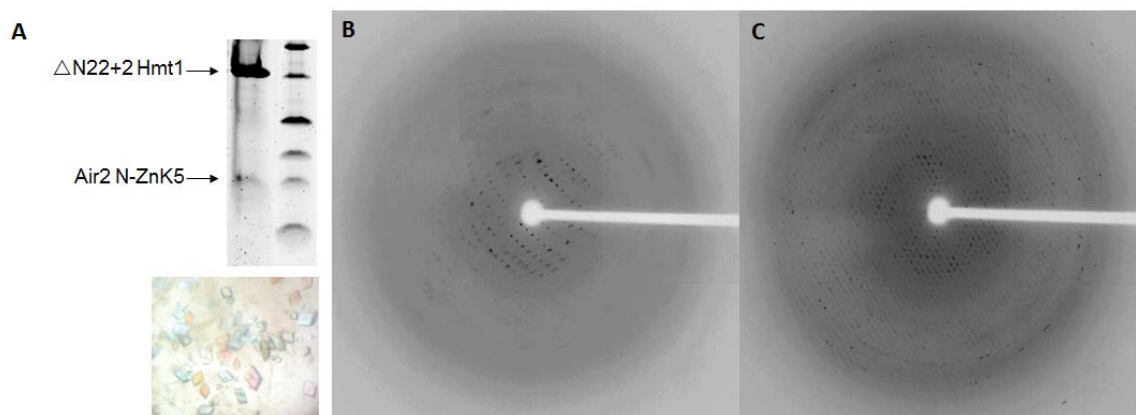


FIGURE 4-9. Air2 N-ZnK5 and $\Delta N22+2$ Hmt1 complex crystals and diffraction patterns. (A) SDS-PAGE analysis of crystal composition shows that both proteins are present in the crystals which are shown below. (B) Initial ~ 10 Å diffraction observed prior to optimization of crystallization conditions. (C) Typical diffraction image from 3.2 Å dataset collected after crystal optimization.

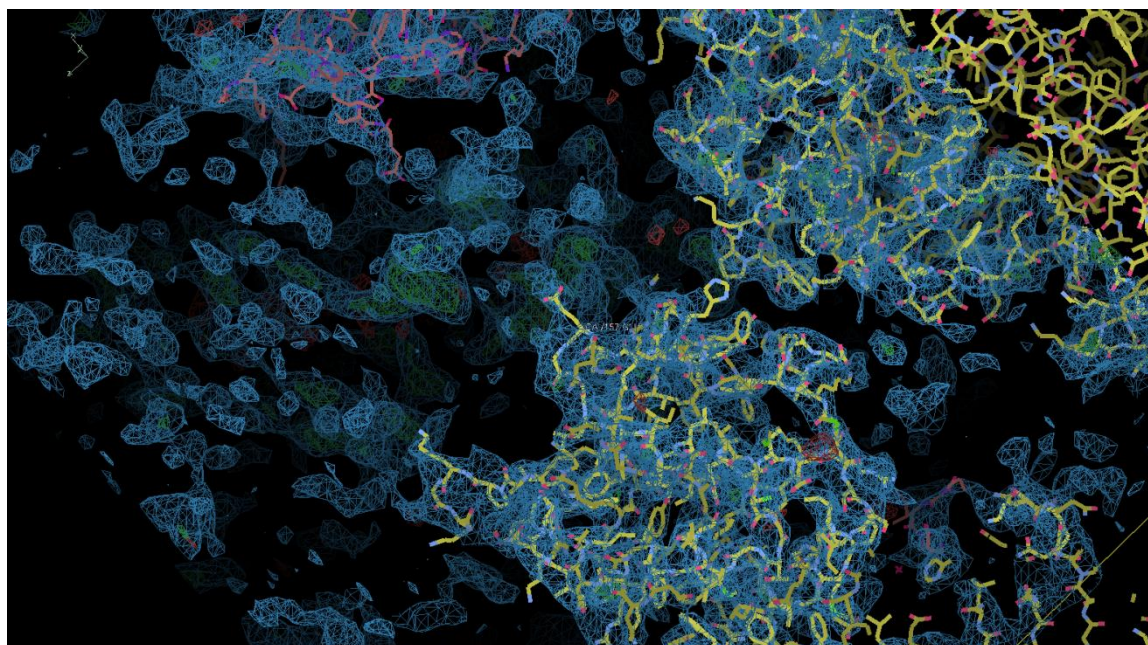


FIGURE 4-10. Initial Air2-Hmt1 electron density map created after molecular replacement using $\Delta N22+2$ Hmt1 hexamer as search model. Hmt1 hexamer is shown in yellow and symmetry molecules are shown in pink. Empty density will be examined and used to build the Air2 structure.

Table 4-1. Data collection statistics for Air2-Hmt1 crystal

Data Collection	
Space Group	C121
Cell dimensions	
<i>a</i> , <i>b</i> , <i>c</i> (Å)	239.4, 103.3, 118.1
α , β , γ (deg)	90.0, 91.97, 90
Resolution (Å)	50-3.45 (3.6-3.45) ^a
R _{sym}	0.224 (0.987)
<i>I</i> / σ <i>I</i>	6.64 (2.03)
Completeness (%)	99.8 (99.9)
Redundancy	6.5 (6.4)

^a Values in parenthesis are for highest-resolution shell.

DISCUSSION

This collaborative work has begun to examine the regulation of Hmt1 by the Air1/2 proteins. We have been able to determine the first functional difference between the Air proteins by showing that Air2 is unable to regulate the methylation of Npl3 by Hmt1 (Figure 4-5). It should be noted that regulation of Hmt1 by Air2 cannot be discounted since no other substrates have been tested. One approach to search for Hmt1 substrates that are methylated under the influence Air2 control is to use hypomethylated yeast cell extracts from an Air2-null background to test for Hmt1 activity in the absence and presence of Air2 in order to test whether Air2 may be a substrate-dependent Hmt1 regulator. Additionally, it was recently reported that Air2 is an Hmt1 substrate and can be methylated at two arginines on the C-terminal tail (41). Arginine methylation of the Air2 C-terminal tail was shown to increase the interaction between Air2 and Npl3 (41), indicating that this region, which was not included in any of the constructs tested in this work is important and should be retained in any future attempts to determine whether Air2 is able to regulate Hmt1.

We have been able to corroborate that Air1 regulates Hmt1 and have identified the region between zinc knuckles 4 and 5 as responsible for this regulatory effect (Figure 4-7). Although unable to fulfill the initial goal of characterizing the mechanism of inhibition (competitive vs. noncompetitive) due to limitations obtaining clean Air1 protein, we were able to narrow down the region responsible for inhibition to a ~60 amino acid stretch of Air1. Analysis of this region has allowed us to identify specific residues for targeted mutagenesis to learn their effect on Hmt1 activity. Additionally, smaller constructs (for example, Air1 ZnK4+linker4 and Air1 linker4+ZnK5) should be created to hone in on the minimal Air1 region required for Hmt1 regulation. Depending on the length of a minimal construct, peptides can be ordered and used to characterize the mechanism of inhibition if protein production continues to be an issue.

We confirmed that Air1 regulates the methylation of Npl3 (20). Only one additional protein substrate, histone H4, was tested in this work. H4 methylation was also inhibited by the presence of Air1 (data not shown). The methylation of all peptide substrates tested (JMH1W, R3, and RKK peptides) was also inhibited by Air1 (data not shown). However, as is the case with Air2, methyltransferase reactions should be performed on hypomethylated yeast cell extracts in the absence or presence of Air1 in order to fully assess if Air1 is a broad spectrum Hmt1 regulator or if the effects are substrate dependent.

A continuation of work started by the Johnson lab (33) has recently produced exciting results in the form of a full 3.2 Å X-ray diffraction dataset which will be used to solve the structure of an Air2/ Δ Hmt1 complex (Table 4-1). A similar strategy has also been recently initiated to solve the crystal structure of an Air1/ Δ Hmt1 complex. This would be the first structure of Air1, and the first structure detailing how Hmt1 interacts

with a regulatory protein. Obtaining the crystal structure of an Air1/ Δ Hmt1 complex would be a *significant* addition to the black-box that is PRMT regulation.

It is often the case that preliminary results, such as those here presented, are unable to answer many specific questions. However, there is immense value in the new questions which arise from data such as these. Since it has been shown that Air1 ZnK4 has a role in promoting RNA target recognition in the context of the TRAMP complex (42), and we have now shown that Air1 ZnK4-5 are implicated in regulating Hmt1 activity, we are left with the intriguing question of whether Hmt1 binding to the Air proteins may modulate their RNA binding ability or selectivity. It is also interesting to wonder since the TRAMP helicase Mtr4 has recently been shown to interact with Hmt1 (43), an interesting question is whether TRAMP has a role in inhibiting Hmt1. Other important questions include: What may be the bigger implication of Air1 regulation given the important role of Hmt1 in the regulation of mRNA export? Does the human homolog of Air1 (ZCCHC7) regulate human PRMT1 activity? There is clearly much work that still needs to be done and a vast extent that remains to be learned about the activity and regulation of the PRMTs.

REFERENCES

1. Bedford, M. T., and Clarke, S. G. (2009) Protein arginine methylation in mammals: who, what, and why. *Mol. Cell* **33**, 1-13
2. Bedford, M. T., and Richard, S. (2005) Arginine methylation an emerging regulator of protein function. *Mol. Cell* **18**, 263-272
3. Yang, Y., and Bedford, M. T. (2013) Protein arginine methyltransferases and cancer. *Nat. Rev. Cancer* **13**, 37-50

4. Savoia, C., Ebrahimian, T., Lemarie, C. A., Paradis, P., Iglarz, M., Amiri, F., Javeshgani, D., and Schiffrin, E. L. (2010) Countervailing vascular effects of rosiglitazone in high cardiovascular risk mice: role of oxidative stress and PRMT-1. *Clin. Sci. (Lond.)* **118**, 583-592
5. Chen, Y., Xu, X., Sheng, M., Zhang, X., Gu, Q., and Zheng, Z. (2009) PRMT-1 and DDAHs-induced ADMA upregulation is involved in ROS- and RAS-mediated diabetic retinopathy. *Exp. Eye Res.* **89**, 1028-1034
6. Wells, S. M., Buford, M. C., Migliaccio, C. T., and Holian, A. (2009) Elevated asymmetric dimethylarginine alters lung function and induces collagen deposition in mice. *Am. J. Respir. Cell Mol. Biol.* **40**, 179-188
7. Kim, J. K., Mastronardi, F. G., Wood, D. D., Lubman, D. M., Zand, R., and Moscarello, M. A. (2003) Multiple sclerosis: an important role for post-translational modifications of myelin basic protein in pathogenesis. *Mol. Cell. Proteomics* **2**, 453-462
8. Basso, M., and Pennuto, M. (2015) Serine phosphorylation and arginine methylation at the crossroads to neurodegeneration. *Exp. Neurol.* **271**, 77-83
9. Lu, T. M., Ding, Y. A., Charng, M. J., and Lin, S. J. (2003) Asymmetrical dimethylarginine: a novel risk factor for coronary artery disease. *Clin. Cardiol.* **26**, 458-464
10. Scaramuzzino, C., Casci, I., Parodi, S., Lievens, P. M., Polanco, M. J., Milioto, C., Chivet, M., Monaghan, J., Mishra, A., Badders, N., Aggarwal, T., Grunseich, C., Sambataro, F., Basso, M., Fackelmayer, F. O., Taylor, J. P., Pandey, U. B., and Pennuto, M. (2015) Protein arginine methyltransferase 6 enhances polyglutamine-expanded androgen receptor function and toxicity in spinal and bulbar muscular atrophy. *Neuron* **85**, 88-100
11. Copeland, R. A., Solomon, M. E., and Richon, V. M. (2009) Protein methyltransferases as a target class for drug discovery. *Nat. Rev. Drug Discov.* **8**, 724-732
12. Low, J. K., and Wilkins, M. R. (2012) Protein arginine methylation in *Saccharomyces cerevisiae*. *FEBS J.* **279**, 4423-4443
13. Niewmierzycka, A., and Clarke, S. (1999) S-Adenosylmethionine-dependent methylation in *Saccharomyces cerevisiae*. Identification of a novel protein arginine methyltransferase. *J. Biol. Chem.* **274**, 814-824

14. Ma, X. J., Lu, Q., and Grunstein, M. (1996) A search for proteins that interact genetically with histone H3 and H4 amino termini uncovers novel regulators of the Swe1 kinase in *Saccharomyces cerevisiae*. *Genes Dev.* **10**, 1327-1340
15. Young, B. D., Weiss, D. I., Zurita-Lopez, C. I., Webb, K. J., Clarke, S. G., and McBride, A. E. (2012) Identification of methylated proteins in the yeast small ribosomal subunit: a role for SPOUT methyltransferases in protein arginine methylation. *Biochemistry* **51**, 5091-5104
16. Gary, J. D., Lin, W. J., Yang, M. C., Herschman, H. R., and Clarke, S. (1996) The predominant protein-arginine methyltransferase from *Saccharomyces cerevisiae*. *The Journal of Biological Chemistry* **271**, 12585-12594
17. Tang, J., Frankel, A., Cook, R. J., Kim, S., Paik, W. K., Williams, K. R., Clarke, S., and Herschman, H. R. (2000) PRMT1 is the predominant type I protein arginine methyltransferase in mammalian cells. *J. Biol. Chem.* **275**, 7723-7730
18. Pang, C. N., Gasteiger, E., and Wilkins, M. R. (2010) Identification of arginine- and lysine-methylation in the proteome of *Saccharomyces cerevisiae* and its functional implications. *BMC Genomics* **11**, 92
19. Shen, E. C., Henry, M. F., Weiss, V. H., Valentini, S. R., Silver, P. A., and Lee, M. S. (1998) Arginine methylation facilitates the nuclear export of hnRNP proteins. *Genes Dev.* **12**, 679-691
20. Inoue, K., Mizuno, T., Wada, K., and Hagiwara, M. (2000) Novel RING finger proteins, Air1p and Air2p, interact with Hmt1p and inhibit the arginine methylation of Npl3p. *The Journal of Biological Chemistry* **275**, 32793-32799
21. Houseley, J., Kotovic, K., El Hage, A., and Tollervey, D. (2007) Trf4 targets ncRNAs from telomeric and rDNA spacer regions and functions in rDNA copy number control. *EMBO J.* **26**, 4996-5006
22. Lemay, J. F., D'Amours, A., Lemieux, C., Lackner, D. H., St-Sauveur, V. G., Bahler, J., and Bachand, F. (2010) The nuclear poly(A)-binding protein interacts with the exosome to promote synthesis of noncoding small nucleolar RNAs. *Mol. Cell* **37**, 34-45
23. Vanacova, S., Wolf, J., Martin, G., Blank, D., Dettwiler, S., Friedlein, A., Langen, H., Keith, G., and Keller, W. (2005) A new yeast poly(A) polymerase complex involved in RNA quality control. *PLoS Biol.* **3**, e189
24. Wyers, F., Rougemaille, M., Badis, G., Rousselle, J. C., Dufour, M. E., Boulay, J., Regnault, B., Devaux, F., Namane, A., Seraphin, B., Libri, D., and Jacquier, A.

- (2005) Cryptic pol II transcripts are degraded by a nuclear quality control pathway involving a new poly(A) polymerase. *Cell* **121**, 725-737
25. LaCava, J., Houseley, J., Saveanu, C., Petfalski, E., Thompson, E., Jacquier, A., and Tollervey, D. (2005) RNA degradation by the exosome is promoted by a nuclear polyadenylation complex. *Cell* **121**, 713-724
 26. Houseley, J., and Tollervey, D. (2009) The many pathways of RNA degradation. *Cell* **136**, 763-776
 27. Anderson, J. T., and Wang, X. (2009) Nuclear RNA surveillance: no sign of substrates tailing off. *Crit. Rev. Biochem. Mol. Biol.* **44**, 16-24
 28. Gorelick, R. J., Henderson, L. E., Hanser, J. P., and Rein, A. (1988) Point mutants of Moloney murine leukemia virus that fail to package viral RNA: evidence for specific RNA recognition by a "zinc finger-like" protein sequence. *Proc. Natl. Acad. Sci. U. S. A.* **85**, 8420-8424
 29. Koster, M., Kuhn, U., Bouwmeester, T., Nietfeld, W., el-Baradi, T., Knochel, W., and Pieler, T. (1991) Structure, expression and in vitro functional characterization of a novel RNA binding zinc finger protein from *Xenopus*. *EMBO J.* **10**, 3087-3093
 30. K, M. J., and Laxmi, A. (2014) DUF581 is plant specific FCS-like zinc finger involved in protein-protein interaction. *PLoS One* **9**, e99074
 31. Nagai, K., Nakaseko, Y., Nasmyth, K., and Rhodes, D. (1988) Zinc-finger motifs expressed in *E. coli* and folded in vitro direct specific binding to DNA. *Nature* **332**, 284-286
 32. Hamill, S., Wolin, S. L., and Reinisch, K. M. (2010) Structure and function of the polymerase core of TRAMP, a RNA surveillance complex. *Proceedings of the National Academy of Sciences* **107**, 15045-15050
 33. Bakelar, J. W. (2015) *Binding Interactions of (R)- and (S)-hydroxypropyl-CoM Dehydrogenases and the Zinc Knuckle Proteins Air1 and Air2*. Doctor of Philosophy, Utah State University
 34. Suh-Lailam, B. B., and Hevel, J. M. (2010) A fast and efficient method for quantitative measurement of S-adenosyl-L-methionine-dependent methyltransferase activity with protein substrates. *Anal. Biochem.* **398**, 218-224
 35. McCoy, A. J., Grosse-Kunstleve, R. W., Adams, P. D., Winn, M. D., Storoni, L. C., and Read, R. J. (2007) Phaser crystallographic software. *J. Appl. Crystallogr.* **40**, 658-674

36. Adams, P. D., Afonine, P. V., Bunkoczi, G., Chen, V. B., Davis, I. W., Echols, N., Headd, J. J., Hung, L. W., Kapral, G. J., Grosse-Kunstleve, R. W., McCoy, A. J., Moriarty, N. W., Oeffner, R., Read, R. J., Richardson, D. C., Richardson, J. S., Terwilliger, T. C., and Zwart, P. H. (2010) PHENIX: a comprehensive Python-based system for macromolecular structure solution. *Acta Crystallogr.* **66**, 213-221
37. Schmidt, K., Xu, Z., Mathews, D. H., and Butler, J. S. (2012) Air proteins control differential TRAMP substrate specificity for nuclear RNA surveillance. *RNA* **18**, 1934-1945
38. Holub, P., Lalakova, J., Cerna, H., Pasulka, J., Sarazova, M., Hrazdilova, K., Arce, M. S., Hobor, F., Stefl, R., and Vanacova, S. (2012) Air2p is critical for the assembly and RNA-binding of the TRAMP complex and the KOW domain of Mtr4p is crucial for exosome activation. *Nucleic Acids Res.* **40**, 5679-5693
39. Ghaemmaghami, S., Huh, W. K., Bower, K., Howson, R. W., Belle, A., Dephoure, N., O'Shea, E. K., and Weissman, J. S. (2003) Global analysis of protein expression in yeast. *Nature* **425**, 737-741
40. Weiss, V. H., McBride, A. E., Soriano, M. A., Filman, D. J., Silver, P. A., and Hogle, J. M. (2000) The structure and oligomerization of the yeast arginine methyltransferase, Hmt1. *Nat. Struct. Biol.* **7**, 1165-1171
41. Erce, M. A., Abeygunawardena, D., Low, J. K., Hart-Smith, G., and Wilkins, M. R. (2013) Interactions affected by arginine methylation in the yeast protein-protein interaction network. *Mol. Cell. Proteomics* **12**, 3184-3198
42. Fasken, M. B., Leung, S. W., Banerjee, A., Kodani, M. O., Chavez, R., Bowman, E. A., Purohit, M. K., Rubinson, M. E., Rubinson, E. H., and Corbett, A. H. (2011) Air1 zinc knuckles 4 and 5 and a conserved IWRXY motif are critical for the function and integrity of the Trf4/5-Air1/2-Mtr4 polyadenylation (TRAMP) RNA quality control complex. *J. Biol. Chem.* **286**, 37429-37445
43. Jackson, C. A., and Yu, M. C. (2014) Detection of protein arginine methylation in *Saccharomyces cerevisiae*. *Methods Mol. Biol.* **1163**, 229-247

CHAPTER 5
INVESTIGATING THE EFFECTS OF PHOSPHORYLATION
ON HMT1 ACTIVITY

ABSTRACT

Protein arginine methyltransferases (PRMTs) are a family of enzymes that can methylate arginine residues in substrate proteins. This posttranslational methylation can alter the interactome of the modified substrate protein, thereby extending the range of its functions. Given that dysregulation or loss of arginine methyltransferase activity has severe biological effects, proper regulation of the arginine methyltransferases is of paramount importance. It was recently reported that regulation of Hmt1, the major type I PRMT in yeast, through posttranslational phosphorylation is necessary for fine tuning cell-cycle progression to environmental conditions. Phosphorylation at Serine 9 of Hmt1 resulted in an increase in the *in vivo* methylation of the RNA binding protein Npl3. Additionally, the *in vivo* effects observed could be mimicked using a glutamate residue at position 9 of Hmt1. However, because *in vitro* studies were not performed, it remains unclear if phosphorylation affects the intrinsic activity of Hmt1, or if phosphorylation results in the recruitment of another factor, leading to increased activity. Herein, we aimed to characterize how phosphorylation affects the methyltransferase activity of Hmt1 *in vitro* through the use of the S9E phosphomimetic and S9A nonphosphorylatable Hmt1 variants. We have been unable to obtain clear results and can therefore neither confirm nor negate the claim that phosphorylation of Hmt1 is necessary for activation. Our results, however,

do indicate that assay conditions, and even the protein tags used can greatly influence the rate of Hmt1 activity and should be taken into account for future work.

INTRODUCTION

Protein arginine methyltransferases (PRMTs) catalyze the addition of one or two methyl groups to protein substrates at arginine residues, thereby altering their function. Arginine methylation has been shown to mediate protein-RNA, protein-DNA, and protein-protein interactions (1). In *Saccharomyces cerevisiae* the methylation of arginine residues by the major yeast methyltransferase Hmt1 is associated with several biological functions such as nucleocytoplasmic shuttling (2), mRNA and rRNA processing (3), splicing (4), translation (5), and transcription through both histone and non-histone proteins (5,6). However, despite the lack of a known demethylase and of the magnitude of processes affected by arginine methylation, little is known about how arginine methyltransferases are regulated.

The only current report of Hmt1 regulation via a posttranslational modification showed that Hmt1 could be phosphorylated at serine 9 in the Hmt1 N-terminal region. In a 2013 *Cell* paper, Messier *et al.* reported that Hmt1 activity and oligomerization are dependent on phosphorylation (7). In this study they generated phosphomimetic (S9E Hmt1) and nonphosphorylatable (S9A Hmt1) variants and performed methylation assays with immunoprecipitated TAP-S9EHmt1 or TAP-S9AHmt1 from yeast cells. They showed that Npl3 was methylated by yeast-purified S9E Hmt1 *in vitro*, while yeast-purified S9A Hmt1 was unable methylate Npl3. This led to the conclusion that Hmt1 phosphorylation at

serine 9 is required for activity. They also concluded from immunoprecipitation experiments that phosphorylation is necessary for Hmt1 oligomerization. However, immunoprecipitation of Hmt1 also comes with the possibility that other protein factors were co-immunoprecipitated, a possibility that was never addressed in the paper. Since the authors of this report elegantly demonstrated that the phosphorylation effects could be mimicked using a glutamate substitution at position 9, we set out to investigate, *in vitro*, the mechanism by which phosphorylation affects Hmt1 activity. S9E Hmt1 (phosphomimetic) and S9A Hmt1 (nonphosphorylatable) constructs were expressed, purified, and their activities measured in order to corroborate the *in vivo* published results. However, it has been impossible to validate the *in vivo* results with our *in vitro* quantitative methylation assay (8). This discrepancy hints at the possibility that the published results were a result of recruitment of an unknown factor, rather than solely due to the phosphorylation event. We end with a discussion of the methods that can be used to finally ascertain whether Hmt1 phosphorylation causes an intrinsic effect on methyltransferase activity, or if this posttranslational modification affects a change through interactions with an unknown regulatory factor.

EXPERIMENTAL PROCEDURES

Materials— AdoMet was purchased from Sigma as a chloride salt ($\geq 80\%$, from yeast). [^3H]AdoMet (83.1 Ci/mmol) was purchased from Perkin Elmer. The R3 peptide (acGGRGGFGGRGGFGGRGGRG) was synthesized by the Keck Institute (Yale University) and purified to $\geq 95\%$. The lyophilized peptide was dissolved in water and its

concentration was determined by mass or by UV spectroscopy ($\epsilon_{280 \text{ nm}} = 5,690 \text{ M}^{-1}\text{cm}^{-1}$). ZipTip[®]_{C4/C18} pipette tips were purchased from Millipore.

Plasmid Generation—A His₆-tagged full length wild type Hmt1 plasmid (pPS1319) was received from Dr. Anne McBride (Bowdoin University) (9). Constructs containing a His₆-TEV-T7 (HTT7) tag were created in the Hevel Lab as described in chapter 3. Briefly, a pET24b+ vector was used to insert a NdeI_His₆-TEV-T7 (HTT7)_BamHI_Npl3_SacI construct into the NdeI and SacI sites. The Npl3 construct was cut out using the BamHI and SacI restriction sites, and a full length wild type Hmt1 construct was inserted using the same restriction sites. Hmt1 phosphorylation variant proteins were generated using the QuikChange[®] Site-Directed Mutagenesis kit (Stratagene) with sets of complementary oligonucleotide primers spanning the desired site of mutation. For each PCR reaction, the pPS1319 vector (from Dr. Anne McBride), or the pET24b+HTT7 vector, containing the gene that codes for full length Hmt1 (pET15b-Hmt1 and pET24b+HTT7-Hmt1, respectively) (9) was used as a template. Desired mutations (S9A and S9E) were confirmed through DNA sequencing.

Expression and Purification of Hmt1 Constructs—*E. coli* BL21 cells expressing either His₆-tagged Hmt1 (WT, S9A, or S9E), His₆-TEV-T7 (HTT7) Hmt1 (WT, S9A, or S9E), or tagless Hmt1 (WT, S9A, S9E) were grown in Luria Broth media at 37° C to OD₆₀₀ reached 0.6, followed by induction with 0.5 mM IPTG at 22° C for 20 hours. Cell pellets were resuspended in two times cell volume lysis buffer (50 mM sodium phosphate pH 7.5, 100 mM NaCl, 20 mM imidazole, or 5 mM imidazole when purifying tagless constructs) and lysed using sonication. The cell lysate was clarified via centrifugation and incubated with Nickel resin (GoldBio) in a 1:1 cell mass: resin ratio for 1-2 hours at 4° C. The resin

was washed eight times with eight times column volume of lysis buffer, followed by three washes with eight times column volume of wash buffer (50 mM sodium phosphate pH 7.5, 100 mM NaCl, 70 mM imidazole). The protein was then eluted off the resin five times with two column volumes of elution buffer (50 mM sodium phosphate pH 7.5, 100 mM NaCl, 250 mM imidazole). Elutions were pooled and dialyzed into 50 mM sodium phosphate pH 7.5, 100 mM NaCl, 10% glycerol. For samples in which the His tag was cleaved from the HTT7 tag, 1 mg of each protein was dialyzed into storage buffer (50 mM sodium phosphate pH 7.5, 100 mM NaCl, 10% glycerol) for 1 hour, then into TEV cleavage buffer (50 mM sodium phosphate pH 7.5, 100 mM NaCl, 10% glycerol, 1 mM EDTA, 10 mM β -mercaptoethanol) for 1 hour prior to the addition of 0.2 mg TEV protease. The protease was added and allowed to work overnight at 4° C in a new bucket of TEV cleavage buffer. After 12 hours, the proteins were dialyzed back into storage buffer for 1 hour. The TEV cleaved proteins were then loaded onto a 1 ml HisTrap column (GE) which bound the cleaved tag and the TEV protein, while the cleaved Hmt1 constructs were collected in the unbound fraction. The protein was then concentrated to ≥ 1 mg/ml, beaded in liquid nitrogen, and stored at -80° C.

Expression and Purification of Npl3 Protein— *E. coli* BL21 Ni-Co (DE3) cells expressing His-TEV-T7 tagged full length Npl3 protein were grown in Luria Broth media at 37° C to OD₆₀₀ reached 0.6, followed by induction with 0.5 mM IPTG at 22° C for 20 hours. Cell pellets were resuspended in two times cell volume lysis buffer (50 mM sodium phosphate pH 7.5, 100 mM NaCl, 20 mM imidazole) and lysed using sonication. The cell lysate was clarified via centrifugation and incubated with Nickel resin (GoldBio) in a 2:1 cell mass: resin ratio for 1-2 hours at 4° C. The resin was washed eight times with eight

times column volume of lysis buffer, followed by three washes with eight times column volume of wash buffer (50 mM sodium phosphate pH 7.5, 100 mM NaCl, 70 mM imidazole). The protein was then eluted off the resin five times with two column volumes of elution buffer (50 mM sodium phosphate pH 7.5, 100 mM NaCl, 500 mM imidazole). Elutions were pooled, filtered and further purified using MonoQ and Heparin columns (GE) in tandem. Fractions containing Npl3 were pooled and dialyzed into 50 mM sodium phosphate pH 7.5, 100 mM NaCl, 10% glycerol. The protein was then concentrated to \geq 1mg/ml, beaded in liquid nitrogen, and stored at -80° C.

Methyltransferase Activity Assays— Hmt1 methylation rates were measured according to an established methyltransferase activity assay (8) with the following modifications. 100 nM Hmt1 (WT, S9A, or S9E) was incubated with 10 nM AdoHcy nucleosidase (MTAN), 0.38 μ M BSA, 1 μ M (or 10 μ M) AdoMet (Sigma), and 1 μ M [3 H]-AdoMet (Perkin Elmer, specific activity 83.1 Ci/mmol) in 50 mM sodium phosphate buffer pH 8.0 at 4° C for 10 minutes prior to initiation with substrate and incubation at 30° C. Substrates used were 200 μ M R3 peptide or Npl3 (0.1 μ M to 1 μ M).

RESULTS

Initial Activity Measurements of Hmt1 Phosphorylation Variants— In order to investigate the effects of phosphorylation on Hmt1 activity, His₆-tagged wild type (WT Hmt1), phosphomimetic (S9E Hmt1), and nonphosphorylatable (S9A Hmt1) constructs were recombinantly expressed and purified from *E. coli* cells. Using an established quantitative methyltransferase activity assay (8), the ability of each Hmt1 construct to

methylate recombinant Npl3 was measured. An *in vitro* confirmation of the previously published results should show weak to zero activity from non-phosphorylated WT Hmt1 and S9A Hmt1, while the phosphomimetic S9E Hmt1 construct would be expected to have robust methyltransferase activity on the Npl3 substrate, as was shown *in vivo* (7). However, our initial findings did not yield these results. Instead, we observed the opposite of these predictions (Figure 5-1). The nonphosphorylatable (S9A Hmt1) variant showed robust methyltransferase activity, while WT Hmt1 and S9E Hmt1 proteins methylated Npl3, at a much lower rate. We were surprised by these results, prompting us to re-sequence the plasmids, re-express, purify, and again measure Npl3 methylation by these proteins, but the second set of results were very similar to the first (see error bars in Figure 5-1), indicating that an error was not committed on our part.

AdoMet Concentrations Affect Activity of Hmt1 S9A— The typical steady-state methyltransferase assay conditions used in the Hevel lab employ saturating concentrations of arginine-containing substrate, but only use 2 μM AdoMet (SAM) which is below the reported K_M for PRMT1 of $6 \pm 1 \mu\text{M}$ (10). While the concentration of AdoMet used in the *Cell* paper was not reported, 2 μM [AdoMet] is fairly standard. To examine a potential influence of AdoMet concentration on PRMT1 activity, the rates of Npl3 methylation by the Hmt1 phosphorylation variants at both 2 μM and 11 μM AdoMet ([AdoMet] used in Figure 5-1) were compared. At 2 μM AdoMet, the extreme difference in the methylation rates between the various Hmt1 constructs was not observed. Instead, the S9E Hmt1 and S9A Hmt1 rates become comparable.

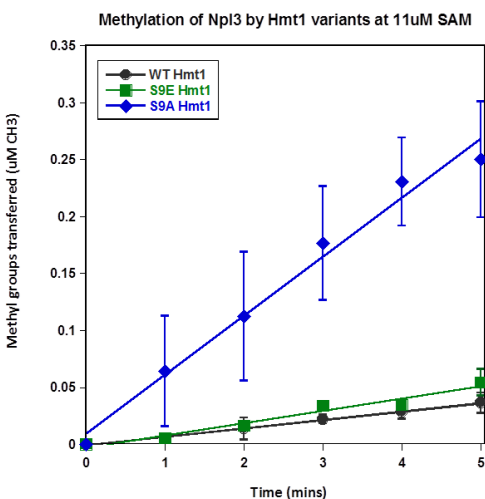


FIGURE 5-1. Methylation of Npl3 by Hmt1 phosphorylation variants. The reactions were carried out with 100 nM Hmt1 (WT, S9E, or S9A), 10 μM AdoMet + 1 μM [³H]AdoMet, and 1 μM Npl3 substrate in 50 mM sodium phosphate buffer pH 8.0 at 30° C. Error bars indicate the standard deviation from the average between two biological replicates.

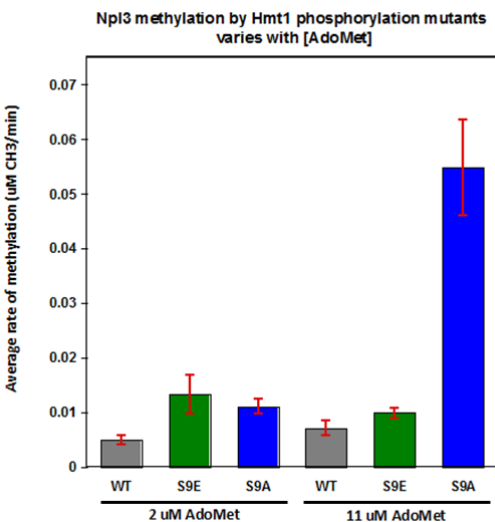


FIGURE 5-2. Activity of Hmt1 phosphorylation variants at two AdoMet concentrations. The average rate of methyl group transferred is shown for each Hmt1 phosphorylation variant in the presence of 1 μM Npl3 and either 2 μM or 11 μM AdoMet. Error bars shown represent the standard deviation between two biological replicated.

Further attempts to replicate the conditions used in the reactions with yeast purified TAP-Hmt1 constructs focused on varying the concentration of the Npl3 substrate, since the original report used 700 nM Npl3 and our conditions used 1 μ M. However, the S9A Hmt1 construct that was unable methylate 700 nM Npl3 when purified from yeast cells, efficiently methylated 700 nM Npl3 *in vitro* (Figure 5-3-A). It must be noted that the data in Figure 5-3-A represents the measurement of only one rate for each Npl3 concentration per Hmt1 construct and therefore no attempts were made to fit the data to a Michaelis-Menten equation. Since no clear distinction in the rate of methyl transfer was observed for the Hmt1 phosphorylation variants using the Npl3 protein substrate, the rates of methylation of R3 peptide substrate (ac-GGRGGFGGRGGFGGRGGFGG) were also measured (Figure 5-3-B). Again, no significant difference in the overall methylation rates was observed.

Effect of N-terminal Tag on the Activity of Hmt1 Phosphorylation Variants—

Although TAP-Hmt1 constructs tested by Messier *et al.* have not been used in the Hevel lab, the activity of TAP-tagged WT Hmt1 is known to be consistently very poor (conversations with Dr. Michael Yu), while the activity of recombinant WT Hmt1 (with a Histidine tag) in the Hevel lab has typically been robust. Therefore, the Hmt1 phosphorylation variants were expressed with different affinity tags to determine if N-terminal tags can affect the activity of the Hmt1 phosphorylation variants. The N-terminal Histidine tag that we employed does seem to have a direct effect on the overall activity of all of our constructs (Figure 5-4). The highest level of activity is shown by the constructs with the longest tag (HTT7 tag is 40 amino acids long, cleaved HTT7 (cHTT7) is 12 amino acids long, while the His₆ tag is 6 amino acids long). Interestingly, the HTT7-tagged Hmt1

phosphorylation variants were able to methylate 1 μM Npl3 in a parallel to the results of Messier *et al.* (S9A Hmt1 significantly more impaired than S9E Hmt1). The TAP-Hmt1 constructs used to immunoprecipitate the Hmt1 phosphorylation variants from yeast cells code for ProteinA-TEV-CBP-Hmt1, meaning that after TEV cleavage, the constructs used for methyltransferase assay by Messier *et al.* retained a 26 amino acid calmodulin binding protein (CBP) tag on the N-terminus of Hmt1. Our results, while only single data points, suggest that perhaps the observations made by Messier *et al.* could have been influenced by the use of a purification tag.

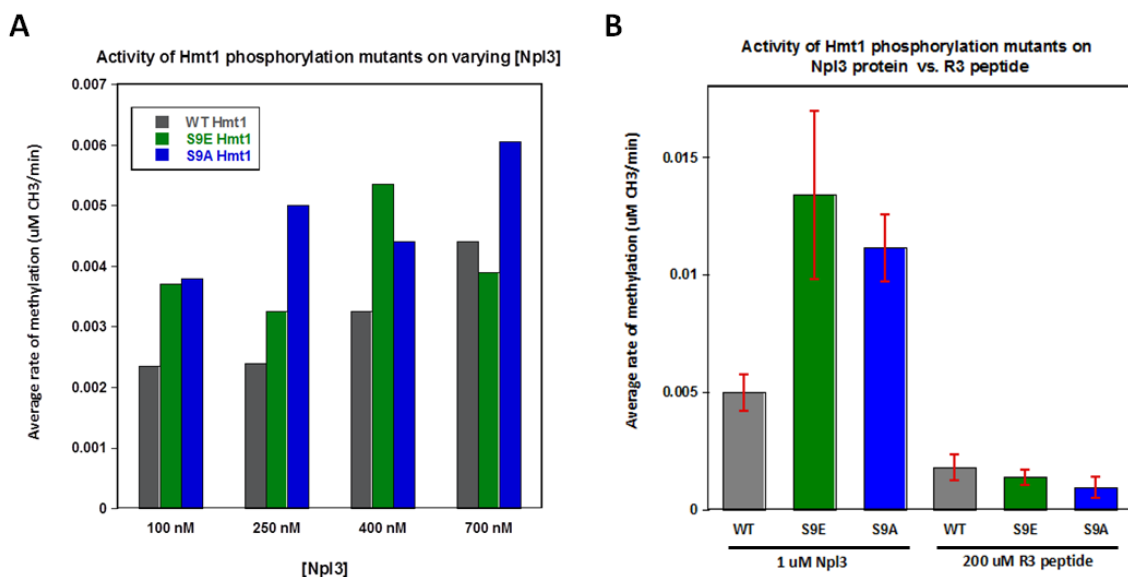


FIGURE 5-3. Activity of Hmt1 phosphorylation variants with varying [Npl3], or with R3 peptide. The rates of methyl group transfer are shown for each Hmt1 phosphorylation variant with varied substrate concentration at 2 μM AdoMet. Error bars, when shown, indicate the standard deviation between at least two biological replicates.

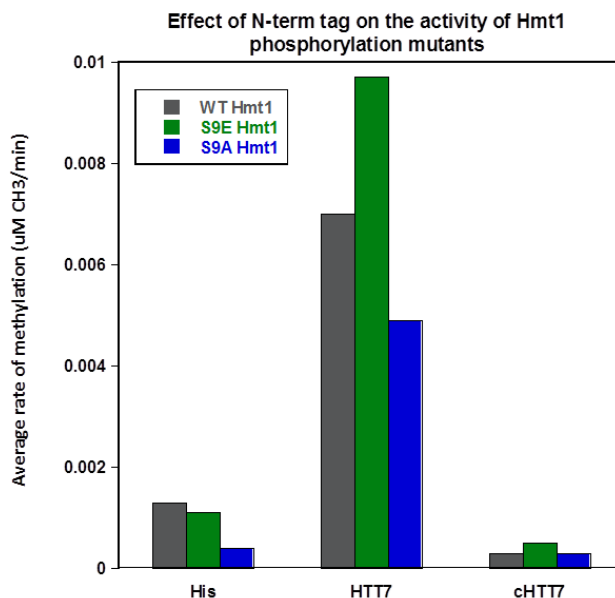


FIGURE 5-4. Effect of N-terminal tags on Npl3 methylation by Hmt1 phosphorylation variants. Single rate measurements are shown for the various Hmt1 phosphorylation variants with one of the following N-terminal tags: His₆ tag, His₆-TEV-T7 (HTT7) tag, or TEV-cleaved HTT7 tag. The methyltransferase activity of these constructs was measured in the presence of 1 µM Npl3, and 2 µM AdoMet.

DISCUSSION

The proper regulation of PRMT1 activity is critical for organismal well-being. Regulation of protein activity can be achieved many ways, including posttranslational phosphorylation which regulates many proteins, including several PRMT isoforms (11-13). Recently, the yeast PRMT1 homolog, Hmt1, was reported to be activated *in vivo* through phosphorylation on an N-terminal serine residue (7). In this report, it was also shown that a phosphomimetic Hmt1 variant (S9E) immunoprecipitated from yeast cells could mimic the activity and oligomerization of phosphorylated Hmt1, while a nonphosphorylatable yeast-purified S9A Hmt1 variant had no activity. However, there is precedent for the need to corroborate results observed *in vivo* with *in vitro* methods. One

well known example was the misclassification of PRMT7 as a type II PRMT due to contamination of immunoprecipitated type III PRMT7 with the type II PRMT5 (14). Since the report by Messier *et al.* did not address the possibility that their results may have been affected by the co-immunoprecipitation of an unknown factor with Hmt1, we determined to characterize the activity of recombinant Hmt1 phosphorylation variants (S9E and S9A) using a quantitative *in vitro* methyltransferase assay developed in our lab (8). We were unable to replicate the *in vivo* observations and find that the N-terminal tags used to purify Hmt1 may affect the measurement of Hmt1 activity. Tag-free constructs of the Hmt1 phosphorylation variants should be used to be sure that our inability to reproduce the *in vivo* results is not a result of the tags attached to the protein.

A possible experiment to ascertain whether phosphorylation at serine 9 of Hmt1 has an intrinsic effect on Hmt1 activity, or affects activity through the recruitment of an unknown factor is to determine the activity of tag-free, recombinantly expressed phosphomimetic S9E Hmt1 and nonphosphorylatable S9A Hmt1 with and without an Hmt1-null yeast cell lysate. If an unknown yeast factor binds to and activates phosphorylated Hmt1, a stark difference should be noted between the methylation of S9E Hmt1 in the presence or absence of yeast lysate, whereas no significant difference would indicate an intrinsic effect on Hmt1 activity from phosphorylation.

REFERENCES

1. Bedford, M. T., and Clarke, S. G. (2009) Protein arginine methylation in mammals: who, what, and why. *Molecular cell* **33**, 1-13

2. Herrmann, F., and Fackelmayer, F. O. (2009) Nucleo-cytoplasmic shuttling of protein arginine methyltransferase 1 (PRMT1) requires enzymatic activity. *Genes Cells* **14**, 309-317
3. Yu, M. C., Bachand, F., McBride, A. E., Komili, S., Casolari, J. M., and Silver, P. A. (2004) Arginine methyltransferase affects interactions and recruitment of mRNA processing and export factors. *Genes Dev.* **18**, 2024-2035
4. Chen, Y. C., Milliman, E. J., Goulet, I., Cote, J., Jackson, C. A., Vollbracht, J. A., and Yu, M. C. (2010) Protein arginine methylation facilitates cotranscriptional recruitment of pre-mRNA splicing factors. *Mol. Cell. Biol.* **30**, 5245-5256
5. Xu, C., Henry, P. A., Setya, A., and Henry, M. F. (2003) In vivo analysis of nucleolar proteins modified by the yeast arginine methyltransferase Hmt1/Rmt1p. *RNA* **9**, 746-759
6. Low, J. K., and Wilkins, M. R. (2012) Protein arginine methylation in *Saccharomyces cerevisiae*. *FEBS J.* **279**, 4423-4443
7. Messier, V., Zenklusen, D., and Michnick, S. W. (2013) A nutrient-responsive pathway that determines M phase timing through control of B-cyclin mRNA stability. *Cell* **153**, 1080-1093
8. Suh-Lailam, B. B., and Hevel, J. M. (2010) A fast and efficient method for quantitative measurement of S-adenosyl-L-methionine-dependent methyltransferase activity with protein substrates. *Anal. Biochem.* **398**, 218-224
9. Shen, E. C., Henry, M. F., Weiss, V. H., Valentini, S. R., Silver, P. A., and Lee, M. S. (1998) Arginine methylation facilitates the nuclear export of hnRNP proteins. *Genes Dev.* **12**, 679-691
10. Rust, H. L., Zurita-Lopez, C. I., Clarke, S., and Thompson, P. R. (2011) Mechanistic studies on transcriptional coactivator protein arginine methyltransferase 1. *Biochemistry* **50**, 3332-3345
11. Higashimoto, K., Kuhn, P., Desai, D., Cheng, X., and Xu, W. (2007) Phosphorylation-mediated inactivation of coactivator-associated arginine methyltransferase 1. *Proceedings of the National Academy of Sciences* **104**, 12318-12323
12. Feng, Q., He, B., Jung, S. Y., Song, Y., Qin, J., Tsai, S. Y., Tsai, M. J., and O'Malley, B. W. (2009) Biochemical control of CARM1 enzymatic activity by phosphorylation. *The Journal of Biological Chemistry* **284**, 36167-36174

13. Liu, F., Zhao, X., Perna, F., Wang, L., Koppikar, P., Abdel-Wahab, O., Harr, M. W., Levine, R. L., Xu, H., Tefferi, A., Deblasio, A., Hatlen, M., Menendez, S., and Nimer, S. D. (2011) JAK2V617F-mediated phosphorylation of PRMT5 downregulates its methyltransferase activity and promotes myeloproliferation. *Cancer Cell* **19**, 283-294
14. Zurita-Lopez, C. I., Sandberg, T., Kelly, R., and Clarke, S. G. (2012) Human protein arginine methyltransferase 7 (PRMT7) is a type III enzyme forming omega-NG-monomethylated arginine residues. *J. Biol. Chem.* **287**, 7859-7870

CHAPTER 6
REDOX CONTROL OF PROTEIN ARGININE METHYLTRANSFERASE 1
(PRMT1) ACTIVITY¹

ABSTRACT

Elevated levels of asymmetric dimethylarginine (ADMA) correlate with risk factors for cardiovascular disease. ADMA is generated by the catabolism of proteins methylated on arginine residues by protein arginine methyltransferases (PRMTs), and is degraded by dimethylarginine dimethylaminohydrolase (DDAH). Reports have shown that DDAH activity is down regulated and PRMT1 protein expression is upregulated under oxidative stress conditions, leading many to conclude that ADMA accumulation occurs via increased synthesis by PRMTs and decreased degradation. However, we now report that the methyltransferase activity of PRMT1, the major PRMT isoform in humans, is impaired under oxidative conditions. Oxidized PRMT1 displays decreased activity, which can be rescued by reduction. This oxidation event involves one or more cysteine residues that become oxidized to sulfenic acid (-SOH). We demonstrate a hydrogen peroxide concentration-dependent inhibition of PRMT1 activity that is readily reversed under physiological H₂O₂ concentrations. Our results challenge the unilateral view that increased

¹Morales, Y., Nitzel, D. V., Price, O. M., Gui, S., Li, J., Qu, J., and Hevel, J. M. (2015) Redox Control of Protein Arginine Methyltransferase 1 (PRMT1) Activity. *The Journal of biological chemistry* **290**, 14915-14926

PRMT1 expression necessarily results in increased ADMA synthesis, but rather demonstrate that enzymatic activity can be regulated in a redox-sensitive manner.

INTRODUCTION

Endothelial dysfunction plays a major role in cardiovascular disease, the leading cause of death in the United States (1). Several factors have been suggested to contribute to endothelial dysfunction such as decreased activity and/or expression of endothelial nitric oxide synthase (eNOS) and/or increased vascular formation of oxygen-derived free radicals (2,3). Asymmetric dimethylarginine (ADMA) is an endogenously synthesized inhibitor of NOS that has been gaining increased attention in the cardiovascular field (2,4-9). In the heart, ADMA and other NOS inhibitors cause reduced heart rate and cardiac output (10,11). Interestingly, in addition to decreasing levels of nitric oxide, evidence suggests that ADMA may also uncouple NOS (conditions under which NOS generates superoxide anion), thus increasing oxidative stress and inducing additional endothelial dysfunction (7,12). Furthermore, ADMA was shown to increase endothelial oxidative stress and up-regulate expression of redox-sensitive genes that encode endothelial adhesion molecules (13), increasing propensity for plaque buildup. Taken together, the available data indicates that ADMA levels represent a risk factor for the development of endothelial dysfunction.

ADMA is generated through the degradation of cellular proteins containing asymmetrically dimethylated arginine residues (Fig. 6-1). Arginine residues in certain proteins can be modified by the addition of one or two methyl groups; this modification is catalyzed by the protein arginine methyltransferase (PRMT) family of enzymes. Nine

human PRMT isoforms can be subdivided into three types determined by their final methylation products. Type 1 PRMTs (such as PRMT1) form monomethylarginine (MMA) and/or ADMA and represent the majority of identified PRMTs. Type 2 PRMTs form MMA and/or symmetric dimethylarginine (SDMA), and type 3 PRMTs produce only MMA (14). Each of the methylated arginine products (MMA, ADMA, and SDMA) can induce different biological responses in the cell; however, only MMA and ADMA are inhibitors of NOS activity (9,14). ADMA in the body is metabolized by dimethylarginine dimethylaminohydrolase (DDAH) to citrulline and dimethylamine (15). Thus, the amount of free ADMA at any given time is a reflection of PRMT, proteasome, and DDAH activities.

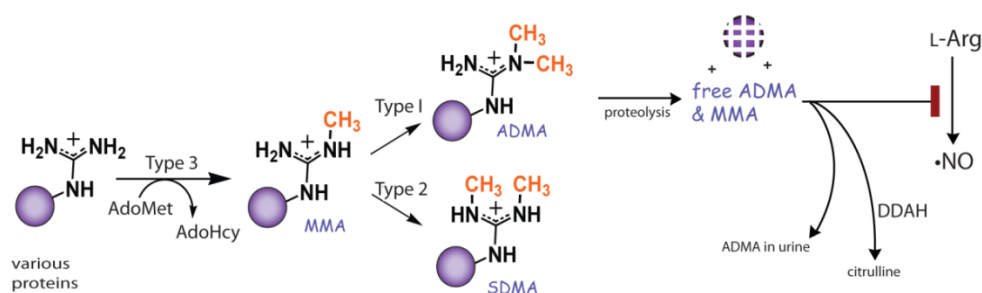


FIGURE 6-1. ADMA formation and degradation. Protein arginine methyltransferases (PRMTs) transfer a methyl group from donor AdoMet to arginine residues in substrate proteins. Type 1 PRMTs can transfer one or two methyl groups to the same terminal guanidino nitrogen producing monomethyl arginine (MMA) or asymmetric dimethylarginine (ADMA), respectively. Upon degradation of the methylated proteins, free MMA and ADMA inhibit NO synthesis by acting as competitive inhibitors of nitric oxide synthase. Free ADMA is catabolized by dimethylarginine dimethylaminohydrolase (DDAH) to citrulline and dimethylamine, or excreted in urine.

Evidence has shown that under oxidative stress, a condition linked to a variety of disease states, free ADMA levels are increased. In many instances these studies also showed that PRMT1 RNA or protein expression is increased and DDAH activity is decreased (11,16-20). This has led many to conclude that the increased expression of PRMT1 protein results in increased protein methylation, giving rise to a larger pool of the precursors for free ADMA (6,18,21). While it is clear that elevated ADMA levels are connected to oxidative stress, the assumption that increased levels of PRMT1 protein expression are directly responsible for increased free ADMA production has not been validated. In fact, a recent report showed a significant reduction in the production of ADMA-containing polypeptides in both replicative and H₂O₂-induced premature senescent cells (22). In order to clarify the role of PRMT1 in free ADMA accumulation under oxidative stress conditions, we set out to investigate if oxidative conditions affect PRMT1 catalytic activity.

Here we report that PRMT1, the major human PRMT isoform, is susceptible to oxidation. Oxidized rat PRMT1, which differs from human PRMT1 at just one residue, is characterized by impaired enzymatic activity that can be rescued by reduction. We demonstrate a reversible, concentration-dependent inhibition of PRMT1 activity by H₂O₂. Furthermore, we show that this oxidation event involves at least two cysteines which are oxidized to sulfenic acid (-SOH). Our results provide the first direct evidence that PRMT1 enzymatic activity can be regulated in a redox-sensitive manner.

EXPERIMENTAL PROCEDURES

Materials— AdoMet was purchased from Sigma as a chloride salt ($\geq 80\%$, from yeast). [^3H]AdoMet (83.1 Ci/mmol) was purchased from Perkin Elmer. R3 peptide (acGGRGGFGGRGGFGGRGGRG) was synthesized by the Keck Institute (Yale University) and purified to $\geq 95\%$. The lyophilized peptide was dissolved in water and its concentration was determined by mass or by UV spectroscopy ($\epsilon_{280\text{ nm}} = 5,690\text{ M}^{-1}\text{cm}^{-1}$). Bulk histones from calf thymus were purchased from Sigma. Histone 4 protein was purchased from New England Biolabs. ZipTip[®]_{C4/C18} pipette tips were purchased from Millipore. DCP-Rho1 sulfenic acid probe was purchased from Kerafast and 5IAF thiol-specific probe was purchased from Life Technologies.

Plasmid Generation— The His₆-ratPRMT1 plasmid (HisPRMT1) was previously generated (23). To create a construct with a cleavable His₆-tag, a DNA segment coding for a tobacco etch virus (TEV) cleavage site was designed with both N- and C-terminal *NdeI* restriction sites. The *NdeI* restriction enzyme was used to cut open the vector at an *NdeI* site between the His₆-tag and the enzyme coding sequence, and the designed TEV insert ligated using the Quick Ligation[™] kit (New England Biolabs) to form the His₆-TEV-ratPRMT1 plasmid (HisTevPRMT1). The C101S, C342S, C254S, C208S, C101S/C208S variants were generated using the HisTevPRMT1 plasmid (or confirmed HisTevPRMT1 C101S plasmid for C101S/C208S) as a PCR template for site directed mutagenesis using the QuikChange Lightning Kit (Stratagene) and sets of complementary oligonucleotide primers spanning the desired site of mutation. To replace all 11 cysteine residues of PRMT1 with serines and create HisTevPRMT1 \square cys (or cys-), properly coded DNA with N-terminal *NdeI* and C-terminal *BamHI* restriction sites was ordered from GenScript. The

PRMT1 sequence in His₆-TEV-PRMT1 was excised with *NdeI/BamHI* and replaced with the synthetic PRMT1 \square cys insert. The cysteine-less with C101 reintroduced (cys-C¹⁰¹), cysteine-less with C208 reintroduced (cys-C²⁰⁸), and cysteine-less with both C101 and C208 reintroduced (cys-C¹⁰¹C²⁰⁸) variants were generated using the HisTevPRMT1 \square cys plasmid as a PCR template for site directed mutagenesis using the QuikChange Lightning Kit (Stratagene) and sets of complementary oligonucleotide primers spanning the desired site of mutation. All plasmids were transformed using the *E.coli* DH5 α cell line. Plasmids were purified (Qiagen Plasmid Mini Kit) and sequenced to confirm the correctness of the open reading frame prior to protein expression.

Recombinant Protein Expression and Purification— Full-length His-tagged PRMT1 (residues 1-353) was expressed and purified as described previously (23). Briefly, *E. coli* BL21 cells were transformed with the above constructs and grown on Luria Broth medium / kanamycin agar plates. Selected colonies were grown in Luria Broth to A₆₀₀ = 0.6 and induced with 0.5 mM IPTG for 24 hours at 25⁰ C. Cell pellets were resuspended in lysis/wash buffer (50 mM sodium phosphate [pH 7.6], and 20 mM imidazole), sonicated, and centrifuged at 47,000 \times g for 20 minutes at 4⁰ C. The clarified supernatant was incubated with Nickel Sepharose 6 Fast Flow resin (Qiagen) rotating for 2 hours at 4⁰ C. The binding reaction was pelleted at 700 \times g, the supernatant discarded, and the resin washed 4 times with lysis/wash buffer, 7 times with wash buffer containing 70 mM imidazole, and then eluted in 6 washes with 250 mM imidazole buffer. The elutions were pooled and dialyzed into storage buffer (50 mM sodium phosphate [pH 7.6], and 10 % glycerol), concentrated to greater than 1 mg/mL, and beaded in liquid nitrogen for storage at -80⁰ C. To generate cleaved constructs, half of the His₆-TEV enzymes were put into

cleavage buffer (50 mM sodium phosphate, 1 mM DTT, 2 mM EDTA, and 5 % glycerol); the TEV enzyme added and allowed to cleave overnight. The cleaved enzyme was dialyzed into storage buffer, re-incubated with nickel resin (removal of TEV and remaining His₆-tag), and the subsequent supernatant was dialyzed, concentrated, and stored the same as the His₆-tagged elutions. Enzyme cleavage and purity (> 90%) were assessed during and after purification using SDS-page. pET21a TbPRMT7 and pET28b human PRMT6 were purified as PRMT1. pET28a human PRMT3 (residues 211-531) was grown and purified as described in Wang *et al.* (24). Protein concentrations were determined by UV spectroscopy (PRMT1 $\epsilon_{280 \text{ nm}} = 54,945 \text{ M}^{-1}\text{cm}^{-1}$, PRMT3 $\epsilon_{280 \text{ nm}} = 37735 \text{ M}^{-1}\text{cm}^{-1}$, PRMT7 $\epsilon_{280 \text{ nm}} = 37150 \text{ M}^{-1}\text{cm}^{-1}$, PRMT6 $\epsilon_{280 \text{ nm}} = 59040 \text{ M}^{-1}\text{cm}^{-1}$) and by the Bradford assay with bovine serum albumin as a standard.

Kinetic Assays of PRMT1 Constructs— Conditions of methylation reactions were as published previously (23). Briefly, enzyme activity was assessed at 37° C in assays containing 100 nM PRMT1, 2 μM AdoMet (1 μM [³H]AdoMet), 0.38 μM bovine serum albumin, 100 nM AdoHcy nucleosidase (MTAN, purified as described in ref. (25)) and initiated with 200 μM peptide substrate or 2 μM protein substrate. Reactions in the presence of DTT were performed by pre-incubation of the reaction with 1 mM DTT for 10 minutes at 4° C prior to initiation with substrate. At different time points, 5 μL samples were removed from reactions and quenched with 6 μL of 8 M guanidinium hydrochloride. Samples were processed with ZipTip®_{C4/C18} pipette tips (Millipore) (for protein or peptide substrates, respectively) to separate the unreacted [³H]AdoMet and the radiolabeled product (26). Time-dependent incorporation of radiolabel into substrates was quantified using a scintillation counter (Beckman Coulter). Methyltransferase activity for hPRMT3,

hPRMT6, and TbPRMT7 were performed as above, except 1 mM bulk histones (Sigma), and 1 mM Histone 4 protein (NEB) were used as substrates for hPRMT6 and TbPRMT7, respectively.

Conditions for testing the effect of hydrogen peroxide on enzymatic activity were published previously (27) and were modified as follows. PRMT1 was pre-reduced in 1mM DTT for 2 hours on ice then rapidly desalted on a 7 kDa Zeba™ Spin desalting column (Thermo Scientific). PRMT1 (2 μM final concentration) was oxidized with 0, 0.4 μM, 4 μM, 40 μM, 200 μM, 400 μM, or 800 μM H₂O₂ for 10 minutes at 37⁰ C and then incubated with catalase (300 U/ml) for 1 minute at 37⁰ C. The mixture was then kept on ice and used for kinetic assays as above. Methyltransferase activity was unaffected by the addition of catalase (data not shown). In all cases, data reported is the average of at least three independent measurements.

Size Exclusion Chromatography— Gel filtration chromatography was performed on a Superdex™ 200 10/300GL column (GE Healthcare) in 50 mM sodium phosphate pH 7.6, 150 mM NaCl, and 5 % glycerol at 0.4 ml/min flow rate. Freshly purified PRMT1 variants were allowed to equilibrate overnight into gel filtration buffer, with or without the addition of 1 mM DTT, 2 mM EDTA prior to examination. All constructs were analyzed by loading 300 μL of enzyme at a concentration of 10-20 μM and run at 0.4 mL/min for 75 minutes.

In Vitro DCP-Rho1 Labeling of Sulfenic Acid in Recombinant PRMT1—

DCP-Rho1 labeling of purified PRMT1 was modified from the method described in Poole *et al.*(28). Briefly, 2.5 μM recombinantly expressed, air oxidized WT PRMT1, cysteine-less PRMT1, cysteine-lessC¹⁰¹, cysteine-lessC²⁰⁸, or cysteine-lessC¹⁰¹C²⁰⁸

enzymes were incubated with 1 mM DTT or with buffer in the presence of 6 M urea for 1 hour at 22° C prior to addition of 10 μM DCP-Rho1 for 20 minutes at 22° C in a final reaction volume of 25 μl. The labeling reaction was quenched by addition of 4X SDS loading dye and boiling for 5 minutes. Labeled proteins were separated from unreacted label by 12 % SDS-PAGE, and band quantification was performed using the Image Lab software from BioRad and is reported as the average of three independent measurements.

In Vitro 5IAF Labeling of Free Thiol Content in Recombinant PRMT1—

5IAF labeling of purified PRMT1 was modified from the method described in Wu *et al.* (29) with optimization conditions aided by Hansen *et al.* (30). Briefly, 2.5 μM recombinantly expressed, air oxidized WT PRMT1, cysteine-less PRMT1, cysteine-lessC¹⁰¹, cysteine-lessC²⁰⁸, or cysteine-lessC¹⁰¹C²⁰⁸ enzymes were incubated with 1 mM DTT or with buffer in the presence of 6 M urea for 1 hour at 22° C prior to addition of 2.5 mM 5IAF for 1 hour at 22° C in a final reaction volume of 25 μl. The labeling reaction was quenched by addition of 4X SDS loading dye and boiling for 5 minutes. Labeled proteins were separated from unreacted label by 12 % SDS-PAGE, and band quantification was performed using the Image Lab software from BioRad and is reported as the average of three independent measurements.

LC-MS/MS Analysis of Sulfenic Acid Content in Recombinant PRMT1—

120 μg WT PRMT1 was treated with 5 mM dimedone in the presence of 6 M urea for 2 hours at 22° C. The sample was then buffer exchanged twice into 50 mM ammonium bicarbonate to remove excess dimedone and all urea. After reduction and alkylation, the labeled sample was precipitated by stepwise addition of 6 volumes of cold acetone with continuous vortexing and then incubated overnight at -20° C. After centrifugation at 20,000

g for 30 minutes at 4° C, the supernatant was removed, and the pellet was allowed to air-dry. Two consecutive digestions steps were employed for the on-pellet-digestion. In step 1 (digestion-aided pellet dissolution), Tris buffer (50 mM, pH 8.5) containing trypsin at an enzyme/substrate ratio of 1:40 (w/w) was added and incubated at 37° C for 6 hours with vortexing at 500 rpm in a ThermoMixer shaking incubator (Eppendorf); in step 2 (complete cleavage), another portion of trypsin solution was added at an enzyme/substrate ratio of 1:40 (w/w) in a 50 µl final volume. The mixture was incubated at 37° C for 12 hours to achieve a complete digestion. The digestion was terminated by adding 1 % (v:v) formic acid and centrifuged at 20,000 g for 30 min at 4° C; the supernatant was used for LC-MS/MS analysis.

Four µl of the digested solution was analyzed by nanospray LC-MS/MS, which constitutes an Orbitrap Fusion Tribrid mass spectrometer with ETD (Thermo Fisher Scientific, San Jose, CA) coupled to an ultra-high pressure Eksigent ekspert NanoLC 425 system (Dublin, CA) with a autosampler of Eksigent NLC 400 (Made in the Netherlands). A nano-LC/nanospray setup was used to obtain a comprehensive separation of the complex peptide mixture and sensitive detection. Mobile phases A and B were 0.1 % formic acid in 1 % acetonitrile and 0.1 % formic acid in 88 % acetonitrile, respectively. Samples were loaded onto a large ID trap (300 µm ID × 5 mm, packed with Zorbax 5 µm C18 material) with 1 % B at a flow rate of 10 µL/min for 3 min. A series of nanoflow gradients was used to back-flush the trapped samples onto the nano-LC column (75 µm ID × 100 cm, packed with Pepmap 3-µm C18 material). The column was heated at 52 °C to improve both chromatographic resolution and reproducibility. Gradient profile was as follows: i) a linear increase from 3 to 8% B over 5 min; ii) an increase from 8 to 27 % B over 117 min; iii) an

increase from 27 to 45 % B over 10 min; iv) an increase from 45 to 98 % B over 20 min; and v) isocratic at 98 % B for 20 min.

The mass spectrometry was operating under data-dependent product ion mode. A 3 second scan cycle included an MS1 scan (Orbitrap) followed by MS2 scans (dual-cell ion trap) by alternating CID and ETD activation, was programmed. The parameters used for MS and MS/MS data acquisition under the CID mode were: top speed mode with 3s cycle time; Orbitrap: scan range (m/z) = 400-1600; resolution = 120 K; AGC target = 5×10^5 ; maximum injection time (ms) = 50; Filter: precursor selection range = 400-1500; include charge state = 2-7; dynamic exclude after n times = 1, duration time 60 s; Decision: data dependent mode: top speed, precursor priority = most intense; for CID, isolation mode = quadrupole; isolation window = 1.6; collision energy (%) = 30; detection type: Ion trap; iontrap scan rate: Rapid; AGC target = 1×10^4 ; maximum injection time (ms) = 50; microscan = 1; and for ddMS2 (ETD), ETD reaction time (ms) 200; ETD reagent target 1.0×10^6 ; Maximum ETD reagent injection time (ms): 200; AGC target = 1×10^4 ; maximum injection time (ms) = 50; microscan = 1.

CID and ETD activation spectra were processed using Peaks 7. Briefly, raw files were searched against the sequence of PRMT1, with the precursor mass tolerance of 20 ppm and peptide fragment mass tolerance of 1 Da. And the static side chain modifications of carbamidomethyl (57.021), and dynamic side chain modifications of oxidation (15.995) and dimedone (138.068) controlled the protein FDR as 0.1 %.

RESULTS

PRMT1 Activity is Reversibly Inhibited by Oxidation— The elevated levels of free ADMA that are observed under oxidative stress conditions (7) could arise from a few distinct mechanisms. Both proteosomal degradation and methyltransferase activities could affect the rate of free ADMA formation. Increased synthesis of ADMA-containing proteins (the precursors to free ADMA) could occur by increasing the expression of PRMT proteins while maintaining normal enzyme activity, or by increasing the methyltransferase activity of the current pool of PRMT proteins. Since PRMT1 is responsible for ~85% of arginine methylation in cells and is the primary source of ADMA (31), altered expression and/or activity of this isoform would be expected to contribute greatly to altering levels of ADMA. In order to determine if oxidative conditions induce any changes in PRMT1 activity, we treated fully reduced recombinant PRMT1 with hydrogen peroxide, a common cellular oxidant, and measured the resulting methyltransferase activity.

Recombinantly expressed PRMT1 was pre-reduced with dithiothreitol (DTT), and rapidly desalted to remove residual DTT. The reduced PRMT1 was then incubated with various concentrations of H₂O₂ (0.4—800 μM final concentration) followed by the addition of catalase to remove any remaining H₂O₂. Surprisingly, when the peroxide-treated PRMT1 was assayed, methyltransferase activity was found to be significantly inhibited by peroxide in a dose-dependent manner (Fig. 6-2A). At concentrations of hydrogen peroxide greater than 4 μM, PRMT1 activity was significantly impaired and could not be fully recovered (data not shown). However, at the physiologically relevant concentration of 0.4 μM (physiological levels in mammals range from 0.001 μM to 0.7 μM)(32), hydrogen peroxide was also able to inhibit PRMT1 activity, and subsequent reduction with DTT

resulted in full recovery of activity (Fig. 6-2B). These experiments provide the first evidence that PRMT1 enzymatic activity is susceptible to reversible oxidative impairment under physiologically relevant oxidative conditions.

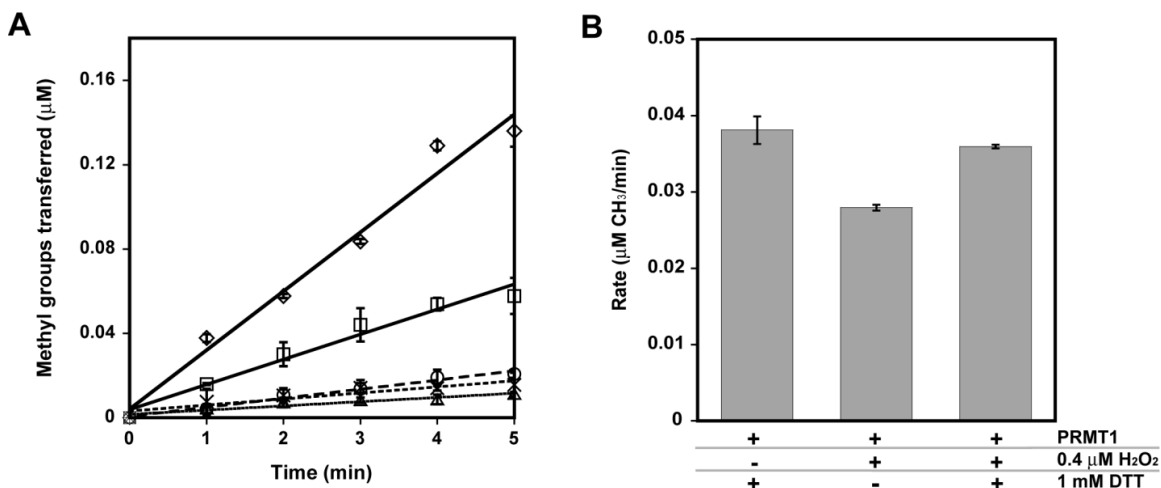


FIGURE 6-2. PRMT1 activity is (A) inhibited by H_2O_2 in a concentration dependent manner and (B) activity lost can be recovered by reduction. In (A), reduced PRMT1 was incubated with 0 (\diamond), 40 (\square), 200 (\circ), 400 (\times), or 800 (\triangle) $\mu\text{M H}_2\text{O}_2$ for 10 minutes at 37°C , followed by the addition of catalase. Methyltransferase activity of the treated PRMT1 was measured with 200 μM R3 peptide as a substrate as described in Experimental Procedures. In (B), reduced PRMT1 was treated with a physiologically-relevant concentration of hydrogen peroxide or phosphate-buffered saline (PBS) and subsequently treated with 1mM DTT or PBS prior to methyltransferase assays.

PRMT1 Enzymatic Activity Increases After Reduction— In order to better understand the sensitivity of PRMT1 to oxidation, we purified recombinant PRMT1 in the absence of reductant and measured methyltransferase activity in the absence and presence of a reductant. Pre-incubation with DTT increased methyltransferase activity by greater than 10-fold with the R3 peptide substrate (Fig. 6-3A). We examined the duration of this effect by rapidly desalting PRMT1 following the DTT pre-incubation step. The activity of

the desalted PRMT1 was increased only by 2-fold using the R3 peptide (Fig. 6-3A), indicating that the effect of DTT is transient and that PRMT1 oxidation occurs quickly in the absence of a reductant. We further studied the relationship between enzymatic activity and the concentration of DTT by comparing PRMT1 activity with varied concentrations of DTT ranging from 0.1 mM to 10 mM (Fig. 6-3B). Our results indicate that the effect of DTT is concentration-dependent, achieving a maximal rate enhancement at 1.5-2 mM DTT (Fig. 6-3B). During the course of this study, more than 50 human and rat PRMT1 proteins were purified in the absence of reductant and showed anywhere from a 1.8-fold to 70-fold increase in methyltransferase activity when DTT was included in the reaction or the enzyme was pre-incubated with DTT (data not shown). We note that in many cases, our purification protocol can be accomplished in as few as ~8 hours. These results demonstrate that PRMT1 is sensitive to oxidation by not only hydrogen peroxide, but also cellular conditions and/or the mild conditions used for purification.

Methylation of the sulfhydryl groups in DTT was previously observed with small molecule plant O-methyltransferases, where it acted as an intermediate acceptor molecule (33). Even though DTT methylation was not detected in our control reactions lacking peptide substrate (control Fig. 6-3A), we replaced DTT in our assay with an alternative thiol-free reductant, Tris(2-carboxyethyl)phosphine (TCEP). When 1 mM TCEP was used to reduce PRMT1, the rate enhancement with the R3 peptide was identical to that observed using 1 mM DTT (Fig. 6-3A). We conclude that the enhancement of HisPRMT1 methyltransferase activity is due to the reducing power of the DTT or TCEP additives.

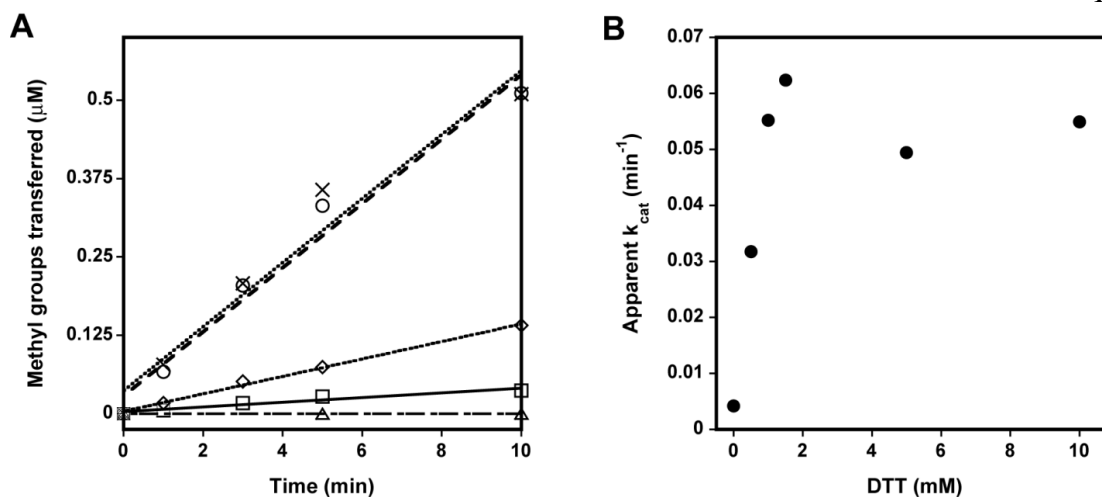


FIGURE 6-3. The effect of reducing agents on PRMT1 enzymatic activity. In (A) PRMT1 methyltransferase activity was measured without substrate (Δ), or with 200 μ M R3 peptide in the absence (\square) and presence of DTT (\circ) or TCEP (\times), or after desalting following a 10 minute pre-incubation with DTT (\diamond). In (B), methyltransferase activity was measured as a function of DTT concentration.

Several different affinity tags are used for PRMT1 purification and variable methylation rates have been observed (34-36). We questioned whether our His₆-tag was influencing the observed rate changes upon reduction. To address this concern, we expressed a tag-less version of rat PRMT1. However, this version of PRMT1 was unstable and lost activity rapidly (data not shown). As an alternative strategy, we created a His₆-tagged, tobacco etch virus (TEV) cleavable, rat PRMT1 construct (HisTevPRMT1) which allowed us to cleave the tag after an initial purification step and then use the tag-free version (tag-freePRMT1) for kinetic assays. Both tagged and tag-free versions of PRMT1 exhibited rate enhancement upon reduction, although the tag-free version was markedly more active than the tagged version even without DTT in the assay (Fig. 6-4). This observation is easily explained when the method for acquiring tag-free protein is taken into consideration. The protocol for TEV cleavage includes an overnight dialysis step in a

buffer containing 1 mM DTT and 2 mM EDTA and therefore the resulting tag-free enzyme used in the activity assays is already somewhat pre-reduced. To confirm this theory, we again purified the cleavable (HisTevPRMT1) enzyme by nickel chromatography. Purified enzyme was divided into two separate dialysis bags. TEV was added to one, and the other was left uncleaved; however, both tagged and cleaved samples were dialyzed overnight in the same 1 mM DTT, 2 mM EDTA containing buffer. Methyltransferase activity of these newly purified tagged and tag-free PRMT1 enzymes revealed no significant rate enhancement upon addition of DTT (Fig. 6-4). The addition of only EDTA had no significant effect on methyltransferase activity (Fig. 6-4). These results confirm that it is not the tag, but rather the reducing treatment of the tag-free enzyme which enhanced the enzymatic activity of PRMT1.

Reduction Alters the Oligomeric State of PRMT1— It has been shown that PRMT1 forms at least a homo dimer in order to be catalytically active (36-38). Feng *et al.* introduced the idea that changing the oligomeric state of PRMT1 affects its enzymatic activity (34). Since reduction of PRMT1 results in increased activity, we wondered if reduction had an effect on the oligomeric state of the enzyme. Size exclusion chromatography experiments in the presence or absence of DTT were carried out to determine the oligomeric state of PRMT1 under different redox environments (Fig. 6-5). Unreduced PRMT1 migrates over a broad range of oligomeric states, with the majority of the protein existing in oligomers that migrate at molecular weights above 660 kDa. As a reference, PRMT1 is thought to be active as an 80 kDa dimer (although a dimer form has not been observed on size exclusion chromatography) (36,39). Overnight incubation with 1 mM DTT and 2 mM EDTA results in a shift towards a homogeneous oligomeric state

migrating between 200 and 450 kDa (Fig. 6-5). Analytical ultracentrifugation, a more sensitive technique for determining molecular weights, showed the same shift towards a smaller oligomeric species upon reduction as was observed using size exclusion chromatography (data not shown). In conclusion, oxidized PRMT1 forms a large molecular weight functional aggregate, while reduction of PRMT1 causes a shift towards a smaller, more uniform, oligomeric state that correlated with an increase in enzymatic activity.

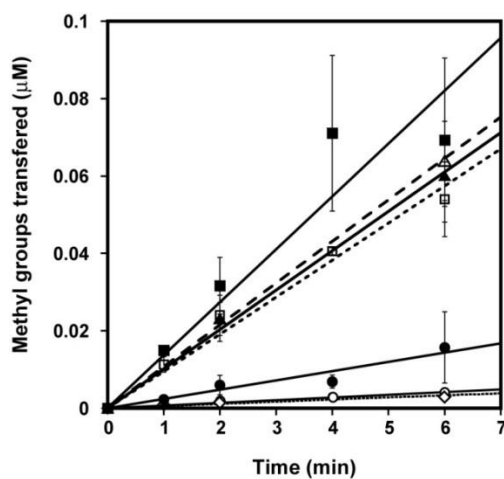


FIGURE 6-4. The enhancing effect of DTT on PRMT1 methyltransferase activity is independent of the His₆-tag. Enzymatic activity of HisTevPRMT1 (○), cleaved PRMT1 (△), and dialyzed HisTevPRMT1 (□) measured with 200 μM R3 peptide in the absence (open) and presence (closed symbols) of DTT respectively, as well as HisTevPRMT1 treated with EDTA only as a control (◇).

Reduction Alters the Oligomeric State of PRMT1— It has been shown that PRMT1 forms at least a homo dimer in order to be catalytically active (36-38). Feng *et al.* introduced the idea that changing the oligomeric state of PRMT1 affects its enzymatic activity (34). Since reduction of PRMT1 results in increased activity, we wondered if reduction had an effect on the oligomeric state of the enzyme. Size exclusion

chromatography experiments in the presence or absence of DTT were carried out to determine the oligomeric state of PRMT1 under different redox environments (Fig. 6-5). Unreduced PRMT1 migrates over a broad range of oligomeric states, with the majority of the protein existing in oligomers that migrate at molecular weights above 660 kDa. As a reference, PRMT1 is thought to be active as an 80 kDa dimer (although a dimer form has not been observed on size exclusion chromatography) (36,39). Overnight incubation with 1 mM DTT and 2 mM EDTA results in a shift towards a homogeneous oligomeric state migrating between 200 and 450 kDa (Fig. 6-5). Analytical ultracentrifugation, a more sensitive technique for determining molecular weights, showed the same shift towards a smaller oligomeric species upon reduction as was observed using size exclusion chromatography (data not shown). In conclusion, oxidized PRMT1 forms a large molecular weight functional aggregate, while reduction of PRMT1 causes a shift towards a smaller, more uniform, oligomeric state that correlated with an increase in enzymatic activity.

The Oxidation-Dependent Effects on PRMT1 Activity Require a Cysteine(s) Residue— One of the most common mechanisms for oxidative damage is the oxidation of cysteine residues (40-43). We took a broad approach to evaluate whether any cysteine residues were responsible for the effects of oxidation/reduction by creating a PRMT1 variant where all eleven rat PRMT1 cysteine residues were mutated to serine (HisTevPRMT1 Δ cys or cys-). Interestingly, the cysteine-less PRMT1 showed no enhancement in methyltransferase activity upon pre-incubation with DTT (Fig. 6-6). In addition to activity measurements, the oligomeric state of the cysteine-less PRMT1 variant was assessed by size-exclusion chromatography (Fig. 6-5). The cysteine-less PRMT1

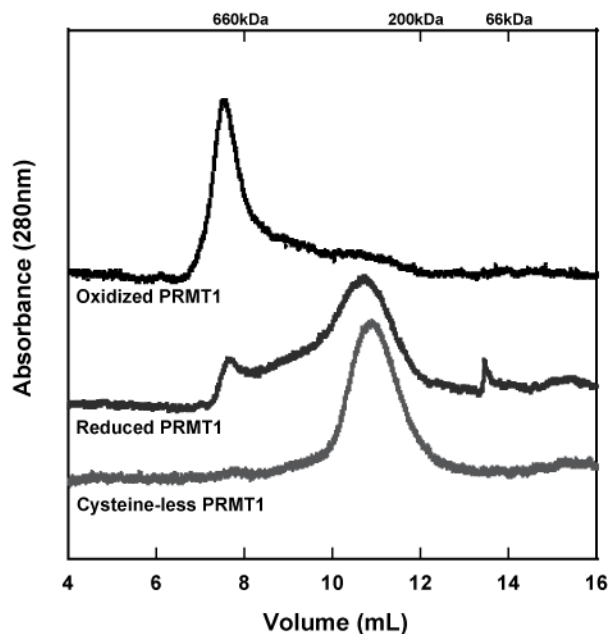


FIGURE 6-5. Oligomeric state of PRMT1 proteins assessed by size exclusion chromatography. PRMT1 without DTT treatment (top) or incubated overnight with 1 mM DTT and 2 mM EDTA (middle), compared to Cysteine-less PRMT1 which migrates at the same position regardless of treatment with DTT or EDTA. Reduction of PRMT1 or removal of all cysteine residues results in a shift towards a smaller oligomeric state.

enzyme exhibited a migration pattern similar to that of the maximally active, reduced PRMT1, regardless of its treatment (data not shown). We conclude from these observations that indeed one (or more) cysteine(s) are responsible for the redox switching of PRMT1 activity.

C101, C342, C254, and C208 are not Individually Responsible for Reductive Effects— We examined the rat PRMT1 crystal structures (36) for cysteine residues capable of undergoing oxidation and found that out of the eleven cysteines present in rat PRMT1, cysteines 101, 208, 232, 254, and 342, are all solvent accessible (Fig. 6-8). Cysteines 9 and 15 are not visible in the crystal structure and were not considered in this study since a human PRMT1 variant lacking the first 27 amino acids exhibits enhanced activity after

reduction (data not shown). A recent quantitative reactivity profiling study identified C101 as hyper-reactive with 4-hydroxyl-2-nonenal (HNE) (44), indicating that C101 may be susceptible to oxidation. Cysteine 101 is situated on the far edge of the AdoMet binding pocket and directly interacts with the adenine ring structure of AdoMet (see Fig. 6-8), and thus, seemed like an excellent target to control enzymatic activity depending on its redox state. Mutation of C101 to serine results in a construct mimicking wild type methyltransferase activity, including the response to DTT (Fig. 6-6). Closer evaluation of our rat PRMT1 M48L crystal structure (23) showed additional electron density around cysteine 342, suggesting possible oxidation of the thiolate moiety to a reducible sulfenic acid moiety. Although this residue is relatively removed from the active site, it has been suggested that residues distant from the active site can regulate PRMT substrate specificity (45). However, the C342S variant also mimicked wild type enzymatic activity, including the DTT enhancement (Fig. 6-6). The PRMT1 crystal structure (36) also shows that C254 forms an intermolecular disulfide bond with another PRMT1 dimer, and was therefore also mutated to determine if reduction of this disulfide caused the increase in activity and the corresponding shift towards a smaller oligomeric state. However, as we saw with the other two individual cysteine variants, C254S activity was still enhanced upon reduction with DTT (Figure 6-6). The C254S PRMT1 variant also behaved as WT PRMT1 when run on size exclusion chromatography (data not shown)(36).

As previously mentioned, it is believed that PRMT1 dimerization is necessary for catalytic activity. In fact, all currently available Type 1 and Type 2 PRMT structures reveal a conserved mode of dimerization between catalytic subunits (36-38,46,47). Each subunit contains a dimerization helix-turn-helix dimerization arm (blue in Fig. 6-8) that extends

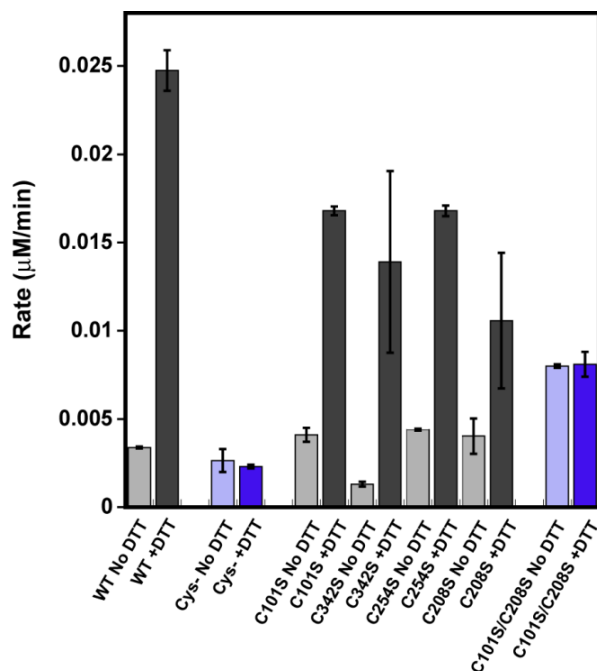


FIGURE 6-6. Methyltransferase activity of PRMT1 cysteine variants in the absence or presence of DTT. WT PRMT1, Cysteine-less PRMT1, C101S PRMT1, C342S PRMT1, C254S PRMT1, C208S PRMT1, and C101S/C208S PRMT1 methylated 200 μM R3 peptide in the absence (light gray/purple) or presence (dark gray/purple) of DTT. Results shown correspond to the average of at least two biological replicates. Removing all cysteine residues from PRMT1, or making C101 and C208 unavailable for oxidation resulted in abolished redox control over PRMT1 catalytic activity.

from the C-terminal β -barrel (dark gray in Fig. 6-8) and rests upon the N-terminal AdoMet binding domain (light gray in Fig. 6-8) of the other subunit; coming together to form an active dimer with a central cavity and two opposing active sites (Fig. 6-8).

Zhang, X. *et al.* reported that removal of the helix-turn-helix dimerization arm of PRMT1 not only eliminated homodimerization, but also AdoMet binding and methyltransferase activity. It was thus suggested that the dimer interaction is required to engage the residues on the other side of the structural elements to interact with AdoMet properly (36). In the analysis of another type 1 PRMT structure, Cheng, Y. *et al.* computed the atomic position fluctuations (APFs) of the monomer and dimer to determine the impact

of dimerization of the motion of atPRMT10, also a type 1 PRMT. They found two regions to have lower APFs in dimeric form than in monomeric form: the $\alpha\gamma$ -loop- αZ (40-68 in atPRMT10) (orange in Fig. 6-8) and the dimerization arm (187-235 in atPRMT10) (blue in Fig. 6-8), suggesting that these regions are stabilized upon dimer formation. The $\alpha\gamma$ -loop- αZ region is directly involved in AdoMet binding and the formation of the substrate binding groove I (36). It was also suggested that stabilization of this region by dimerization likely improves the binding of AdoMet and substrate proteins (37). Additionally, Higashimoto *et al.* demonstrated that in PRMT4 (CARM1), phosphorylation of S229, located on the outer face of the AdoMet binding domain, compromised dimerization, negatively regulated methyltransferase activity, and lowered AdoMet binding (48). The presence of a charged functional group adjacent to the hydrophobic dimerization arm binding surface likely destabilizes dimerization interactions. Cysteine 208 of PRMT1 is located on the PRMT1 dimer interface (Fig. 6-8). Given the importance of dimerization for PRMT activity and the predicted susceptibility to oxidation, this residue was also deemed likely to be culpable for the effect of oxidation in impairing methyltransferase activity. Additionally, use of the Cysteine Oxidation Prediction Algorithm (COPA) which uses distance to the nearest cysteine sulfur, solvent accessibility, and pKa as parameters for thiol oxidation susceptibility, suggested Cysteine 208 is susceptible to oxidation by exposure (49). However, measurement of the enzymatic activity of the individual C208S variant revealed this construct was also enhanced by DTT (Fig. 6-6).

If PRMT1 dimerization is indeed stabilizing substrate binding, we rationalized that oxidation of C208 in the dimerization arm in conjunction with C101 in the AdoMet binding pocket could be responsible for the diminished methyltransferase activity observed under

oxidizing conditions. In order to explore this hypothesis, a C101S/C208S variant of PRMT1 was created, and methyltransferase activity was measured in the presence and absence of DTT. Remarkably, methyltransferase activity of the double variant was the same under both oxidizing and reducing conditions (Fig. 6-6). We note that the activity of the double variant (C101S/C208S) is lower than the activity of reduced wild type enzyme, suggesting that these residues may have an additional role in PRMT1 activity. Surprisingly, when both C101 and C208 are unavailable for oxidation, the protein does not completely shift to a smaller oligomeric state as the cysteine-less construct (data not shown). In conclusion, making C101 and C208 unavailable for oxidation resulted in abolished redox control over PRMT1 catalytic activity.

Sulfenic Acid Formation at C101 and C208 In Vitro— In order to further analyze the oxidation events occurring at C101 and C208, we used the sulfenic acid-specific probe DCP-Rho1, which contains a rhodamine attached to the functional core of dimedone. To detect sulfenic acids, air oxidized wild type PRMT1 (WT), cysteine-less with C101 reintroduced (cys-C¹⁰¹), cysteine-less with C208 reintroduced (cys-C²⁰⁸), and cysteine-less with both C101 and C208 reintroduced (cys-C¹⁰¹C²⁰⁸) were incubated with DCP-Rho1 or DMSO as a negative control in the presence or absence of reductant under denaturing conditions. Cysteine-less PRMT1 (cys-) was also subjected to labeling as a negative control. Analysis of the fluorescent label incorporation (Fig. 6-7-A and B) clearly shows the presence of sulfenic acid at cysteine 101 and 208 of PRMT1. Interestingly, while both cysteine 101 and 208 are necessary for oxidative impairment of C101, we consistently observed more sulfenic acid formation at C208, suggesting either that C101 is less susceptible to oxidation than C208, or that the sulfenic acid form of C101 is transient and

can be further oxidized to sulfinic or sulfonic acid. The possibility that these two cysteine residues may somehow be involved in a disulfide linkage was ruled out using Native PAGE analysis (data not shown). Free thiol content analysis using the 5IAF probe (Fig. 6-7-C and D) and performed in parallel with the DCP-Rho1 labeling, shows similar free thiol content for cys-C¹⁰¹ and cys-C²⁰⁸. When analyzed together, these results are consistent with a higher propensity for irreversible oxidation at C101. In addition to the fluorescent probes, WT PRMT1 treated with sulfenic-acid-specific dimedone was subjected to LC-MS/MS analysis to further confirm sulfenic acid formation. Using this method, dimedone incorporation was observed at both C101 and C208 (Figure 6-7-E and F), confirming the fluorescent probe results. In conclusion, the reversible activity impairment observed under oxidative conditions is consistent with sulfenic acid formation at C101 and C208 of PRMT1.

DISCUSSION

Elevated ADMA concentrations have been proposed to predict cardiovascular mortality in patients with chronic renal insufficiency (50) and acute coronary events (8). Additionally, ADMA is not only a marker, but also a mediator of oxidative stress within vascular tissue (7). Given that PRMT1 is the primary source of ADMA in eukaryotes, it is of the utmost importance to understand how PRMT1 activity and ADMA synthesis are regulated under oxidative stress conditions. Here, we have shown that PRMT1 activity is decreased *in vitro* under physiologically relevant oxidative conditions, an effect which is readily reversed upon reduction and is associated with cysteine oxidation to sulfenic acid.

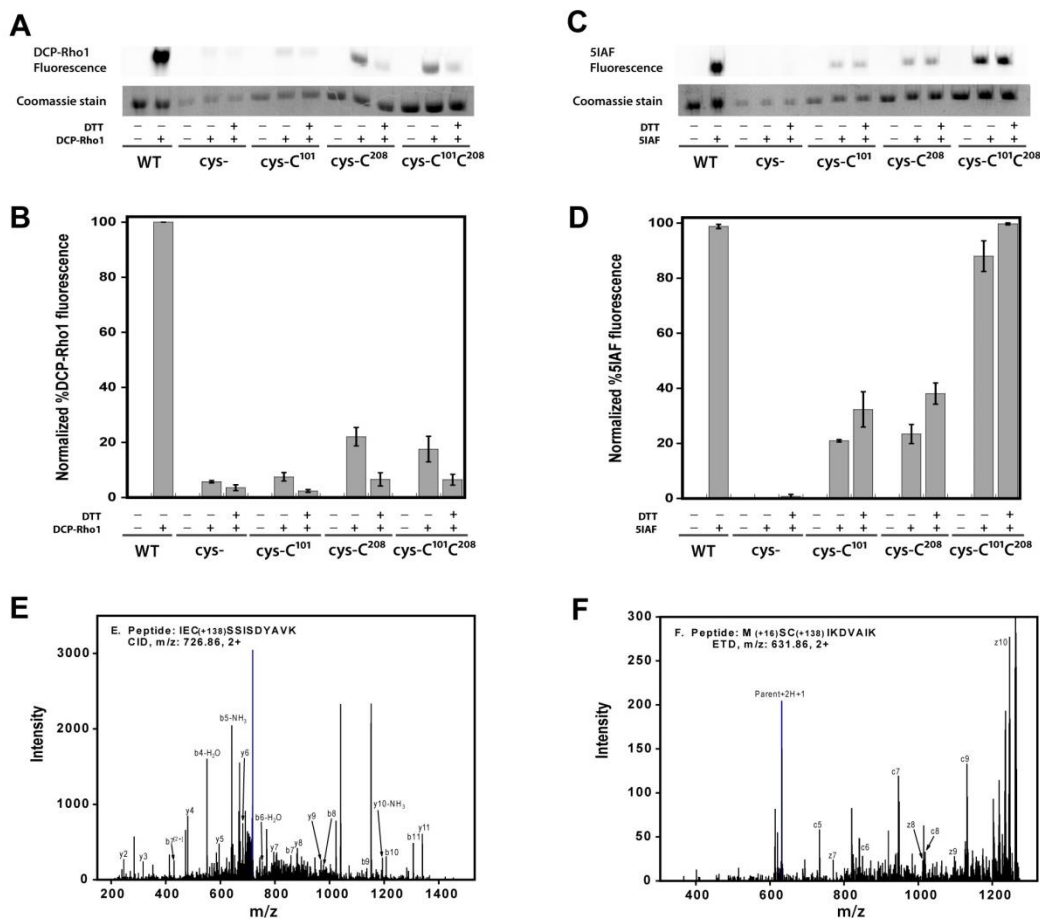


FIGURE 6-7. Sulfenic acid detection and free thiol content in PRMT1. In (A), (B), (C), and (D) Air oxidized wild type PRMT1 (WT), cysteine-less (cys-), cysteine-less with C101 reintroduced (cys-C¹⁰¹), cysteine-less with C208 reintroduced (cys-C²⁰⁸), and cysteine-less with both C101 and C208 reintroduced (cys-C¹⁰¹C²⁰⁸) were denatured in 6M urea and incubated with 1 mM DTT or buffer prior to addition of 10 μ M DCP-Rho1 or 2.5 mM 5IAF. Labeled samples were resolved by SDS-PAGE. (A) shows a representative image of the rhodamine fluorescence signal and the corresponding coomassie bands. (B) graphical representation of triplicate gel analysis. Normalized percent DCP-Rho1 fluorescence represents the percentage of fluorescent signal divided by the amount of protein observed in the coomassie bands which is interpreted as the relative amount of sulfenic acid present. (C) shows a representative image of the 5IAF fluorescence signal and the corresponding coomassie bands. (D) graphical representation of triplicate 5IAF gel analysis, interpreted as relative amount of free thiols present. (E) and (F) show a representative MS/MS fragmentation spectra for peptides containing dimedone-modified sulfenic acids in PRMT1. In (E), the CID fragments of peptide IECSSISDYAVK labeled with dimedone at C101. (F) ETD fragments of peptide MCSIKDVAIK labeled with dimedone at C208. The mass shift by the modification is 138.068 (exact number), as denoted in peptide sequence.

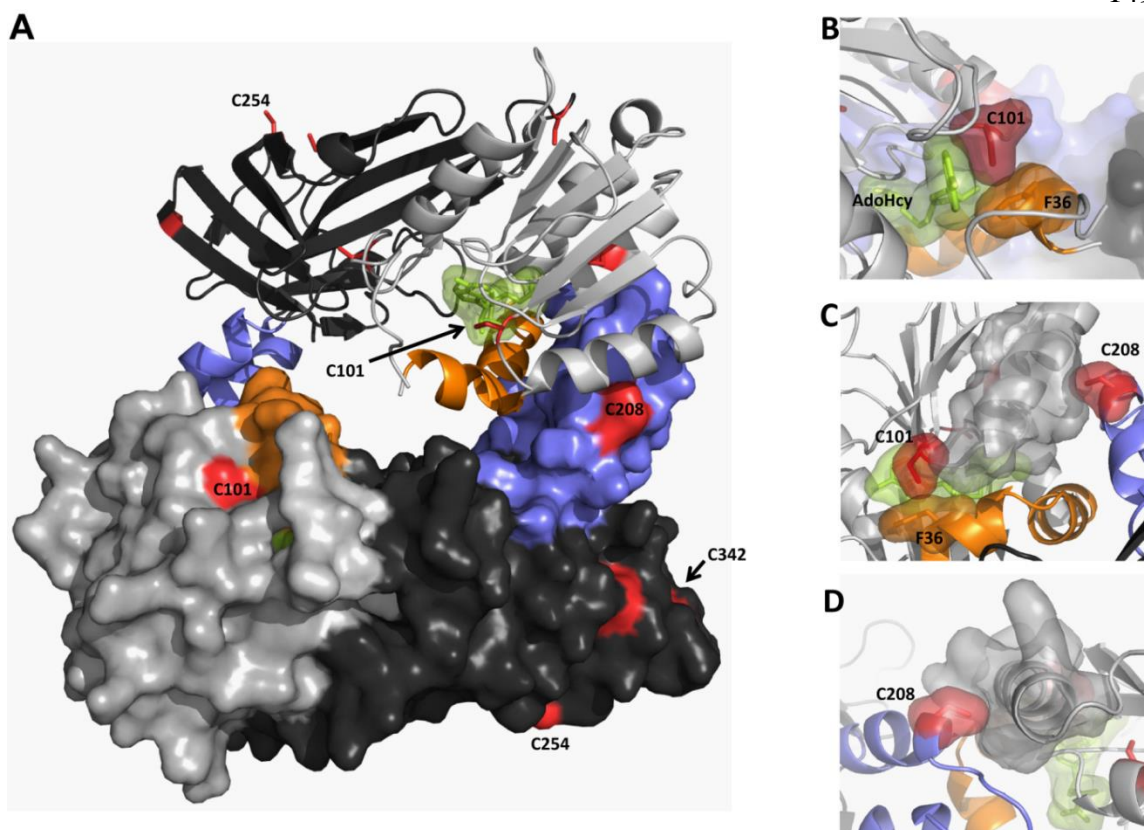


FIGURE 6-8. Cysteine residues in rPRMT1. PRMT1 dimer (1OR8) colored as described in text (AdoMet binding domain in light gray, β -barrel domain in dark gray, dimerization arm in blue, α γ -loop- α Z in orange, AdoHcy in green, and cysteine residues in red. Residues 26-39 were modeled based on the position of this helix in the PRMT3 structure (1F3L). (A) PRMT1 dimer (B) Surface representation showing close active site interactions between AdoHcy, C101 and F36. (C) Top view of dimerization arm in one monomer interacting with AdoMet binding site in other monomer. (D) Back view showing packing of C208 in one monomer with alpha helix in AdoMet binding domain of other monomer.

Our results complicate the view that the increased PRMT1 protein expression observed under oxidative stress conditions is responsible for increased ADMA levels, by supporting a model in which PRMT1 activity can be regulated in a redox-sensitive manner. While it has long been known that DDAH breakdown of ADMA is under redox control, we provide

the first evidence that the activity of enzymes involved in the formation of ADMA precursors are regulated in a redox-sensitive fashion.

Removal of two cysteine residues implicated in PRMT1 dimerization and cofactor binding eliminates the redox-dependent control over PRMT1 methyltransferase activity. Dimerization is strictly conserved in all known PRMTs and seems necessary for methyltransferase activity (36-38). One of the pathways proposed for signal communication between the dimer interface and the catalytic center uses the mainly hydrophobic dimer interactions between the $\alpha\gamma$ -loop- αZ (orange in Fig. 6-8) of one monomer and the helix-turn-helix dimerization arm of another (blue in Fig.6-8) (36,37,46). It has been proposed that this dimer interaction is required to engage residues into proper conformation for interaction with the AdoMet cofactor (36). It is feasible that oxidation of residues involved in this cooperative effort could disrupt PRMT1 methyltransferase activity by affecting AdoMet binding. Interestingly, cysteine 208 is conserved in PRMT3 and PRMT6, while both cysteine 101 and 208 are conserved in PRMT8. Remarkably, the type III PRMT7 from *Trypanosoma brucei*, which contains only three cysteine residues that do not align with any cysteines in PRMT1, but does contain a cysteine at a different location in its dimerization arm, also shows increased activity upon reduction. Activity measurements using human PRMT3, human PRMT6, and TbPRMT7 demonstrate that these type 1 and type 3 PRMTs are also under redox control (Figure 6-9). Ongoing studies will help provide insight as to how these residues affect AdoMet interactions and PRMT methyltransferase activity.

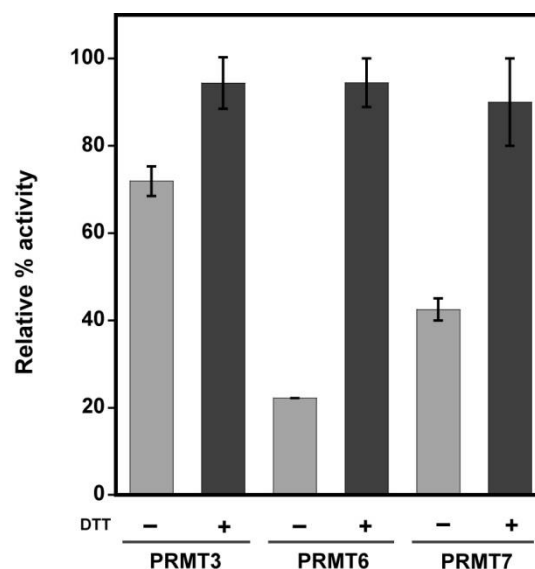


FIGURE 6-9. Redox control is conserved among PRMT family members. Human PRMT3 (residues 211-531), human PRMT6, and TbPRMT7 activities were tested with R3 peptide, bulk histones, or Histone 4 respectively in the absence or presence of DTT. The average of three activity measurements are shown as relative percent activity for each isoform with its corresponding substrate.

While the active form of PRMT1 is expected to be a dimer, size exclusion chromatography analysis, as well as dynamic light scattering, have shown the enzyme typically migrates as a high molecular weight oligomer (34,36,38,51,52). Feng *et al.* suggested that PRMT1 multi-oligomerization (i.e., greater than a dimer) is concentration dependent in the range of 0-0.5 μM and that the final PRMT1 multi-oligomeric complex is the most active form (34). It is important to note that the Feng study was done with fully reduced PRMT1 and at significantly lower enzyme concentrations than those used in this study. Our results show that oxidized PRMT1, which displays less activity, shifts from a large oligomeric species to a smaller, but still large oligomeric state under reducing conditions. While our results seem to be at odds with the Feng study, they only serve to highlight the high degree of complexity that exists in relating PRMT1 oligomerization and

activity. Interestingly, while cysteine-less PRMT1 remains a smaller oligomer under both reducing and oxidizing conditions, the C101S/C208S PRMT1 variant presents as a mix of both large and smaller oligomers under reducing conditions (data not shown). It is difficult to assess what may be causing PRMT1 to form such large oligomeric aggregates, and the link between PRMT1 cysteine oxidation and protein oligomerization remains to be determined. While our results add to the larger story, much remains to be discovered on the impact of oligomeric state on PRMT1 activity.

It is also important to point out that much of the work in the PRMT field is carried out exclusively under reducing conditions. Our work emphasizes the importance of PRMT1 as a redox-sensitive enzyme and the need for careful control of its redox environment. Since PRMT1 activity is under redox control, it is possible that experiment conditions might inadvertently alter activity and/or interaction partners. In the future, it will be highly important to take into account the redox environment of experiments before reaching conclusions. Additionally, while the different affinity tags that were used in this study did not change the increase in activity observed upon PRMT1 reduction, the overall methyltransferase activity was generally lower for HisTevPRMT1 constructs than for HisPRMT1 constructs. Since the tags are located on the N-terminal end of the enzyme, this observation may hint at the importance of the N-terminal PRMT1 sequence in controlling enzymatic activity.

In addition to providing ADMA precursor pools, growing evidence supports the involvement of PRMT1 in the cellular oxidative stress response as a modifier of signal transduction. PRMT1 has recently been reported to be involved in the transcriptional regulation of the human ferritin gene, up-regulation of which is an important cellular

defense response to oxidative stress (53). It was also recently reported that PRMT1 methylation is involved in the transcriptional repression of HIF α (54), a protein needed to activate the cellular adaptive response to hypoxia, another condition linked to high levels oxidative stress. Finally, we note that oxidative stress in HEK293 cells was reported to enhance PRMT1-mediated methylation of FOXO1 in the nucleus (55). The observed increase in FOXO1 methylation seems contradictory to our results and highlights the importance of further investigating the effect of oxidation *in vivo* on PRMT1 substrate specificity, and/or cellular localization. In future studies, it will also be interesting to determine how redox regulation affects the role of PRMT1 in signal transduction.

In summary, this work has demonstrated that PRMT1 is a redox-responsive enzyme. Oxidation at two cysteine residues potentially destabilizes dimerization leading to diminished methyltransferase activity, while reduction readily reverses the effects of oxidation under physiologically relevant conditions, consistent with sulfenic acid formation observed at both cysteine residues. Our results provide the first direct evidence that PRMT1 enzymatic activity can be regulated in a redox-sensitive manner and raise the concern that the current paradigm used to explain free ADMA accumulation *in vivo* may be incomplete.

REFERENCES

1. Go, A. S., Mozaffarian, D., Roger, V. L., Benjamin, E. J., Berry, J. D., Blaha, M. J., Dai, S. F., Ford, E. S., Fox, C. S., Franco, S., Fullerton, H. J., Gillespie, C., Hailpern, S. M., Heit, J. A., Howard, V. J., Huffman, M. D., Judd, S. E., Kissela, B. M., Kittner, S. J., Lackland, D. T., Lichtman, J. H., Lisabeth, L. D., Mackey, R. H., Magid, D. J., Marcus, G. M., Marelli, A., Matchar, D. B., McGuire, D. K., Mohler, E. R., Moy, C. S., Mussolino, M. E., Neumar, R. W., Nichol, G., Pandey,

- D. K., Paynter, N. P., Reeves, M. J., Sorlie, P. D., Stein, J., Towfighi, A., Turan, T. N., Virani, S. S., Wong, N. D., Woo, D., Turner, M. B., Comm, A. H. A. S., and Subcomm, S. S. (2014) Heart Disease and Stroke Statistics-2014 Update A Report From the American Heart Association. *Circulation* **129**, E28-E292
2. Lu, T. M., Ding, Y. A., Charng, M. J., and Lin, S. J. (2003) Asymmetrical dimethylarginine: a novel risk factor for coronary artery disease. *Clinical cardiology* **26**, 458-464
 3. Chen, X., Niroomand, F., Liu, Z., Zankl, A., Katus, H. A., Jahn, L., and Tiefenbacher, C. P. (2006) Expression of nitric oxide related enzymes in coronary heart disease. *Basic research in cardiology* **101**, 346-353
 4. Antoniades, C., Shirodaria, C., Leeson, P., Antonopoulos, A., Warrick, N., Van-Assche, T., Cunnington, C., Tousoulis, D., Pillai, R., Ratnatunga, C., Stefanadis, C., and Channon, K. M. (2009) Association of plasma asymmetrical dimethylarginine (ADMA) with elevated vascular superoxide production and endothelial nitric oxide synthase uncoupling: implications for endothelial function in human atherosclerosis. *European heart journal* **30**, 1142-1150
 5. Boger, R. H., Bode-Boger, S. M., Szuba, A., Tsao, P. S., Chan, J. R., Tangphao, O., Blaschke, T. F., and Cooke, J. P. (1998) Asymmetric dimethylarginine (ADMA): a novel risk factor for endothelial dysfunction: its role in hypercholesterolemia. *Circulation* **98**, 1842-1847
 6. Luneburg, N., Harbaum, L., and Hennigs, J. K. (2014) The Endothelial ADMA/NO Pathway in Hypoxia-Related Chronic Respiratory Diseases. *BioMed research international* **2014**, 501612
 7. Sydow, K., and Munzel, T. (2003) ADMA and oxidative stress. *Atherosclerosis. Supplements* **4**, 41-51
 8. Valkonen, V. P., Paiva, H., Salonen, J. T., Lakka, T. A., Lehtimaki, T., Laakso, J., and Laaksonen, R. (2001) Risk of acute coronary events and serum concentration of asymmetrical dimethylarginine. *Lancet* **358**, 2127-2128
 9. Vallance, P., and Leiper, J. (2004) Cardiovascular biology of the asymmetric dimethylarginine:dimethylarginine dimethylaminohydrolase pathway. *Arteriosclerosis, thrombosis, and vascular biology* **24**, 1023-1030
 10. Achan, V., Broadhead, M., Malaki, M., Whitley, G., Leiper, J., MacAllister, R., and Vallance, P. (2003) Asymmetric dimethylarginine causes hypertension and cardiac dysfunction in humans and is actively metabolized by dimethylarginine dimethylaminohydrolase. *Arteriosclerosis, thrombosis, and vascular biology* **23**, 1455-1459

11. Kielstein, J. T., Impraim, B., Simmel, S., Bode-Boger, S. M., Tsikas, D., Frolich, J. C., Hoeper, M. M., Haller, H., and Fliser, D. (2004) Cardiovascular effects of systemic nitric oxide synthase inhibition with asymmetrical dimethylarginine in humans. *Circulation* **109**, 172-177
12. Burgoyne, J. R., Mongue-Din, H., Eaton, P., and Shah, A. M. (2012) Redox signaling in cardiac physiology and pathology. *Circulation research* **111**, 1091-1106
13. Chan, J. R., Boger, R. H., Bode-Boger, S. M., Tangphao, O., Tsao, P. S., Blaschke, T. F., and Cooke, J. P. (2000) Asymmetric dimethylarginine increases mononuclear cell adhesiveness in hypercholesterolemic humans. *Arteriosclerosis, thrombosis, and vascular biology* **20**, 1040-1046
14. Bedford, M. T., and Clarke, S. G. (2009) Protein arginine methylation in mammals: who, what, and why. *Molecular cell* **33**, 1-13
15. Ogawa, T., Kimoto, M., and Sasaoka, K. (1987) Occurrence of a new enzyme catalyzing the direct conversion of NG,NG-dimethyl-L-arginine to L-citrulline in rats. *Biochemical and biophysical research communications* **148**, 671-677
16. Boger, R. H., Sydow, K., Borlak, J., Thum, T., Lenzen, H., Schubert, B., Tsikas, D., and Bode-Boger, S. M. (2000) LDL cholesterol upregulates synthesis of asymmetrical dimethylarginine in human endothelial cells: involvement of S-adenosylmethionine-dependent methyltransferases. *Circulation research* **87**, 99-105
17. Chobanyan-Jurgens, K., Pham, V. V., Stichtenoth, D. O., and Tsikas, D. (2011) Asymmetrical dimethylarginine, oxidative stress, and atherosclerosis. *Hypertension* **58**, e184-185; author reply e186
18. Jiang, J. L., Zhang, X. H., Li, N. S., Rang, W. Q., Feng, Y., Hu, C. P., Li, Y. J., and Deng, H. W. (2006) Probucol decreases asymmetrical dimethylarginine level by alternation of protein arginine methyltransferase I and dimethylarginine dimethylaminohydrolase activity. *Cardiovascular drugs and therapy / sponsored by the International Society of Cardiovascular Pharmacotherapy* **20**, 281-294
19. Chen, Y., Xu, X., Sheng, M., Zhang, X., Gu, Q., and Zheng, Z. (2009) PRMT-1 and DDAHs-induced ADMA upregulation is involved in ROS- and RAS-mediated diabetic retinopathy. *Experimental eye research* **89**, 1028-1034
20. Tyagi, N., Sedoris, K. C., Steed, M., Ovechkin, A. V., Moshal, K. S., and Tyagi, S. C. (2005) Mechanisms of homocysteine-induced oxidative stress. *American journal of physiology. Heart and circulatory physiology* **289**, H2649-2656

21. Wilcox, C. S. (2012) Asymmetric dimethylarginine and reactive oxygen species: unwelcome twin visitors to the cardiovascular and kidney disease tables. *Hypertension* **59**, 375-381
22. Lim, Y., Lee, E., Lee, J., Oh, S., and Kim, S. (2008) Down-regulation of asymmetric arginine methylation during replicative and H₂O₂-induced premature senescence in WI-38 human diploid fibroblasts. *Journal of biochemistry* **144**, 523-529
23. Gui, S., Wooderchak, W. L., Daly, M. P., Porter, P. J., Johnson, S. J., and Hevel, J. M. (2011) Investigation of the molecular origins of protein-arginine methyltransferase I (PRMT1) product specificity reveals a role for two conserved methionine residues. *The Journal of biological chemistry* **286**, 29118-29126
24. Wang, R., Ibanez, G., Islam, K., Zheng, W., Blum, G., Sengelaub, C., and Luo, M. (2011) Formulating a fluorogenic assay to evaluate S-adenosyl-L-methionine analogues as protein methyltransferase cofactors. *Molecular bioSystems* **7**, 2970-2981
25. Cornell, K. A., Swarts, W. E., Barry, R. D., and Riscoe, M. K. (1996) Characterization of recombinant *Escherichia coli* 5'-methylthioadenosine/S-adenosylhomocysteine nucleosidase: analysis of enzymatic activity and substrate specificity. *Biochemical and biophysical research communications* **228**, 724-732
26. Suh-Lailam, B. B., and Hevel, J. M. (2010) A fast and efficient method for quantitative measurement of S-adenosyl-L-methionine-dependent methyltransferase activity with protein substrates. *Analytical biochemistry* **398**, 218-224
27. Atmane, N., Dairou, J., Paul, A., Dupret, J. M., and Rodrigues-Lima, F. (2003) Redox regulation of the human xenobiotic metabolizing enzyme arylamine N-acetyltransferase 1 (NAT1). Reversible inactivation by hydrogen peroxide. *The Journal of biological chemistry* **278**, 35086-35092
28. Nelson, K. J., Klomsiri, C., Codreanu, S. G., Soito, L., Liebler, D. C., Rogers, L. C., Daniel, L. W., and Poole, L. B. (2010) Use of dimedone-based chemical probes for sulfenic acid detection methods to visualize and identify labeled proteins. *Methods in enzymology* **473**, 95-115
29. Wu, Y., Kwon, K. S., and Rhee, S. G. (1998) Probing cellular protein targets of H₂O₂ with fluorescein-conjugated iodoacetamide and antibodies to fluorescein. *FEBS letters* **440**, 111-115

30. Hansen, R. E., and Winther, J. R. (2009) An introduction to methods for analyzing thiols and disulfides: Reactions, reagents, and practical considerations. *Analytical biochemistry* **394**, 147-158
31. Tang, J., Frankel, A., Cook, R. J., Kim, S., Paik, W. K., Williams, K. R., Clarke, S., and Herschman, H. R. (2000) PRMT1 is the predominant type I protein arginine methyltransferase in mammalian cells. *The Journal of biological chemistry* **275**, 7723-7730
32. Stone, J. R., and Yang, S. (2006) Hydrogen peroxide: a signaling messenger. *Antioxidants & redox signaling* **8**, 243-270
33. Coiner, H., Schroder, G., Wehinger, E., Liu, C. J., Noel, J. P., Schwab, W., and Schroder, J. (2006) Methylation of sulfhydryl groups: a new function for a family of small molecule plant O-methyltransferases. *The Plant journal : for cell and molecular biology* **46**, 193-205
34. Feng, Y., Xie, N., Jin, M., Stahley, M. R., Stivers, J. T., and Zheng, Y. G. (2011) A transient kinetic analysis of PRMT1 catalysis. *Biochemistry* **50**, 7033-7044
35. Kleinschmidt, M. A., Streubel, G., Samans, B., Krause, M., and Bauer, U. M. (2008) The protein arginine methyltransferases CARM1 and PRMT1 cooperate in gene regulation. *Nucleic acids research* **36**, 3202-3213
36. Zhang, X., and Cheng, X. (2003) Structure of the predominant protein arginine methyltransferase PRMT1 and analysis of its binding to substrate peptides. *Structure* **11**, 509-520
37. Cheng, Y., Frazier, M., Lu, F., Cao, X., and Redinbo, M. R. (2011) Crystal structure of the plant epigenetic protein arginine methyltransferase 10. *Journal of molecular biology* **414**, 106-122
38. Weiss, V. H., McBride, A. E., Soriano, M. A., Filman, D. J., Silver, P. A., and Hogle, J. M. (2000) The structure and oligomerization of the yeast arginine methyltransferase, Hmt1. *Nature structural biology* **7**, 1165-1171
39. Kolbel, K., Ihling, C., Bellmann-Sickert, K., Neundorf, I., Beck-Sickinger, A. G., Sinz, A., Kuhn, U., and Wahle, E. (2009) Type I Arginine Methyltransferases PRMT1 and PRMT-3 Act Distributively. *The Journal of biological chemistry* **284**, 8274-8282
40. Di Simplicio, P., Franconi, F., Frosali, S., and Di Giuseppe, D. (2003) Thiolation and nitrosation of cysteines in biological fluids and cells. *Amino acids* **25**, 323-339

41. Berlett, B. S., and Stadtman, E. R. (1997) Protein oxidation in aging, disease, and oxidative stress. *The Journal of biological chemistry* **272**, 20313-20316
42. Stadtman, E. R. (1993) Oxidation of free amino acids and amino acid residues in proteins by radiolysis and by metal-catalyzed reactions. *Annual review of biochemistry* **62**, 797-821
43. Carter, E. L., and Ragsdale, S. W. (2014) Modulation of nuclear receptor function by cellular redox poise. *Journal of inorganic biochemistry* **133**, 92-103
44. Weerapana, E., Wang, C., Simon, G. M., Richter, F., Khare, S., Dillon, M. B., Bachovchin, D. A., Mowen, K., Baker, D., and Cravatt, B. F. (2010) Quantitative reactivity profiling predicts functional cysteines in proteomes. *Nature* **468**, 790-795
45. Osborne, T. C., Obiany, O., Zhang, X., Cheng, X., and Thompson, P. R. (2007) Protein arginine methyltransferase 1: positively charged residues in substrate peptides distal to the site of methylation are important for substrate binding and catalysis. *Biochemistry* **46**, 13370-13381
46. Troffer-Charlier, N., Cura, V., Hassenboehler, P., Moras, D., and Cavarelli, J. (2007) Functional insights from structures of coactivator-associated arginine methyltransferase 1 domains. *The EMBO journal* **26**, 4391-4401
47. Yue, W. W., Hassler, M., Roe, S. M., Thompson-Vale, V., and Pearl, L. H. (2007) Insights into histone code syntax from structural and biochemical studies of CARM1 methyltransferase. *The EMBO journal* **26**, 4402-4412
48. Higashimoto, K., Kuhn, P., Desai, D., Cheng, X., and Xu, W. (2007) Phosphorylation-mediated inactivation of coactivator-associated arginine methyltransferase 1. *Proceedings of the National Academy of Sciences of the United States of America* **104**, 12318-12323
49. Sanchez, R., Riddle, M., Woo, J., and Momand, J. (2008) Prediction of reversibly oxidized protein cysteine thiols using protein structure properties. *Protein science : a publication of the Protein Society* **17**, 473-481
50. Zoccali, C., Bode-Boger, S., Mallamaci, F., Benedetto, F., Tripepi, G., Malatino, L., Cataliotti, A., Bellanuova, I., Fermo, I., Frolich, J., and Boger, R. (2001) Plasma concentration of asymmetrical dimethylarginine and mortality in patients with end-stage renal disease: a prospective study. *Lancet* **358**, 2113-2117
51. Tang, J., Gary, J. D., Clarke, S., and Herschman, H. R. (1998) PRMT 3, a type I protein arginine N-methyltransferase that differs from PRMT1 in its oligomerization, subcellular localization, substrate specificity, and regulation. *The Journal of biological chemistry* **273**, 16935-16945

52. Lim, Y., Kwon, Y. H., Won, N. H., Min, B. H., Park, I. S., Paik, W. K., and Kim, S. (2005) Multimerization of expressed protein-arginine methyltransferases during the growth and differentiation of rat liver. *Biochimica et biophysica acta* **1723**, 240-247
53. Huang, B. W., Ray, P. D., Iwasaki, K., and Tsuji, Y. (2013) Transcriptional regulation of the human ferritin gene by coordinated regulation of Nrf2 and protein arginine methyltransferases PRMT1 and PRMT4. *FASEB journal : official publication of the Federation of American Societies for Experimental Biology* **27**, 3763-3774
54. Lafleur, V. N., Richard, S., and Richard, D. E. (2014) Transcriptional repression of hypoxia-inducible factor-1 (HIF-1) by the protein arginine methyltransferase PRMT1. *Molecular biology of the cell* **25**, 925-935
55. Yamagata, K., Daitoku, H., Takahashi, Y., Namiki, K., Hisatake, K., Kako, K., Mukai, H., Kasuya, Y., and Fukamizu, A. (2008) Arginine methylation of FOXO transcription factors inhibits their phosphorylation by Akt. *Molecular cell* **32**, 221-231

CHAPTER 7

SUMMARY AND FUTURE DIRECTIONS

The protein arginine methyltransferases catalyze the post-translational modification of proteins implicated in a variety of fundamental cellular pathways, and unsurprisingly, their dysregulation has been linked to many human diseases (reviewed in Chapter 2). As the predominant PRMT in cells (31), PRMT1 methylation must be tightly regulated in order to respond adequately to specific cellular needs. However, despite the critical need for proper PRMT1 regulation, very little is actually known about the factors that influence PRMT1 substrate selection, product made (MMA vs. ADMA), and overall methyltransferase activity. The work presented here has combined structural and kinetic approaches to better understand how PRMT1 binds its substrates, and how overall methyltransferase activity can be regulated. A summary of each project and future directions along with existing preliminary data are described below.

Investigation of the In Vivo Effects of Oxidation on PRMT1— We discovered that PRMT1 (as well as PRMT3, PRMT6, and PRMT7) methyltransferase activity can be regulated by the redox environment *in vitro*. To determine whether this regulatory mechanism is relevant in cells, we have collaborated with the lab of Dr. Michael Yu (State University of New York, Buffalo) to test the methyltransferase activity of PRMT1 after treating cells with increasing amount of oxidants. The Yu lab grew human embryonic kidney (HEK293 that had been transfected to over express FLAG-tagged PRMT1) cells to about 85% confluency prior to treatment with hydrogen peroxide (0, 0.6 mM, or 1.2 mM

H₂O₂) for 1 hour at 37° C to mimic increasing cellular oxidative stress conditions. They then used magnetic beads containing anti-FLAG antibody to immunoprecipitate FLAG-tagged PRMT1 from these cells. The immunoprecipitated PRMT1 (IP PRMT1) was then sent to our lab where we used a gel-based methyltransferase assay to determine the effect of cellular oxidative stress on the ability of PRMT1 to methylate histone H4. As shown in Figure 7-1-A and B, the methyltransferase activity of PRMT1 decreases with increasing levels of cellular oxidative stress. Additionally, the immunoprecipitated PRMT1 samples were also probed for sulfenic acid content using the same sulfenic acid-specific fluorescent probe (DCP-Rho1) used in our *in vitro* studies. As depicted in Figure 7-2, increasing cellular oxidative stress is associated with increasing sulfenic acid formation on PRMT1, suggesting that the redox regulatory mechanism described *in vitro* (discussed in chapter 6) also occurs *in vivo*. The *in vivo* significance of PRMT1 redox regulation remains to be determined. Newly emerging Bioorthogonal Profiling of Protein Methylation (BPPM) approaches (56), may be used for PRMT1 in cells with and without oxidative stress treatment to determine whether substrate preference is affected by the redox state and provide an indication of what specific pathways may be affected by this regulatory mechanism. A more targeted avenue of investigation would be to characterize the effect of PRMT1 redox regulation on pathways that have already linked PRMT1 to the cellular oxidative stress response. Such pathways include the PRMT1-dependent transcriptional regulation of HIF α or of the human ferritin gene, which are needed for the cellular adaptive response to hypoxia and the cellular defense response to oxidative stress, respectively.

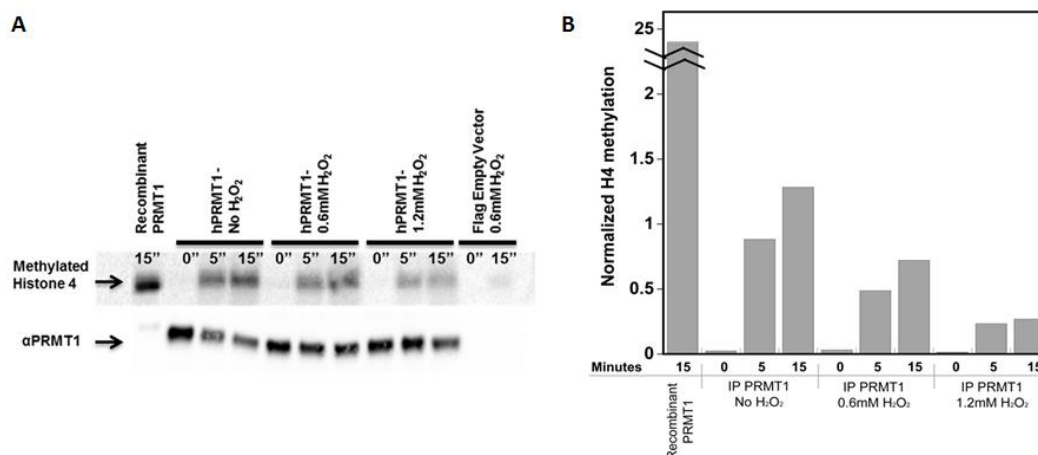


FIGURE 7-1. PRMT1 methyltransferase activity is impaired by oxidation *in vivo*. In (A), immunoprecipitated PRMT1 from HEK293 cells treated with 0, 0.6, or 1.2 mM H₂O₂ was used to methylate 1 μ M histone H4 protein using 2 μ M [³H]AdoMet as the methyl group donor in 50 mM sodium phosphate pH 8.0 at 30° C. At the noted time points, 10 μ l was removed from each reaction, quenched in SDS sample buffer and boiled for 5 minutes prior to running on a 12% SDS-PAGE gel. The proteins were transferred to a PVDF membrane which was dried and exposed to a Tritium imaging screen (BioRad) for 96 hours. After exposure the amount of PRMT1 present in each lane was detected using an anti-PRMT1 antibody (Bethyl). In (B) a graphical representation of (A) is shown, with the activity normalized based on the levels of PRMT1 present.

Impact of Redox Regulation of PRMT1 on Substrate Binding— While we have clearly determined that PRMT1 oxidation at two critical cysteine residues leads to a decrease in the PRMT1 enzymatic activity, the mechanism through which oxidation impacts activity remains undetermined. Methods such as fluorescence quenching, isothermal titration calorimetry (ITC), or fluorescence anisotropy could be used to determine the effect that oxidation on the indicated cysteine residues may have on the ability of PRMT1 to bind AdoMet and peptide substrates in both the unmethylated and monomethylated forms.

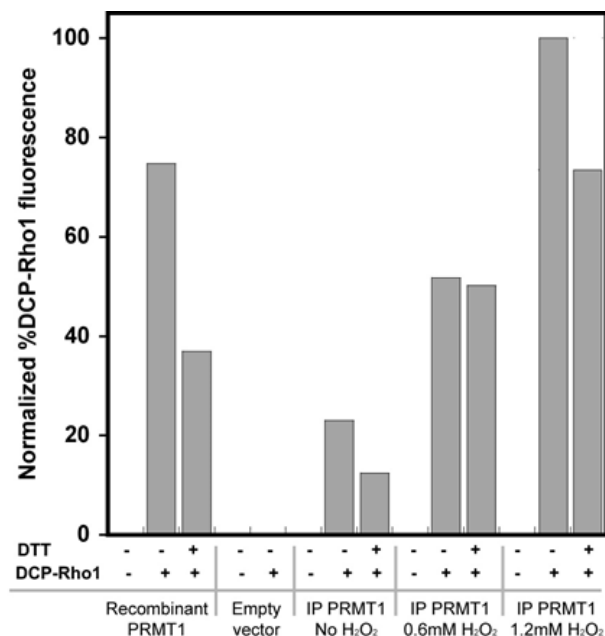


FIGURE 7-2. Sulfenic acid levels in PRMT1 increase with increasing cellular oxidative stress. The sulfenic acid-specific DCP-Rho1 fluorescent probe was used as described in chapter 6 to quantify the sulfenic acid levels in PRMT1 immunoprecipitated from HEK293 cells treated with 0, 0.6, or 1.2 mM H₂O₂.

Mechanism of PRMT6 Redox Regulation—Sequence conservation analysis of the PRMT1 cysteines necessary for redox control of PRMT1 activity led us to identify PRMT3, PRMT6, PRMT7, and PRMT8 as additional PRMT isoforms that may be regulated by oxidative stress since at least one of the two cysteines were conserved in these isoforms (57). As described in chapter 6, we were able to confirm the redox regulation of PRMT3, PRMT6, and PRMT7. While our redox regulation manuscript was under review, the structure of the mouse PRMT6 was solved in both an oxidized and reduced form (58). Although the two structures (PDB ID: 4C03 reduced, 4C05 oxidized) crystallized in different space groups (P₂₁2₁2 and I₄₁, respectively), the monomers of each form overlap

with an rmsd of 0.59. The main difference between the two structures occurs in the positioning of the N-terminal helix αX (orange in Figure 7-3) which is properly folded in the reduced structure (Figure 7-3-B) and unfolded in the oxidized structure (Figure 7-3-A). The oxidized form of the PRMT6 structure shows the presence of a disulfide bond bridging helix αX in the AdoMet binding domain of one monomer to the dimerization arm of the other monomer (disulfide bond links C53 and C232 of two mouse PRMT6 monomers), resulting in a covalent dimer with an unfolded αX helix (58). As discussed in chapter 2, it has long been known that the helix αX is essential for the activity of all PRMTs. In mouse PRMT6, proper folding of the αX helix locks and buries the cofactor in place for catalysis. Additionally, the Y50 and Y54 residues position the double-E-loop E167 in an active conformation for catalysis (Figure 7-4). Therefore, indicating that proper folding of the αX helix is necessary for catalysis, but not for initial cofactor binding.

The determination of this structure in differing conformations that depend on the redox state 1) validates our determination that PRMT6 is under redox control, 2) indicates that PRMT6 likely has a mechanism of redox control that is different from PRMT1 since there is no cysteine present on the PRMT1 αX helix, and 3) serves as a guide for us to begin work to determine the mechanism of PRMT6 redox control.

I have initiated construction of several human PRMT6 cysteine to serine variant constructs (ie. cysteine-less PRMT6) which can be used to determine the mechanism of redox control of PRMT 6 activity. These can be used much like the PRMT1 constructs were to identify the specific cysteines necessary for redox regulation. It will be interesting to determine if only the presence of the two cysteines found to form a disulfide bond are

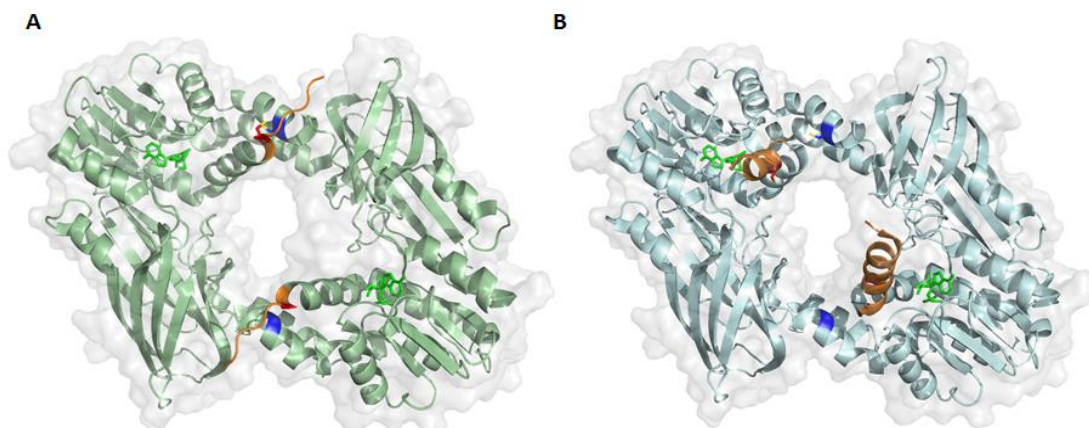


FIGURE 7-3. PRMT6 structures in (A) oxidized and (B) reduced forms. In (A) and (B) the structures of oxidized (PDB: 4C05) and reduced (PDB: 4C03) PRMT6 are shown. The N-terminal helix αX has been colored in orange in both forms. (A) Helix αX is disordered in the oxidized (light green) structure and mouse PRMT6 cysteine 53 (red) forms a disulfide bond with cysteine 232 (blue) of the adjacent monomer. (B) The αX helix of PRMT6 is properly folded over the cofactor and substrate binding pockets in the reduced (light blue) PRMT6 structure.

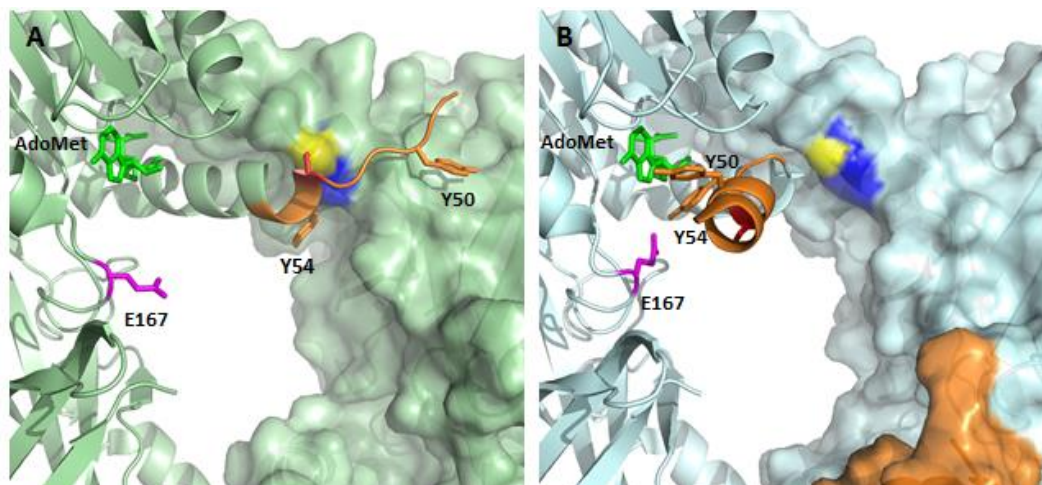


FIGURE 7-4. Position of PRMT6 active site E167 in (A) oxidized and (B) reduced forms. Active site comparison of (A) oxidized and (B) reduced PRMT6, colored as in 7-3. Residue E167 of the double-E loop has been colored in magenta in both. In the reduced structure, residues Y50 and Y54 of the N-terminal helix αX help position E167 in the position required for catalysis.

required, since neither of those are conserved in any other PRMT isoform, or if additional cysteines play a role in the redox regulation of PRMT6 activity.

Interestingly, the PRMT6 structure suggests that the redox state of this enzyme may affect substrate binding and catalysis but have no effect on cofactor binding (58). As suggested for PRMT1, fluorescence quenching, isothermal titration calorimetry (ITC), or fluorescence anisotropy should be used to determine the specific effects of oxidation on the on the ability of PRMT1 to bind AdoMet and peptide substrates in both the unmethylated and monomethylated forms.

Redox Regulation of PRMT1 Product Formation— Another interesting discovery that has emerged since we reported the redox regulation of PRMT1 activity is that the PRMT1 redox state may influence the product formation of the PRMT1 enzyme. Using an HPLC-based PRMT product detection assay (59), my lab mate Tamar Caceres found that reduced PRMT1 forms primarily MMA, while oxidized PRMT1 makes both MMA and ADMA when methylating the R3 peptide (Figure 7-5). I attempted to determine whether oxidized PRMT1 makes more ADMA than reduced PRMT1 when methylating a different substrate, histone H4 protein. Initial results indicate that reduced PRMT1 catalyzed more ADMA on the H4 protein than the oxidized enzyme (data not shown). Although these results are preliminary and will be tested again to confirm these observations, they hint at the possibility that redox regulation of PRMT1 activity may affect the processivity of the enzyme in a substrate dependent manner. This subject will continue to be investigated in the Hevel lab. Similar studies should also assess whether reduction/oxidation affects the processivity of PRMT6.

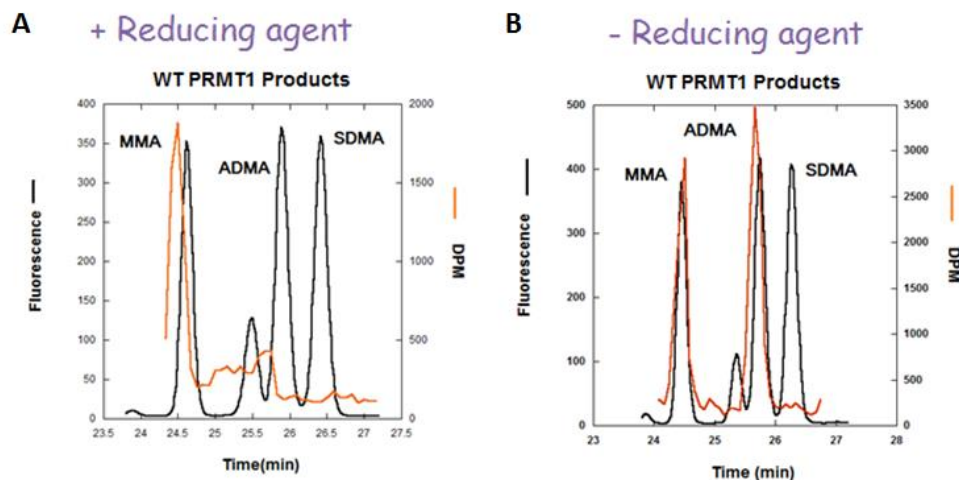


FIGURE 7-5. PRMT1 product formation on the R3 peptide depends on the redox state. Reverse HPLC analysis of the methylation products of the R3 peptide indicate that (A) the presence of a reducing agent impedes ADMA formation, while (B) ADMA formation can be catalyzed in the absence of reducing agent.

SUMMARY

This dissertation provides new insights into regulatory mechanisms that control PRMT methyltransferase activity. New insights into the workings of previously reported PRMT1 regulators, along with the discovery of a novel regulatory mechanism for several members of the PRMT family, provide a strong foundation for future research that will help unravel mechanisms that control PRMT activity.

REFERENCES

1. Go, A. S., Mozaffarian, D., Roger, V. L., Benjamin, E. J., Berry, J. D., Blaha, M. J., Dai, S. F., Ford, E. S., Fox, C. S., Franco, S., Fullerton, H. J., Gillespie, C., Hailpern, S. M., Heit, J. A., Howard, V. J., Huffman, M. D., Judd, S. E., Kissela, B. M., Kittner, S. J., Lackland, D. T., Lichtman, J. H., Lisabeth, L. D., Mackey, R. H., Magid, D. J., Marcus, G. M., Marelli, A., Matchar, D. B., McGuire, D. K., Mohler, E. R., Moy, C. S., Mussolino, M. E., Neumar, R. W., Nichol, G., Pandey, D. K., Paynter, N. P., Reeves, M. J., Sorlie, P. D., Stein, J., Towfighi, A., Turan, T. N., Virani, S. S., Wong, N. D., Woo, D., Turner, M. B., Comm, A. H. A. S., and

- Subcomm, S. S. (2014) Heart Disease and Stroke Statistics-2014 Update A Report From the American Heart Association. *Circulation* **129**, E28-E292
2. Lu, T. M., Ding, Y. A., Charng, M. J., and Lin, S. J. (2003) Asymmetrical dimethylarginine: a novel risk factor for coronary artery disease. *Clin. Cardiol.* **26**, 458-464
 3. Chen, X., Niroomand, F., Liu, Z., Zankl, A., Katus, H. A., Jahn, L., and Tiefenbacher, C. P. (2006) Expression of nitric oxide related enzymes in coronary heart disease. *Basic Res. Cardiol.* **101**, 346-353
 4. Antoniades, C., Shirodaria, C., Leeson, P., Antonopoulos, A., Warrick, N., Van-Assche, T., Cunnington, C., Tousoulis, D., Pillai, R., Ratnatunga, C., Stefanadis, C., and Channon, K. M. (2009) Association of plasma asymmetrical dimethylarginine (ADMA) with elevated vascular superoxide production and endothelial nitric oxide synthase uncoupling: implications for endothelial function in human atherosclerosis. *Eur. Heart J.* **30**, 1142-1150
 5. Boger, R. H., Bode-Boger, S. M., Szuba, A., Tsao, P. S., Chan, J. R., Tangphao, O., Blaschke, T. F., and Cooke, J. P. (1998) Asymmetric dimethylarginine (ADMA): a novel risk factor for endothelial dysfunction: its role in hypercholesterolemia. *Circulation* **98**, 1842-1847
 6. Luneburg, N., Harbaum, L., and Hennigs, J. K. (2014) The Endothelial ADMA/NO Pathway in Hypoxia-Related Chronic Respiratory Diseases. *Biomed Res Int* **2014**, 501612
 7. Sydow, K., and Munzel, T. (2003) ADMA and oxidative stress. *Atheroscler Suppl* **4**, 41-51
 8. Valkonen, V. P., Paiva, H., Salonen, J. T., Lakka, T. A., Lehtimaki, T., Laakso, J., and Laaksonen, R. (2001) Risk of acute coronary events and serum concentration of asymmetrical dimethylarginine. *Lancet* **358**, 2127-2128
 9. Vallance, P., and Leiper, J. (2004) Cardiovascular biology of the asymmetric dimethylarginine:dimethylarginine dimethylaminohydrolase pathway. *Arterioscler. Thromb. Vasc. Biol.* **24**, 1023-1030
 10. Achan, V., Broadhead, M., Malaki, M., Whitley, G., Leiper, J., MacAllister, R., and Vallance, P. (2003) Asymmetric dimethylarginine causes hypertension and cardiac dysfunction in humans and is actively metabolized by dimethylarginine dimethylaminohydrolase. *Arterioscler. Thromb. Vasc. Biol.* **23**, 1455-1459
 11. Kielstein, J. T., Impraim, B., Simmel, S., Bode-Boger, S. M., Tsikas, D., Frolich, J. C., Hoepfer, M. M., Haller, H., and Fliser, D. (2004) Cardiovascular effects of

systemic nitric oxide synthase inhibition with asymmetrical dimethylarginine in humans. *Circulation* **109**, 172-177

12. Burgoyne, J. R., Mongue-Din, H., Eaton, P., and Shah, A. M. (2012) Redox signaling in cardiac physiology and pathology. *Circ. Res.* **111**, 1091-1106
13. Chan, J. R., Boger, R. H., Bode-Boger, S. M., Tangphao, O., Tsao, P. S., Blaschke, T. F., and Cooke, J. P. (2000) Asymmetric dimethylarginine increases mononuclear cell adhesiveness in hypercholesterolemic humans. *Arterioscler. Thromb. Vasc. Biol.* **20**, 1040-1046
14. Bedford, M. T., and Clarke, S. G. (2009) Protein arginine methylation in mammals: who, what, and why. *Molecular cell* **33**, 1-13
15. Ogawa, T., Kimoto, M., and Sasaoka, K. (1987) Occurrence of a new enzyme catalyzing the direct conversion of NG,NG-dimethyl-L-arginine to L-citrulline in rats. *Biochem. Biophys. Res. Commun.* **148**, 671-677
16. Boger, R. H., Sydow, K., Borlak, J., Thum, T., Lenzen, H., Schubert, B., Tsikas, D., and Bode-Boger, S. M. (2000) LDL cholesterol upregulates synthesis of asymmetrical dimethylarginine in human endothelial cells: involvement of S-adenosylmethionine-dependent methyltransferases. *Circ. Res.* **87**, 99-105
17. Chobanyan-Jurgens, K., Pham, V. V., Stichtenoth, D. O., and Tsikas, D. (2011) Asymmetrical dimethylarginine, oxidative stress, and atherosclerosis. *Hypertension* **58**, e184-185; author reply e186
18. Jiang, J. L., Zhang, X. H., Li, N. S., Rang, W. Q., Feng, Y., Hu, C. P., Li, Y. J., and Deng, H. W. (2006) Probucol decreases asymmetrical dimethylarginine level by alternation of protein arginine methyltransferase I and dimethylarginine dimethylaminohydrolase activity. *Cardiovasc. Drugs Ther.* **20**, 281-294
19. Chen, Y., Xu, X., Sheng, M., Zhang, X., Gu, Q., and Zheng, Z. (2009) PRMT-1 and DDAHs-induced ADMA upregulation is involved in ROS- and RAS-mediated diabetic retinopathy. *Exp. Eye Res.* **89**, 1028-1034
20. Tyagi, N., Sedoris, K. C., Steed, M., Ovechkin, A. V., Moshal, K. S., and Tyagi, S. C. (2005) Mechanisms of homocysteine-induced oxidative stress. *Am. J. Physiol. Heart Circ. Physiol.* **289**, H2649-2656
21. Wilcox, C. S. (2012) Asymmetric dimethylarginine and reactive oxygen species: unwelcome twin visitors to the cardiovascular and kidney disease tables. *Hypertension* **59**, 375-381

22. Lim, Y., Lee, E., Lee, J., Oh, S., and Kim, S. (2008) Down-regulation of asymmetric arginine methylation during replicative and H₂O₂-induced premature senescence in WI-38 human diploid fibroblasts. *J. Biochem.* **144**, 523-529
23. Gui, S., Wooderchak, W. L., Daly, M. P., Porter, P. J., Johnson, S. J., and Hevel, J. M. (2011) Investigation of the molecular origins of protein-arginine methyltransferase I (PRMT1) product specificity reveals a role for two conserved methionine residues. *The Journal of Biological Chemistry* **286**, 29118-29126
24. Wang, R., Ibanez, G., Islam, K., Zheng, W., Blum, G., Sengelaub, C., and Luo, M. (2011) Formulating a fluorogenic assay to evaluate S-adenosyl-L-methionine analogues as protein methyltransferase cofactors. *Mol. Biosyst.* **7**, 2970-2981
25. Cornell, K. A., Swarts, W. E., Barry, R. D., and Riscoe, M. K. (1996) Characterization of recombinant *Escherichia coli* 5'-methylthioadenosine/S-adenosylhomocysteine nucleosidase: analysis of enzymatic activity and substrate specificity. *Biochem. Biophys. Res. Commun.* **228**, 724-732
26. Suh-Lailam, B. B., and Hevel, J. M. (2010) A fast and efficient method for quantitative measurement of S-adenosyl-L-methionine-dependent methyltransferase activity with protein substrates. *Anal. Biochem.* **398**, 218-224
27. Atmane, N., Dairou, J., Paul, A., Dupret, J. M., and Rodrigues-Lima, F. (2003) Redox regulation of the human xenobiotic metabolizing enzyme arylamine N-acetyltransferase 1 (NAT1). Reversible inactivation by hydrogen peroxide. *The Journal of Biological Chemistry* **278**, 35086-35092
28. Nelson, K. J., Klomsiri, C., Codreanu, S. G., Soito, L., Liebler, D. C., Rogers, L. C., Daniel, L. W., and Poole, L. B. (2010) Use of dimedone-based chemical probes for sulfenic acid detection methods to visualize and identify labeled proteins. *Methods Enzymol.* **473**, 95-115
29. Wu, Y., Kwon, K. S., and Rhee, S. G. (1998) Probing cellular protein targets of H₂O₂ with fluorescein-conjugated iodoacetamide and antibodies to fluorescein. *FEBS Lett.* **440**, 111-115
30. Hansen, R. E., and Winther, J. R. (2009) An introduction to methods for analyzing thiols and disulfides: Reactions, reagents, and practical considerations. *Anal. Biochem.* **394**, 147-158
31. Tang, J., Frankel, A., Cook, R. J., Kim, S., Paik, W. K., Williams, K. R., Clarke, S., and Herschman, H. R. (2000) PRMT1 is the predominant type I protein arginine methyltransferase in mammalian cells. *J. Biol. Chem.* **275**, 7723-7730

32. Stone, J. R., and Yang, S. (2006) Hydrogen peroxide: a signaling messenger. *Antioxid. Redox Signal.* **8**, 243-270
33. Coiner, H., Schroder, G., Wehinger, E., Liu, C. J., Noel, J. P., Schwab, W., and Schroder, J. (2006) Methylation of sulfhydryl groups: a new function for a family of small molecule plant O-methyltransferases. *Plant J.* **46**, 193-205
34. Feng, Y., Xie, N., Jin, M., Stahley, M. R., Stivers, J. T., and Zheng, Y. G. (2011) A transient kinetic analysis of PRMT1 catalysis. *Biochemistry* **50**, 7033-7044
35. Kleinschmidt, M. A., Streubel, G., Samans, B., Krause, M., and Bauer, U. M. (2008) The protein arginine methyltransferases CARM1 and PRMT1 cooperate in gene regulation. *Nucleic Acids Res.* **36**, 3202-3213
36. Zhang, X., and Cheng, X. (2003) Structure of the predominant protein arginine methyltransferase PRMT1 and analysis of its binding to substrate peptides. *Structure* **11**, 509-520
37. Cheng, Y., Frazier, M., Lu, F., Cao, X., and Redinbo, M. R. (2011) Crystal structure of the plant epigenetic protein arginine methyltransferase 10. *J. Mol. Biol.* **414**, 106-122
38. Weiss, V. H., McBride, A. E., Soriano, M. A., Filman, D. J., Silver, P. A., and Hogle, J. M. (2000) The structure and oligomerization of the yeast arginine methyltransferase, Hmt1. *Nat. Struct. Biol.* **7**, 1165-1171
39. Kolbel, K., Ihling, C., Bellmann-Sickert, K., Neundorff, I., Beck-Sickinger, A. G., Sinz, A., Kuhn, U., and Wahle, E. (2009) Type I Arginine Methyltransferases PRMT1 and PRMT-3 Act Distributively. *J. Biol. Chem.* **284**, 8274-8282
40. Di Simplicio, P., Franconi, F., Frosali, S., and Di Giuseppe, D. (2003) Thiolation and nitrosation of cysteines in biological fluids and cells. *Amino Acids* **25**, 323-339
41. Berlett, B. S., and Stadtman, E. R. (1997) Protein oxidation in aging, disease, and oxidative stress. *The Journal of Biological Chemistry* **272**, 20313-20316
42. Stadtman, E. R. (1993) Oxidation of free amino acids and amino acid residues in proteins by radiolysis and by metal-catalyzed reactions. *Annu. Rev. Biochem.* **62**, 797-821
43. Carter, E. L., and Ragsdale, S. W. (2014) Modulation of nuclear receptor function by cellular redox poise. *The Journal of Inorganic Biochemistry* **133**, 92-103

44. Weerapana, E., Wang, C., Simon, G. M., Richter, F., Khare, S., Dillon, M. B., Bachovchin, D. A., Mowen, K., Baker, D., and Cravatt, B. F. (2010) Quantitative reactivity profiling predicts functional cysteines in proteomes. *Nature* **468**, 790-795
45. Osborne, T. C., Obianyano, O., Zhang, X., Cheng, X., and Thompson, P. R. (2007) Protein arginine methyltransferase 1: positively charged residues in substrate peptides distal to the site of methylation are important for substrate binding and catalysis. *Biochemistry* **46**, 13370-13381
46. Troffer-Charlier, N., Cura, V., Hassenboehler, P., Moras, D., and Cavarelli, J. (2007) Functional insights from structures of coactivator-associated arginine methyltransferase 1 domains. *EMBO J.* **26**, 4391-4401
47. Yue, W. W., Hassler, M., Roe, S. M., Thompson-Vale, V., and Pearl, L. H. (2007) Insights into histone code syntax from structural and biochemical studies of CARM1 methyltransferase. *The EMBO journal* **26**, 4402-4412
48. Higashimoto, K., Kuhn, P., Desai, D., Cheng, X., and Xu, W. (2007) Phosphorylation-mediated inactivation of coactivator-associated arginine methyltransferase 1. *Proceedings of the National Academy of Sciences* **104**, 12318-12323
49. Sanchez, R., Riddle, M., Woo, J., and Momand, J. (2008) Prediction of reversibly oxidized protein cysteine thiols using protein structure properties. *Protein Sci.* **17**, 473-481
50. Zoccali, C., Bode-Boger, S., Mallamaci, F., Benedetto, F., Tripepi, G., Malatino, L., Cataliotti, A., Bellanuova, I., Fermo, I., Frolich, J., and Boger, R. (2001) Plasma concentration of asymmetrical dimethylarginine and mortality in patients with end-stage renal disease: a prospective study. *Lancet* **358**, 2113-2117
51. Tang, J., Gary, J. D., Clarke, S., and Herschman, H. R. (1998) PRMT 3, a type I protein arginine N-methyltransferase that differs from PRMT1 in its oligomerization, subcellular localization, substrate specificity, and regulation. *J. Biol. Chem.* **273**, 16935-16945
52. Lim, Y., Kwon, Y. H., Won, N. H., Min, B. H., Park, I. S., Paik, W. K., and Kim, S. (2005) Multimerization of expressed protein-arginine methyltransferases during the growth and differentiation of rat liver. *Biochim. Biophys. Acta* **1723**, 240-247
53. Huang, B. W., Ray, P. D., Iwasaki, K., and Tsuji, Y. (2013) Transcriptional regulation of the human ferritin gene by coordinated regulation of Nrf2 and protein arginine methyltransferases PRMT1 and PRMT4. *FASEB J.* **27**, 3763-3774

54. Lafleur, V. N., Richard, S., and Richard, D. E. (2014) Transcriptional repression of hypoxia-inducible factor-1 (HIF-1) by the protein arginine methyltransferase PRMT1. *Mol. Biol. Cell* **25**, 925-935
55. Yamagata, K., Daitoku, H., Takahashi, Y., Namiki, K., Hisatake, K., Kako, K., Mukai, H., Kasuya, Y., and Fukamizu, A. (2008) Arginine methylation of FOXO transcription factors inhibits their phosphorylation by Akt. *Mol. Cell* **32**, 221-231
56. Guo, H., Wang, R., Zheng, W., Chen, Y., Blum, G., Deng, H., and Luo, M. (2014) Profiling substrates of protein arginine N-methyltransferase 3 with S-adenosyl-L-methionine analogues. *ACS Chem. Biol.* **9**, 476-484
57. Morales, Y., Nitzel, D. V., Price, O. M., Gui, S., Li, J., Qu, J., and Hevel, J. M. (2015) Redox Control of Protein Arginine Methyltransferase 1 (PRMT1) Activity. *J. Biol. Chem.* **290**, 14915-14926
58. Bonnefond, L., Stojko, J., Mailliot, J., Troffer-Charlier, N., Cura, V., Wurtz, J. M., Cianferani, S., and Cavarelli, J. (2015) Functional insights from high resolution structures of mouse protein arginine methyltransferase 6. *J. Struct. Biol.* **191**, 175-183
59. Gui, S., Wooderchak-Donahue, W. L., Zang, T., Chen, D., Daly, M. P., Zhou, Z. S., and Hevel, J. M. (2013) Substrate-induced control of product formation by protein arginine methyltransferase 1. *Biochemistry* **52**, 199-209

APPENDIX

Copyright Permission Policy

These guidelines apply to the reuse of articles, figures, charts and photos in the *Journal of Biological Chemistry, Molecular & Cellular Proteomics* and the *Journal of Lipid Research*.

For authors reusing their own material:

Authors need **NOT** contact the journal to obtain rights to reuse their own material. They are automatically granted permission to do the following:

- Reuse the article in print collections of their own writing.
- Present a work orally in its entirety.
- Use an article in a thesis and/or dissertation.
- Reproduce an article for use in the author's courses. (If the author is employed by an academic institution, that institution also may reproduce the article for teaching purposes.)
- Reuse a figure, photo and/or table in future commercial and noncommercial works.
- Post a copy of the paper in PDF that you submitted via BenchPress.
 - Only authors who published their papers under the "Author's Choice" option may post the final edited PDFs created by the publisher to their own/departmental/university Web sites.
 - All authors may link to the journal site containing the final edited PDFs created by the publisher.

<http://www.jbc.org/site/home/about/permissions.xhtml>

Permission Letter

Dr. Jun Qu
Department of Pharmaceutical Sciences
State University of New York, University at Buffalo

October 19, 2015

Yalemi Morales
Utah State University
Department of Chemistry and Biochemistry
Logan, UT 84322-0300

This letter grants my permission for Yalemi Morales to use the following publication in part or in full for inclusion in her Ph.D. dissertation.

Morales, Y., Nitzel, D. V., Price, O. M., Gui, S., Li, J., Qu, J., and Hevel, J. M. (2015) Redox Control of Protein Arginine Methyltransferase 1 (PRMT1) Activity. *The Journal of Biological Chemistry* **290**: 14915-14926

Sincerely,

Jun Qu

Permission Letter

Dr. Jun Li
Department of Pharmaceutical Sciences
State University of New York, University at Buffalo

October 19, 2015

Yalemi Morales
Utah State University
Department of Chemistry and Biochemistry
Logan, UT 84322-0300

This letter grants my permission for Yalemi Morales to use the following publication in part or in full for inclusion in her Ph.D. dissertation.

Morales, Y., Nitzel, D. V., Price, O. M., Gui, S., Li, J., Qu, J., and Hevel, J. M. (2015) Redox Control of Protein Arginine Methyltransferase 1 (PRMT1) Activity. *The Journal of Biological Chemistry* **290**: 14915-14926

Sincerely,

Jun Li

Permission Letter

Dr. Shanying Gui
Postdoctoral Researcher
Ohio State University Comprehensive Cancer Center

October 19, 2015

Yalemi Morales
Utah State University
Department of Chemistry and Biochemistry
Logan, UT 84322-0300

This letter grants my permission for Yalemi Morales to use the following publication in part or in full for inclusion in her Ph.D. dissertation.

Morales, Y., Nitzel, D. V., Price, O. M., Gui, S., Li, J., Qu, J., and Hevel, J. M. (2015) Redox Control of Protein Arginine Methyltransferase 1 (PRMT1) Activity. *The Journal of Biological Chemistry* **290**: 14915-14926

Sincerely,

Shanying Gui

Permission Letter

Damon Nitzel
Distribution and Technical Support Representative
Apogee Instruments, Inc.

October 19, 2015

Yalemi Morales
Utah State University
Department of Chemistry and Biochemistry
Logan, UT 84322-0300

This letter grants my permission for Yalemi Morales to use the following publication in part or in full for inclusion in her Ph.D. dissertation.

Morales, Y., Nitzel, D. V., Price, O. M., Gui, S., Li, J., Qu, J., and Hevel, J. M. (2015) Redox Control of Protein Arginine Methyltransferase 1 (PRMT1) Activity. *The Journal of Biological Chemistry* **290**: 14915-14926

Sincerely,

Damon Nitzel

Permission Letter

Owen Price
Department of Chemistry and Biochemistry
Utah State University

October 19, 2015

Yalemi Morales
Utah State University
Department of Chemistry and Biochemistry
Logan, UT 84322-0300

This letter grants my permission for Yalemi Morales to use the following publication in part or in full for inclusion in her Ph.D. dissertation.

Morales, Y., Nitzel, D. V., Price, O. M., Gui, S., Li, J., Qu, J., and Hevel, J. M. (2015) Redox Control of Protein Arginine Methyltransferase 1 (PRMT1) Activity. *The Journal of Biological Chemistry* **290**: 14915-14926

Sincerely,

Owen Price

CURRICULUM VITAE

Yalemi Morales

(Oct. 2015)

EDUCATION

- **Ph.D. in Biochemistry** (2016) Utah State University, Logan UT
Mentor: Joan M. Hevel, Ph.D.
Dissertation: *Characterization of the Substrate Interactions and Regulation of Protein Arginine Methyltransferase 1*
- **B.S. in Biochemistry** (2010) Utah State University, Logan UT

RESEARCH EXPERIENCE

- 2009-2015 Ph.D. Research assistant in the lab of Dr. Joan Hevel, Utah State University. Investigation of the structure and function of protein arginine methyltransferase I (PRMT1) using protein remodeling, X-ray crystallography, kinetic assays, and immunoprecipitation assays. Interested in the interaction of PRMT1 with regulators and substrates, as well as the effect of methylation on the downstream functions of substrates. Dissertation: "Characterization of the Substrate Interactions and Regulation of Protein Arginine Methyltransferase 1"
- 2008-2009 Undergraduate research associate under mentorship of Dr. Joan Hevel and Dr. Sean Johnson, Utah State University. Research focus: Expression, purification and crystallization of PRMT1 with peptide or protein substrate.
- 2007-2008 Undergraduate research fellow in the lab of Dr. Joseph Li, Biology Department, Utah State University. Research focus: investigating apoptotic effect of Blue Tongue Virus infection on mammalian cells after surviving gene silencing using siRNA. Additionally responsible for maintenance and proliferation of all lab mammalian cell lines.
- 2007 Undergraduate research associate in the lab of Dr. Giuseppe Pizzorno, Nevada Cancer Institute, Las Vegas, NV. Research focus: analyzing the effect of mitochondrial gene silencing on apoptosis rate of mammalian cells after chemotherapy drug treatment. Additionally trained in the handling, feeding, breeding, and genotyping of transgenic mice.

Professional/Academic Awards

- 2015 *Thomas F. Emery Outstanding Graduate Student in Biochemistry*, Utah State University. Logan, UT
- 2014 *Utah NASA Space Grant Scholarship*, Utah State University. Logan, UT
- 2014 *Best Poster Award*, Hansen Biochemistry Retreat. Logan, UT
- 2014 *FASEB MRC Program Poster Presentation Travel Award* to present at the SACNAS National Meeting. Los Angeles, CA
- 2014 *Dissertation Fellowship* from the School of Graduate Studies, Utah State University. Logan, UT
- 2014 *Best Oral Presentation* for talk presented at the Intermountain Graduate Research Symposium. Logan, UT
- 2009 *Honorable Mention*, NSF Graduate Research Fellowship
- 2008 *Undergraduate Research Fellowship*, American Heart Association
- 2007 *Dean's Non-resident Transfer Scholarship*, Utah State University. Logan, UT
- 2007 *Undergraduate Research Fellowship*, Utah State University. Logan UT
- 2007 *NIH-INBRE Undergraduate Research Opportunity*, Nevada Cancer Institute. Las Vegas, NV

Publications

- 2015 **Morales, Y.**, Nitzel, D. V., Price, O. M., Gui, S., Li, J., Qu, J., and Hevel, J. M. (2015) Redox Control of Protein Arginine Methyltransferase 1 (PRMT1) Activity. *The Journal of biological chemistry* **290**: 14915-14926
- 2015 **Morales, Y.**, Caceres, T., May, K., Hevel, J. M. (2015) Biochemistry and Regulation of the Protein Arginine Methyltransferases (PRMTs). Invited review manuscript submitted to *Archives of Biochemistry and Biophysics* October 2015.

Oral Research Presentations

- 2015 *Intermountain Graduate Research Symposium*, Logan, UT. "Redox control of Protein Arginine Methyltransferase I (PRMT1) activity"
- 2014 *Hansen Biochemistry Retreat*, Logan, UT. "Hevel lab methyltransferases"
- 2014 *Intermountain Graduate Research Symposium*, Logan, UT. "Exploring the effect of oxidation on PRMT1 activity"
- 2013 *Hansen Biochemistry Retreat*, Logan, UT. "Got CH3?"
- 2008 *American Heart Association Roundtable*, Logan, UT. "Expression, purification, and crystallization of PRMT1"

Poster Research Presentations

- 2014 *51st Annual SACNAS National Meeting*, Los Angeles, CA. “Redox control of Protein Arginine Methyltransferase I (PRMT1) activity.” **Yalemi Morales**, Damon Nitzel, Owen Price, Shanying Gui, Joan M. Hevel.
- 2014 *Hansen Biochemistry Retreat*, Logan, UT. “Redox control of Protein Arginine Methyltransferase I (PRMT1) activity.” **Yalemi Morales**, Damon Nitzel, Owen Price, Shanying Gui, Joan M. Hevel.
- 2014 *FASEB Biological Methylation meeting*, Nassau, Bahamas. “Redox control of Protein Arginine Methyltransferase I (PRMT1) activity.” **Yalemi Morales**, Damon Nitzel, Owen Price, Shanying Gui, Joan M. Hevel.
- 2013 *Hansen Biochemistry Retreat*, Logan, UT. “Protein arginine methylation: characterizing interactions with protein substrates and regulators.” **Yalemi Morales**, Jeremy Bakelar, Joan M. Hevel.
- 2012 *Hansen Biochemistry Retreat*, Logan, UT. “Regulation of protein arginine methylation and its effect on RNA binding.” **Yalemi Morales**, Joan M. Hevel.
- 2011 *Hansen Biochemistry Retreat*, Logan, UT. “Studies of yPRMT1 inhibition by Air1.” **Yalemi Morales**, Jeremy Bakelar, Joan M. Hevel.
- 2009 *237th ACS National Meeting*, Salt Lake City, UT. “How do monomethylated substrates bind PRMT1?” **Yalemi Morales**, Whitney Wooderchak, Joan M. Hevel.
- 2007 *Nevada IDeA Network of Biomedical Research Excellence*, Las Vegas, NV. “Analyzing the effect of MtCH1 and MtCH2 in apoptosis in order to accelerate cancer cell death.” **Yalemi Morales**, G. Pizzorno.

Conferences/Professional Meetings Attended

- 2015 FASEB Helicases and Nucleic-Acid Based Machines, Steamboat Springs, CO
- 2014 51st Annual SACNAS National Meeting, Los Angeles, CA
- 2014 FASEB Biological Methylation Meeting, Nassau, Bahamas
- 2013 50th Annual SACNAS National Meeting, San Antonio, TX
- 2012 Northwest Protein Crystallography Workshop, Bozeman, MT
- 2009 American Chemical Society National Meeting, Salt Lake City, UT

Funding/Support

- 2014 American Heart Association Predoctoral Fellowship Grant Proposal: “Cellular redox regulation of PRMT1 activity and impact on ADMA levels”– **scored 15.8%**, only 10% funded.
- 2014 Dissertation Fellowship Award, Utah State University
- 2014 FASEB MARC Program Poster/Oral Presentation Travel Award
- 2014 Dept. of Chemistry/Biochemistry, Utah State University – Travel Award
- 2014 School of Graduate Studies, Utah State University – Travel Award
- 2009 Honorable Mention, NSF Graduate Research Fellowship

Leadership, Management, and Service

- Train undergraduate and new graduate students (2009-present)
- Mentor undergraduate research projects and undergraduate research proposal development (2009-present)
- Serve as SACNAS (Society for the Advancement of Chicanos and Native Americans in Science) President (organize events, meetings, educational outreach, manage online presence, recruitment, and organize attendance to national meeting) (2013-2015)
- Serve as ACS Chemistry club graduate advisor (educational outreach) (2013-2015)
- Volunteer for Four Paws Rescue (2007-present)

Education Enrichment Activities

- 2013 Grant Writing Workshop, “Getting started as a successful proposal writer and academician.” Logan, UT
- 2012 NSF Responsible Conduct for Research Workshop, Logan, UT
- 2009 Teaching Assistant Workshop, Utah State University, Logan, UT

TEACHING EXPERIENCE

- 2015 (Spring) Advanced Biochemistry I – guest lecture
- 2015 (Spring) Advanced Biochemistry I – guest lecture
- 2014 (Spring) Introductory Biochemistry Laboratory
- 2013 (Fall) Chemical Principles I Laboratory
- 2012 (Fall) Chemical Principles II Laboratory
- 2012 (Spring) Introductory Biochemistry Laboratory
- 2011 (Fall) General Chemistry I Laboratory
- 2010 (Spring) Chemical Principles II Laboratory
- 2009 (Fall) Chemical Principles I Laboratory